Universitat Autònoma de Barcelona

Mathematical Models for Energy and Landscape Integrated Analysis in Agroecosystems

Carme Font Moragón

TESIS DOCTORAL

Mathematical Models for Energy and Landscape Integrated Analysis in Agroecosystems

Carme Font Moragón

Directors:

Dr. Aureli Alabert Romero

Dr. Joan Marull López

Doctorat en Matemàtiques
Departament de Matemàtiques
Universitat Autònoma de Barcelona

2016

Vull agrair als meus directors, el Dr. Aureli Alabert i el Dr. Joan Marull, la implicació, el seguiment i el recolzament durant aquests tres anys; així com a la Dra. Mercè Farré, que tot i no ser oficialment directora, s'ha portat com a tal.

Contents

Chapter 1

Introduction

Mathematical models are used to better explain natural phenomena. Since natural phenomena are very complex, in order to delve into their behaviour and be able to do predictions over them, a simplification process of such systems is needed. In the process of creating the model, the system is translated into mathematical language that allows the study of the system from a new point of view. In this thesis, statistical models are considered to study the behaviour of agroecosystems at different spatial scales.

The aim of this work is to study the relation between energy flows, land cover changes, landscape functionality and the biodiversity that underlies in agroecosystems. For this, models based on such matters are proposed. The main units of analysis will be the land covers, when we work at regional scale, and the land uses, at local scale.

In the second chapter, an intermediate disturbance-complexity model (IDC) of cultural landscapes is presented. This approach is aimed at assessing how different levels of anthropogenic disturbance on ecosystems affect the capacity to host biodiversity depending on the land matrix heterogeneity. It is applied to the Mallorca Island, amidst the Mediterranean biodiversity hotspot, at regional and landscape scales.

The model uses the disturbance exerted by farmers altering the Net Primary Production (NPP) through land use change, as well as removing a share of it, together with Shannon-Wiener index of land use diversity. The model is tested with a twofold-scalar experimental design of a set of landscape units along three time points. Species richness of breeding and wintering birds, taken as a biodiversity proxy, is used in an exploratory factor analysis.

Following the idea presented in the second chapter, in the third chapter we present a method to describe the relation between indicators of the land matrix heterogeneity, and the human appropriation of the net primary production in a given region. These quantities are viewed as functions of the vector of proportions of the different land covers, which is in turn treated as a random vector whose values depend on the particular small terrain cell that is observed.

We illustrate the method assuming first that the vector of proportions follows a uniform distribution on the simplex. We then consider as starting point a raw dataset of proportions for each cell, for which we must first obtain an estimate of its theoretical probability distribution, and secondly generate a sample of large size from it. We apply this procedure to real historical data of the Mallorca Island in three different time points.

The main goal here is to compute the mean value of the land covers diversity as a function of the level of human appropriation of net primary production. This function is related to the so-called Energy-Species hypothesis and to the Intermediate Disturbance Hypothesis.

Finally, fourth chapter is devoted to deal with agroecosystems internal processes. For this purpose, a graph to represent the pattern of energy flows in an agroecosystem is presented. We use this graph model to calculate the level of energy storage within the agroecosystem provided by its ‘internal feedback’, as well as the information embedded in this network of flows, at local and landscape scales.

Thus, we propose an Energy-Landscape Integrated Analysis (ELIA) model that assesses both the complexity of internal energy loops, and the information held in the whole network of socio-metabolic energy fluxes, so as to correlate this energy-information interplay with the functional landscape structure. In the annex, an improvement of the information indicator is suggested. ELIA is tested in the Vallès County of the Barcelona Metropolitan Region.

Chapter 2

Towards an Energy–Landscape Integrated Analysis? Exploring the links between socio-metabolic disturbance and landscape ecology performance (Mallorca Island, Spain, 1956-2011) [1]

2.1 Introduction

The role of agricultural landscapes in biodiversity conservation is an emerging research topic. This is by no means strange in a world where human population will approach nine billion people with a relevant portion of them still suffering malnutrition and hunger, a worrying decrease of species richness, and an unavoidable societal dependence on the environmental services that biodiversity provides. World agriculture is at stake amidst this big challenge (Schröter et al 2005; Godfray et al 2010; Cardinale et al 2012). About half of global usable land is already in intensive farming and grazing—and the more productive indeed. This has been a major driver of biodiversity loss, mainly after the 'Green Revolution' developed from the 1960s onwards (Matson et al 1997; Tilman et al 2002) whereas

---

[1] This work has been published in the journal Landscape Ecology with the participation of Joan Marull, Carme Font, Enric Tello, Nofre Fullana, Elena Domene, Manel Pons, Elena Galan

only some 6-12% is under any sort of nature protection (Bengston et al 2003; Tscharntke et al 2012).

No doubt, society needs other farm systems to meet this global challenge (Gomiero et al 2008). At the same time there is a growing recognition that the environmental impact of agricultural, pastoral and forestry activities is twofold. Depending on the land use intensities and the type of management, agricultural systems may either entail a decrease or increase in biological diversity (Altieri 1999; Swift et al 2004; Cardinale et al 2012). Hence, scientific enquiry needs to focus on the relationship between anthropogenic disturbance exerted on ecological patterns and processes by different agricultural types of farm management and the biodiversity host in cultural landscapes (Tilman et al 2002; Benton et al 2003). This also means looking at farm systems as providers of environmental services as well as producers of food, feed, fibber and fuel (Altieri 1999; Tress et al 2001; Agnoletti, 2006, 2014). If society wants to ensure both agricultural production and ecological services there arises a dilemma between two seemingly opposite strategies: i) a land-sparing approach based on increasing agricultural intensification in some areas so as to devote the others to nature conservation and forest transition (Green et al 2005; Matson and Vitousek 2006); or rather ii) a land-sharing approach based on a wildlife-friendly farming able to provide complex agroecological matrixes connected with natural sites that jointly maintain high species richness at landscape level (Bengston et al 2003; Marull et al 2010; Perfecto and Vandermeer 2010; Tscharntke et al 2012).

Underlying this scientific controversy, that entails important dilemmas for policy-making, there exist contrasting bio-geographical characteristics across the Earth, diverse human settlement patterns and socio-ecological trajectories, together with different intellectual traditions: e.g. island models of a binary landscape vs. continuous and heterogeneous landscape matrix; treating nature and agriculture as being opposite vs. enhancing environmental services in agroecosystems; considering humans separate from nature vs. seeing them as components of ecosystems (McDonnell and Pickett 1993; Farina 2000; Fischer et al 2008). Even those that advocate for combining these contrasting perspectives admit that this requires a major research step forward to know how biodiversity is kept in different landscape patterns and ecological processes (Phalan et al 2011).

Our starting point for this research agenda is to resume the Intermediate Disturbance Hypothesis (IDH), one of the non-equilibrium explanations of the maintenance of biodiversity in ecosystems most debated in ecology (Connell 1978; van der Maarel, 1993; Wilson, 1994; Padisak 1993; Tilman 1994; Reynolds 1995; Chesson and Huntly 1997; Dial and Roughgarden 1998). Several authors had already claimed to apply the IDH to the anthropogenic disturbances exerted by agriculture, forestry and pastoral land uses as well, either from an ecological (Pickett and White 1985; Fahrig and Jonsen 1998), agroecological (Gliessman 1990) or biological conservation (Pierce 2014) viewpoint—and time has come to take this task seriously. Yet the empirical results accumulated over decades remain inconclusive, and the IDH still raises heated debates (Wilkinson 1999). Some authors are proposing its abandonment (Fox 2013), others remain strongly supporters (Huston 2014), whereas some others explain the ambiguous empirical tests by having used different indicators of biodiversity and disturbance measured at different spatial scales without taking into account the differences in biological productivity of each site (Collins and Glenn 1997; Sasaki et al 2009; Svensson et al 2012; Pierce 2014).

Many authors suggest keeping the IDH only as a general framework, and focuses in developing clearer models and more accurate tests of the underlying mechanism that may actually bring about a hump-shaped correlation of spatiotemporal disturbances with species richness (Buckling et al 2000; Sheil and Burslem 2003; Shea et al 2004; Shreeve et al 2004; Barnes et al 2006; Miller at al 2012). There is a growing consensus in pointing out at the spatial environmental variations that create opportunities for a range of dispersal colonizers, either coming from the less undisturbed patches or the survivors in disturbed ones, as the key mechanism that avoids competitive exclusion and maintains a dynamic biodiversity peak at intermediate levels of ecological disturbance. This way undisturbed patches may preserve the ‘ecological memory’ (Bengston et al 2003) needed for an adaptive response to disturbances by the species pool kept at landscape level (Shea and Chesson 2002; Loreau et al 2003; Perfecto and Vandermeer 2010). This approach stresses the spatial component of biological diversity (Tilman 1994), focuses on the interplay between disturbances and land cover diversity, and entails a significant shift towards considering the role of agroecological land management in ecosystem services provision (Tscharntke et al 2005). It also brings into light the insurance role played by the spatial heterogeneity of the land matrix to enhance the ecosystem complexity and resilience in human-dominated environments (Loreau et al 2001, 2003; Elmqvist et al 2003; Benton et al 2003).

These new approaches put foreground the interplay between patch disturbance and land cover diversity as the key mechanism that actually matters in biodiversity maintenance. They also highlight the role of agro-forest mosaics able to offer habitats to different species, and create greater amount of ecotones which provide more opportunities to other species as well (Harper et al 2005). Mainly due to the species-area relationship, much of this biological diversity is located at scales higher than plot or farm level and depends on keeping a landscape-wide variety of land covers. When high species richness is kept at landscape level thanks to land cover heterogeneity, the inevitable decrease of biological diversity in the intensively cropped patches can be compensated (Swift et al 2004). This way, a disturbance-complexity interplay leads to divergent and compensatory trends affecting α-diversity at plot scale (within-patch or within each community), β-diversity at landscape level (between-patch or between communities), and γ-diversity of the species pool hosted at regional scale (Loreau 2000; Roxburgh et al 2004; Gabriel at al 2006). The colonizing capacity of the species hosted in a well-connected mosaic that combines early and late successional niches overrides the local decrease in α-diversity as a result of local or temporal disturbances.

Therefore, the predominance of β-diversity kept by the spatial heterogeneity of a variety of intermingled land covers becomes the key mechanism of biodiversity maintenance in cultural landscapes. A recent review by Tscharnkte et al (2012) stresses that under these circumstances dissimilarity of local communities determines landscape-wide biodiversity, overrides negative local effects of habitat fragmentation, generates spillover effects through the movement of organisms and resources across habitats in all directions (Blitzer at al 2012), and stimulates the selection for distinct traits on populations which facilitates their survival in human-managed landscapes. This landscape complexity enables spatial and temporal insurance, providing higher stability and resilience of ecological processes—such as biological pest control (Bianchi et al 2006). But the effectiveness of farm management in increasing biodiversity reaches a peak at intermediate levels of landscape heterogeneity. This hump-shaped correlation of the disturbance-complexity interplay with the species richness is explained by the fact that simple landscapes tend to behave as a single monoculture poorly endowed of biological diversity, whereas highly complex ones retain great biodiversity anyway. Therefore, a wildlife-friendly agroecological matrix may enhance the overall biological diversity except when it comes to rare specialists species that require specific natural habitats with particular conservation policies.

2.2 Research approach and methods

Testing these hypotheses requires a major research effort to define the thresholds where the disturbance-complexity interplay is more effective in providing biodiversity and ecosystem services. This task has to be undertaken using concepts and methods from different disciplines like conservation biology, agroecology, landscape ecology, land use and land cover change, ecological economics or ecological modelling. It also needs deeper interdisciplinary dialogue among them from a common sustainability science standpoint that seeks solution–oriented knowledge in a participatory manner (Berkes 2007; Rindfuss et al 2008; Lang et al 2012).

Our contribution stands at the crossroads between landscape ecology, land use change, agroecology and ecological economics (Marull et al 2010). We adopt the socio-metabolic accounting of material and energy flow analysis used in ecological economics, as well as in agroecology, as a measure of anthropogenic disturbance carried out on landscape functioning (Haberl 2001; Fischer-Kowalski and Haberl 2007). Drawing on Margalef (2006), we then examine how disturbance exerted by farm systems correlate with landscape mosaics complexity and biodiversity. To this we use GIS methods of land cover and land use change (Lambin and Geist 2006; Agnoletti 2006) to calculate landscape ecology metrics and assess how spatial patterns affect ecological process (Forman 1995; Li 2000; Tischendorf 2001; Turner 2005; Turner et al 2007; Turner and Robbins 2008) which we deem to play a role in biodiversity maintenance through landscape functions (Marull and Mallarach 2005; De Groot, 2006; Marull et al 2007; Helming et al, 2007; Verburg et al 2009; Pino and Marull 2012).

Our approach adopts a comparative long-term perspective (Antrop 2006; Matthews and Selman 2006). It is known that traditional organic farm systems maintained complex land use mosaics, like those of Europe in the 19th century (Tscharntke et al 2005; Marull et al 2010), before the agricultural industrialization fuelled by cheap fossil fuels from the 1960s onwards turned them into increasingly homogeneous land covers polarized between intensive monocultures and afforestation of abandoned lands (Gerard et al 2010; Parcerisas et al 2012; Marull et al 2014). This historical land use change becomes a natural experiment that can be used for a comparative analysis of how different levels of anthropogenic disturbance, within different levels of land use complexity, relate with landscape ecology indicators (Margalef 2006).

We present a mathematical model of how landscape processes are affected by different levels of anthropogenic disturbances on ecosystems exerted when farmers alter Net Primary Production through land use change, and remove a share of it. A multi-scalar experimental design of a set of landscape units in the island of Mallorca from 1956 to 2011 is used to check it empirically. We choose Mallorca for its heritage of a complex agricultural landscape located amidst the Mediterranean biodiversity hotspot (Myers et al 2000; Blondel et al 2010; Marull et al 2015a), and because its unique abundance of historical and cartographical sources allows long-term comparative analysis. The model is tested with a dataset of wintering and breeding birds in Mallorca, following other studies that use the decrease in common farmland bird populations as an indicator of landscape-wide biodiversity loss (Farina 1997; Donald et al 2001; Heikkinen et al 2004; Sirami et al 2008; Inger et al 2014). In the next sub-sections we explain the disturbance variable used and the multi-scalar research design of the Mallorca Island. Then we present the intermediate disturbance-complexity (IDC) model applied to cultural landscapes taking resilience into account. Section three presents and discusses the results, and section four concludes.

2.2.1 Study Area

The Mallorca Island (Figure 2.1) has a total area of 3,603 km^2 of calcareous origin. The mountain range of the Serra de Tramuntana runs parallel to the North coast and reaches 1,445 meters in the highest peak. Between this and the Eastern mountains of Serres de Llevant a plain occupies most of the island. Annual precipitation ranges from 300 mm (in the South) to 1,800 mm (in the North) with an average temperature of 16°C. The vegetation combines scrubland, pines and residual oak forests with a variety of annual crops (grains and vegetables) and arboriculture (olive groves, almonds, figs, carobs, vineyards). Six agro-ecological areas can be distinguished: i) 'Tramuntana' is characterized by its hilly morphology and high precipitation (1,400-1,800 mm) and has most of the land devoted to olive groves and forest (our 3x3 km^2 site is the 'Esporles' scene); ii) 'Raiguer' is the piedmont between Serra de Tramuntana and the inland plane, whose soil, precipitation and edge condition allow intensive cropping of olive groves, vineyards and arboriculture with grains and vegetables (the 3x3 km^2 sites is 'Santa Maria' scene, and also 'Sa Pobla' characterized by watering intensification); iii) 'El Pla' is the central plane most cultivated with grains (the 3x3 km^2 'Sant Joan' scene); iv) the Eastern 'Llevant' combines small elevations with valleys that allow merging cereal cops and arboriculture with agro-forest mosaics, pastures and shrubs (with three 3x3 km^2 scenes: 'Aubocàsser', 'Calicant' and 'Marina'); v) the Southeast 'Migjorn' is characterized by water stress and barren land which largely hinder farming (the 3x3 km^2 site is 'Santanyí' scene). We use this twofold-scalar experimental design in three time points (1956, 1973 and 2000 at regional scale; 1956, 1989 and 2011 at landscape scale) based on land cover maps of Mallorca (see Marull et al 2015a):

1. Regional scale (1:50,000) takes into account the entire island divided into 3x3 km^2 cells, of which only 331 are used to avoid the sea edge effect. Biodiversity information on breeding and wintering birds have been obtained from 5x5 km^2 inland cell database, with 105 and 69 cells respectively (GOB 2008), and used to test our intermediate disturbance-complexity (IDC) model through Exploratory Factor Analysis (EFA) (Costello and Osborne 2005) using as variables the bird species richness, the spatial land pattern, the farming disturbance, and the proportion of land covers in each sample cell.

2. Landscape scale (1:5,000) takes into account eight 3x3 km^2 analysis scenes (Figure 2.1) distributed in five agro-ecological areas of Mallorca. Each scene is divided into nine 1x1 km^2 cells to better grasp the land use change. We relate the farming disturbance with the landscape dynamics captured at this scale by photo-interpretation of the three main land use changes underway: i) abandonment of arboricultural rain-fed crops (almond groves change to cereals; olives groves change to forest); ii) spontaneous afforestation ensuing

woodland abandonment (charcoal making, wood-pastures); and iii) urban sprawl (mainly tourism in coastal areas).

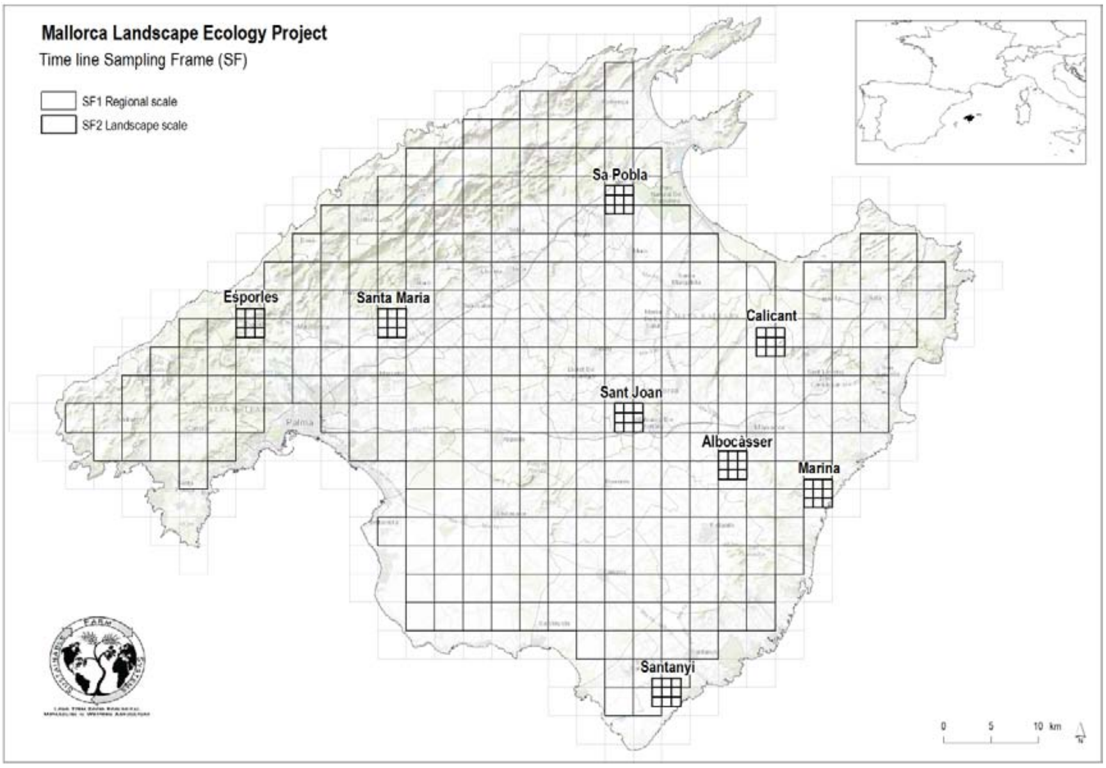

Figure 2.1: Location of the study region in the Mediterranean Sea. Two-scale experimental design: SF-1 (1:50,000); SF-2 (1:5.000).

2.2.2 The Intermediate Disturbance-Complexity Model of Cultural Landscapes

The IDC model is based on variables that describe both spatial land pattern (Shannon-Wiener index - H) and farming disturbance (Human Appropriation of Net Primary Production -$HANPP$), so as to assess how anthropogenic energy-use and land cover and land use change affect landscape ecological functioning. We work with squared cells from land unit (LU) maps, so that:

$$\sum_{i=1}^{k} p_i = 1.$$

Where p_i is the proportion of LU i in a specific cell, and k is the number of LU. We will refer to p as vector $p = (p_1, \ldots, p_k)$. In order to check the IDC with the LU diachronic maps we have first analysed the corresponding shifts in the spatial pattern of the study area, by using H that measures the equi-diversity of LU in a cell.

$$H = -\sum_{i=1}^{k} p_i \log_k p_i.$$

Where k is the total number of LU in the study area, and p_i is the proportion of LU i in a specific cell. H reaches its highest value when: $p_i = \frac{1}{k}$ for $i = 1, \ldots, k$ (i.e., all LU are equally probable). We can prove it by looking at its partial derivatives. Since $p_k = 1 - \sum_{i=1}^{k-1} p_i$, we can rewrite H as $H = -\sum_{i=1}^{k-1} p_i \log_k p_i - (1 - \sum_{i=1}^{k-1} p_i) \log_k(1 - \sum_{i=1}^{k-1} p_i)$. And $\frac{\partial H}{\partial p_j} = \log_k \left(p_j/(1 - \sum_{i=1}^{k-1} p_i) \right)$, that is equal to zero when $p_i = \frac{1}{k}$, for all $i = 1, \ldots, k$.

We use $HANPP$ as indicator of anthropogenic disturbance (Haberl et al 2004, 2007; Wrbka et al 2004; Firbank et al 2008). According to the standard $HANPP$ accountancy, NPP is the net biomass produced by autotrophic organisms over a year that constitutes the main nutritional basis for all food chains. $HANPP$ measures the extent to which farmers reduce the NPP available for other species using the following identities: $HANPP = \Delta NPP_{LU} + NPP_h$; $\Delta NPP_{LU} = NPP_0 - NPP_{act}$. Where NPP_h is the NPP appropriation through harvest, and ΔNPP_{LU} is the change of NPP through human–induced land conversion. ΔNPP_{LU} is defined as the difference between the NPP of the potential (NPP_0), and the actual (NPP_{act}) vegetation. Therefore $HANPP$ can be defined as the difference between the NPP_0 and the NPP remaining in ecosystems after harvest (NPP_t): $HANPP = NPP_0 - NPP_t$; $NPP_t = NPP_{act} - NPP_h$.

$HANPP$ has been assessed to each LU in each period. Hence, site-specific $HANPP$s are calculated multiplying a fixed coefficient (w_i) for some LU i by the surface occupied by this LU. So, $HANPP$ can be expressed as follows:

$$HANPP = \sum_{i=1}^{k} w_i p_i,$$

where w_i denote the weight of LU i. The w_i values (in tonnes of dry matter per surface and year) have been adapted from Schwarzlmüller (2009).

The result is that we have one H and $HANPP$ value for each cell and time period. We are going to analyse the relationship between H and $HANPP$ assuming two LU (i.e.,

$k = 2$) Then:

$$p_1 \in [0,1],\ p_2 = 1 - p_1,$$

$$H = -(p_1 \log_2 p_1 + p_2 \log_2 p_2),$$

$$HANPP = w_1 p_1 + w_2 p_2,$$

when $p_1 = 1$ then $H = 0$ and $HANPP = w_1$ (Figure 2.2a). Insofar as that p_1 decreases in favour of p_2, the graphic *H-HANPP* forms an arc whose peak is given by $p_1 = p_2 = 0.5$, where $H = 1$ and $HANPP = \frac{w_1 + w_2}{2}$.

Supposing three different LU ($k = 3$) we will compare LU by pairs. We can assume $p_i + p_j = 1$, and w_i, w_j their associated weights. The dispersion graphic *H-HANPP* for these values forms an arc whose maximum value is achieved when $p_i = p_j = 0.5$ and corresponds to the point $HANPP = \frac{w_i + w_j}{2}$, and:

$$H = -\frac{1}{2} \log_k 0.5 - \frac{1}{2} \log_k 0.5 = \log_3 2.$$

In Figure 2.2b, starting from the curve formed by $(p_1, p_2, p_3) = (1, 0, 1)$ we get similar but higher curves when increasing p_2 and decreasing p_1 and/or p_3, accordingly. The same occurs starting from the curves $(1, 1, 0)$ and $(0, 1, 1)$. Hence, we get the whole area in Figure 2.2b. Notice that over any weight of $HANPP$ there is a 'leg' formed by non-mosaic points (i.e., which have a predominant LU).

For $k > 3$ we obtain similar results to those in Figure 2.2b. For any $n < k$, if we have exactly n LU such that $p_i > 0$ for these n LU and $p_i = 0$ for the other $k - n$ LU, we can be sure that the corresponding figure achieves its maximum at the point $(\bar{w}, \log_k n)$, where

$$\bar{w} = \frac{1}{n} \sum_{i=1}^{n} w_i,$$

$$\log_k n = -\sum_{i=1}^{n} \frac{1}{n} \log_k \frac{1}{n}.$$

Looking at the figure *HANPP-H* it is clear that any sample data on these variables (obtained from the same LU cartographic data) must bear some relationship (Figure 2.2b). The issue is how to interpret the sample data according to the density of pair values of *HANPP-H*. We assume that Figure 2.2b draws the shape of all possible values adopted by the relationship between farming disturbance and land cover diversity, where the actual values of disturbance-complexity interplays of a given landscape can be represented.

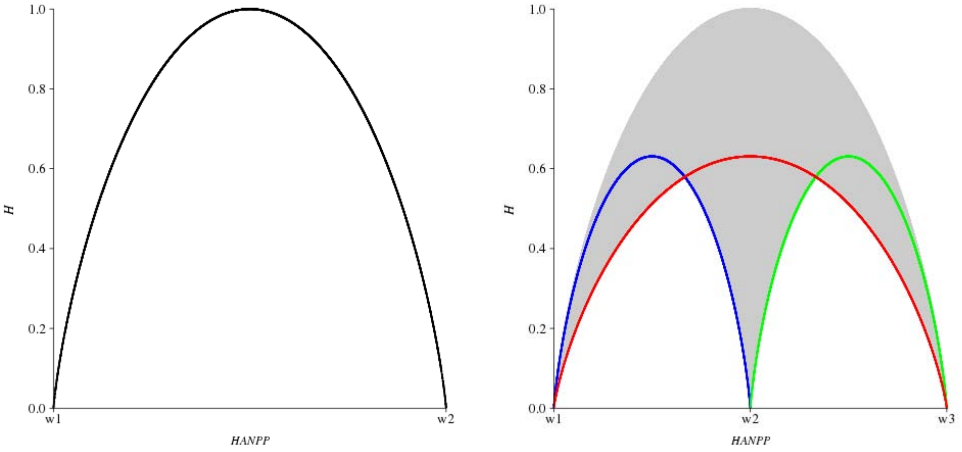

(a) Two LU (w_1, w_2). (b) Three LU (w_1, w_2, w_3).

Figure 2.2: Shannon-Wiener Index (H) - Human Appropriation of Net Primary Production ($HANPP$) theoretical dispersion graphics for two (a) and three (b) land units (LU).

2.2.3 Taking Resilience into account

Resilience is the capacity of a system to recover after disturbance (Folke 2006). As explained, our model assumes that certain levels of disturbance-complexity in an agroecological matrix may lead to an increase in ecological resilience as long as this threshold is kept. Heterogeneous land cover mosaics enhance the resistance to change of the functional landscape structure. In order to test the resilience of the system we look at the variation of $HANPP$ and H with respect to the vector p, the proportion of LU i in a specific cell (Figure 2.2). First of all we should bear in mind that $\sum\limits_{i=1}^{k} p_i = 1$, so $\sum\limits_{i=1}^{k} \Delta p_i = 0$, where Δp_i is the increase of component p_i. We have also to remind that, on the one hand $HANPP$ is a linear combination of p, so the variation of $HANPP$ is quantified directly through Δp_i and Δw_i:

$$\Delta HANPP = \sum_{i=1}^{k} (\Delta w_i \Delta p_i + \Delta w_i p_i + w_i \Delta p_i).$$

In order to measure variations of H we look at the behaviour of $\frac{\partial H}{\partial p_j}$ for each j. We have seen that H reaches its maximum at $p = (\frac{1}{k}, \ldots, \frac{1}{k})$, so $\frac{\partial H}{\partial p_j}\left(\frac{1}{k}\right)$. So, we have to study this function for values of p_j both smaller and bigger than $\frac{1}{k}$,

$$\lim_{p_j \to 0} \left| \frac{\partial H}{\partial p_j}(p_j) \right| = \infty, \quad \lim_{p_j \to 1} \left| \frac{\partial H}{\partial p_j}(p_j) \right| = \infty.$$

This implies that the variation of H for an unbalanced p (i.e., there are some $p_i < 1/k$) are greater than variations of H for a balanced p (mosaics) for the same Δp. This means that the largest vertical variations fall on small p values (i.e., when H is small). This mathematical behaviour is based on the IDC model (Figure 2.2) and can be described as resilience (i.e., the resistance of a point to be moved when it has reached low entropy values—or, conversely, high H). The opposite is observed for points with high values of entropy or lower H (i.e., great variations of entropy $-\Delta H$ allow small changes in human perturbation $-\Delta HANPP$).

To relate the value of entropy with resilience we measure the changes at each point $(HANPP, H)$ by $(\Delta HANPP, \Delta H)$ and look at the slope and magnitude of the vector linking $(HANPP, H)$ with $(HANPP + \Delta HANPP, H + \Delta H)$, to assess the change it has experienced. According to this, resilience can be measured multiplying the slope by the intensity of the movement from a time period to the next one:

$$S = \frac{\Delta H}{|\Delta HANPP| + 1}\sqrt{\Delta H^2 + \Delta HANPP^2}.$$

Where S is both the slope and the intensity of the movement between two time periods. In order to have the trend of ΔH, the absolute value of $\Delta HANPP$ is required, and a term which has been added in order to avoid dividing by zero. Consequently, resilience will be measured looking at S with respect to H. For higher values of H smaller values of S are expected, and vice versa.

2.3 Results and discussion

2.3.1 Socio-metabolic disturbance and land cover patterns (regional scale -SF1)

Figure 2.3 shows the relationship between $HANPP$ and H for data from 1x1km^2 cells at regional scale (SF-1) in the years 1956, 1973 and 2000. We have worked with a total of 10 land covers having a specific w_i for each typology and year. Land covers are divided into three categories, namely ‘semi-natural’, ‘agricultural’ and ‘urban’. Semi-natural land covers include forests (w_1), scrubs (w_2), prairie and bedrock (w_3) and wetlands (w_4). Agricultural land covers include dry cropland (w_5), irrigated cropland (w_6), rain-fed arboricultural groves (w_7), irrigated groves (w_8) and olive groves (w_9). Urban land covers (w_{10}) are both urban and industrial areas. Figure 2.3 shows that the higher point density is concentrated on agricultural land covers (mainly rain-fed groves w_7) which maintain high constant values of $HANPP$ (w_i) along the years. Similar values of H with a decrease in $HANPP$ can be observed along the period.

Three different dynamics can explain these trends seen at regional scale. First, there is a tendency to increase cells with a predominant urban use (urban sprawl), a fact that becomes apparent for 2000 where the value associated to urban areas (w_{10}) appears on the 'leg'. Second, the rain-fed groves (w_7) show a progressive decrease in $HANPP$ due to rural abandonment. Third, there appears a combination between agricultural and forest land covers in the arc connecting these two decks that becomes strongly enhanced, where transition from cropping to woodland becomes apparent.

We have to bear in mind that at regional scale (SF-1) the likelihood of finding agro-forest mosaics increases with cell size and the number of land covers we are working with. Figure 2.4a (3x3 km^2) and 2.4b (5x5 km^2) show how cell's width affects the landscape mosaic. Comparing with Figure 2.3c, it can be seen that the points of the first graph are accumulated between zero and $\log_k 2$ (vertically) and form arches similar to the ones in Figure 2.2a. Conversely, for bigger cell size (2.4a, 2.4b) the point density is closer to 1 and the central part of the graph. In addition, we can observe in Figure 2.3c that points tend to cluster on agricultural land covers (mainly w_7), while diluted densities appear on the other land covers. We infer from this that the latter mesh size is the most suitable for our study.

2.3.2 Testing the 'biodiversity assumption'

As an initial test of this IDC model on biodiversity we have used data on breeding and wintering bird communities observed in Mallorca (GOB, 2008). Considering that it is not disturbance as such but the disturbance-complexity interplay (IDC) what matters, we do

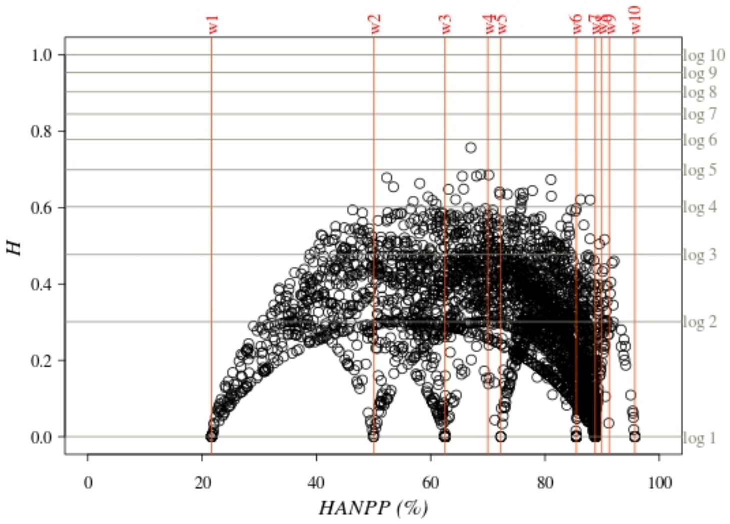

(a) 1956.

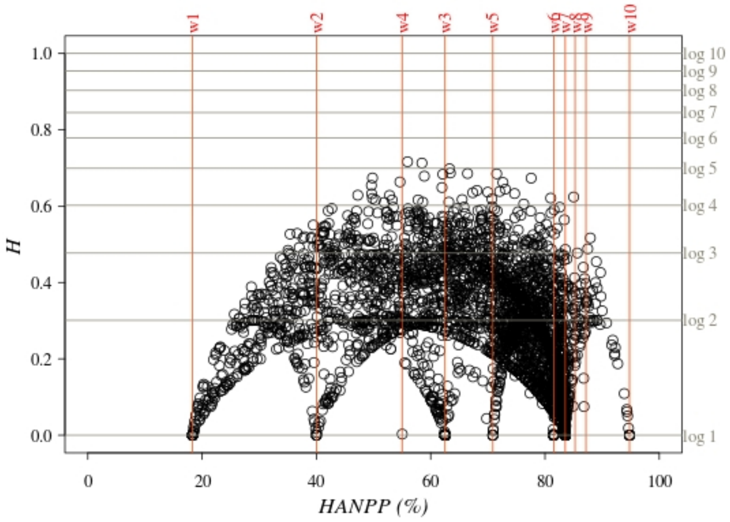

(b) 1973.

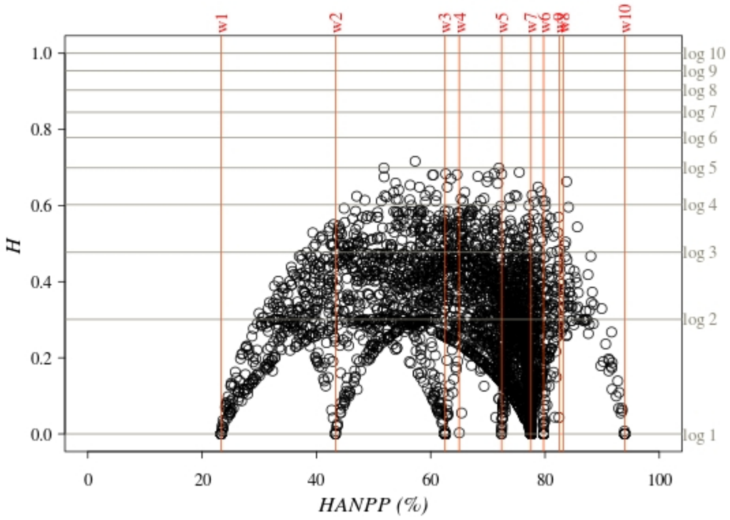

(c) 2000.

Figure 2.3: Applying the Shannon-Wiener Index (H) - Human Appropriation of Net Primary Production ($HANPP$) model to the Mallorca Land Cover Map (SF-1) at three time points (1956, 1973 and 2000; using a 1x1 km^2 sample cell scale).

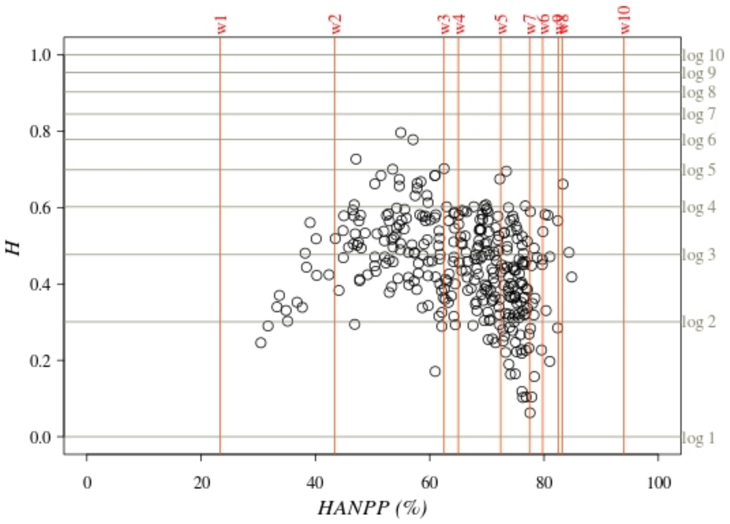

(a) 3x3 km^2 gird.

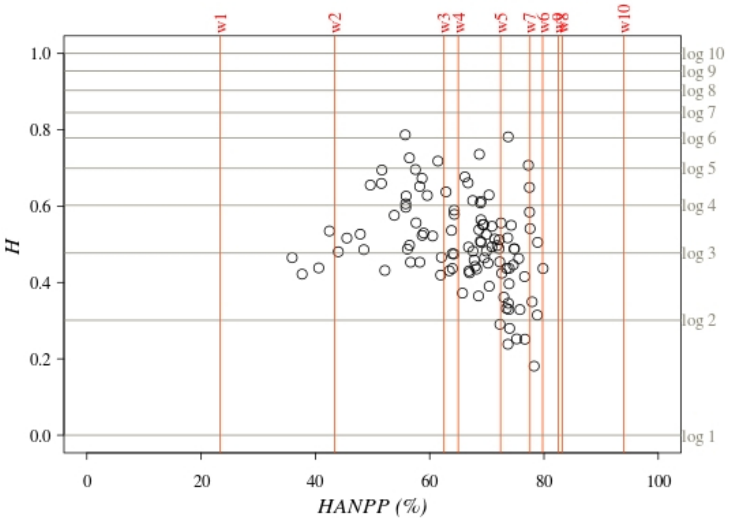

(b) 5x5 km^2 gird.

Figure 2.4: Applying the Shannon-Wiener Index (H) - Human Appropriation of Net Primary Production ($HANPP$) model to the Mallorca Land Cover Map (SF-1) at three different spatial scales (1x1 km^2 –see Figure 2.3c, 3x3 km^2 and 5x5 km^2 sample cells).

not presume a clear statistical relationship between species richness and HANNP when taken separately. Instead, we expect that it does exist between bird species richness and $HANPP$ combined with H and land covers. Exploratory Factor Analysis (EFA) allows us to identify the underlying relationships between measured variables (Darlington 1973, Costello and Osborne 2005). Two EFA have been carried out using breeding and wintering bird data separately, H and $HANPP$ values, and the proportion of land covers in each cell. Since there is a clear relationship among H and $HANPP$, as can be seen in Figures 2.3 and 2.4, we have introduced the variable $H \cdot HANPP$ that is the multiplication of H by $HANPP$, assuming that higher bird species richness for higher values of $H \cdot HANPP$ is expected.

Principal Component Analysis (PCA) is used in order to know the joint behaviour of the variables beyond strong pairwise correlations among them; we can observe how the variables are projected in each dimension and how each dimension is represented by the original variables. Tables 2.2 and 2.4 show the amount of variance of the new components. Following the Kaiser's Criterion (Kaiser, 1960) five components would be retained, since they have eigenvalue greater than 1. However, the Scree Test Criterion (Cattel, 1966) ensures us that values after component three can be passed over, because taking more values does not significantly increases the explained variance. So, three principal components have been chosen to summarize the whole variables.

Figure 2.5 shows the projection of the original variables over each dimension. PCA both for wintering and breeding birds provides arrows placed in a fairly similar way. What changes comparing the two graphs is bird data, wintering birds are better explained between the first and second component than in the case of breeding ones whose arrow is shorter. In both analyses the first component is correlated with the variable $HANPP$ and the land covers olive groves (w_9), prairie and bedrock (w_3), forest (w_1), dry cropland (w_5) and dry groves (w_7). The second component is correlated with the variable $H \cdot HANPP$ and the land covers irrigated cropland (w_6), irrigated groves (w_8), wetlands (w_4) and bird richness. In turn, the variable H is correlated with the first and the second component. Overall the variable $H \cdot HANPP$ results are really important to explain bird species richness owing to the fact that the landscape of Mallorca is mainly a rain-fed agro-ecological matrix.

These results confirm the decrease in European common farmland bird populations associated to the vanishing of heterogeneous landscapes, taken as an indicator of landscape-wide biodiversity loss (Inger et al 2014). While breeding birds are higher correlated with H which implies landscape mosaic preference, wintering birds are more correlated with $H \cdot HANPP$, wetlands (w_4), irrigated groves (w_8) and irrigated cropland (w_6) which means that they look for wet and irrigated land covers in order to find food in winter (Hawkins et al 2003).

Components	variance	percentage of variance	cumulative percentage of variance	Plot of the variance accounted by each component
comp 1	3.576	25.545	25.545	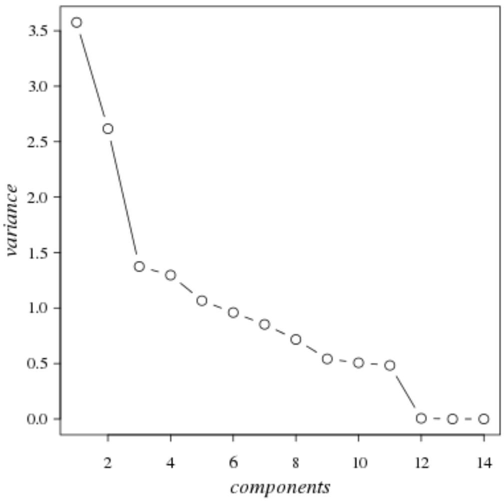
comp 2	2.617	18.689	44.234	
comp 3	1.375	9.82	54.054	
comp 4	1.297	9.266	63.321	
comp 5	1.067	7.62	70.941	
comp 6	0.96	6.858	77.799	
comp 7	0.853	6.093	83.892	
comp 8	0.717	5.121	89.013	
comp 9	0.542	3.873	92.886	
comp 10	0.507	3.622	96.507	
comp 11	0.483	3.452	99.959	
comp 12	0.006	0.041	100	
comp 13	0	0	100	
comp 14	0	0	100	

Table 2.1: Breeding bird species richness PCA

Variables	Component 1	Component 2	Component 3
B. birds	0.177	0.355	-0.485
H	0.711	0.527	0.258
$HANPP$	-0.858	0.417	0.154
$H.HANPP$	0.123	0.847	0.371
w_1 Forest	0.685	-0.397	-0.212
w_2 Scrubs	0.452	-0.087	0.113
w_3 Prairie and bedrock	0.575	-0.051	0.185
w_4 Wetlands	0.050	0.418	-0.682
w_5 Rain-fed annual crops	-0.378	0.174	0.232
w_6 Rain-fed arboriculture	-0.782	-0.321	0.013
w_7 Irrigated crops	-0.095	0.619	-0.420
w_8 Irrigated arboriculture	0.687	0.062	0.191
w_9 Olives	0.043	0.616	0.013
w_{10} Urban	-0.212	0.281	0.295

Table 2.2: Correlation matrix between original variables and rotate new components using breeding bird species.

Components	variance	percentage of variance	cumulative percentage of variance	Plot of the variance accounted by each component
comp 1	3.421	24.434	24.434	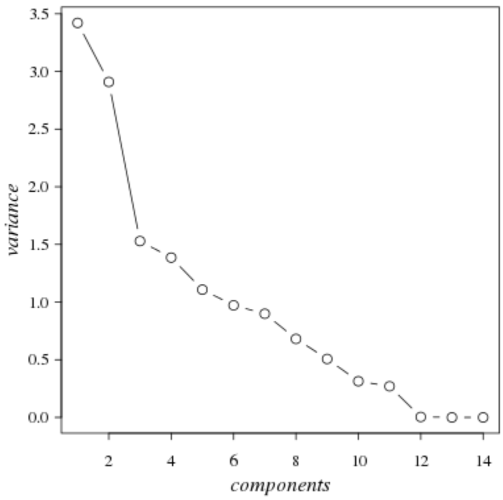
comp 2	2.909	20.776	45.211	
comp 3	1.529	10.924	56.135	
comp 4	1.386	9.898	66.033	
comp 5	1.108	7.912	73.944	
comp 6	0.972	6.945	80.889	
comp 7	0.899	6.421	87.31	
comp 8	0.681	4.867	92.177	
comp 9	0.507	3.618	95.795	
comp 10	0.314	2.246	98.041	
comp 11	0.27	1.927	99.968	
comp 12	0.004	0.031	100	
comp 13	0	0	100	
comp 14	0	0	100	

Table 2.3: Wintering bird species richness PCA

Variables	Component 1	Component 2	Component 2
W. birds	0.193	0.665	-0.526
H	0.783	0.338	0.214
$HANPP$	-0.729	0.569	0.286
$H.HANPP$	0.358	0.707	0.406
w_1 Forest	0.607	-0.485	-0.101
w_2 Scrubs	0.272	-0.27	-0.29
w_3 Prairie and bedrock	0.475	-0.129	0.165
w_4 Wetlands	0.243	0.647	-0.515
w_5 Rain-fed annual crops	-0.4	0.27	0.038
w_6 Rain-fed arboriculture	-0.878	-0.168	0.126
w_7 Irrigated crops	0.09	0.623	-0.248
w_8 Irrigated arboriculture	0.644	-0.162	0.428
w_9 Olives	0.157	0.447	0.496
w_{10} Urban	-0.081	0.265	0.255

Table 2.4: Correlation matrix between original variables and rotate new components using wintering bird species.

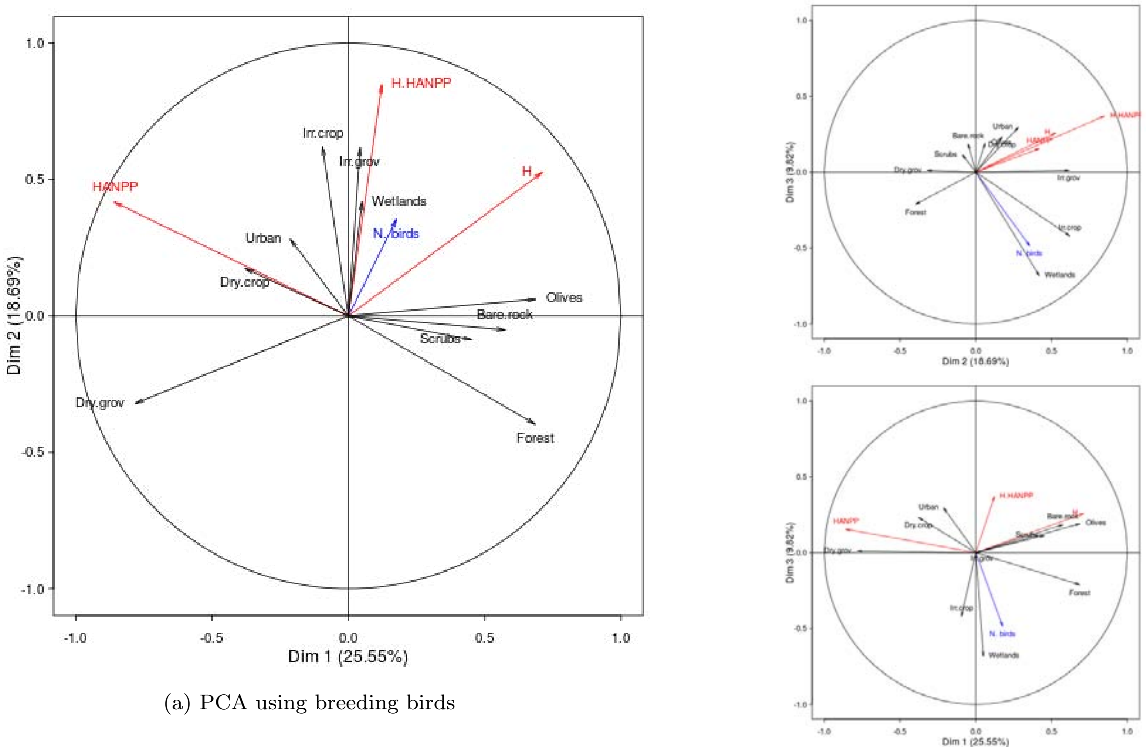

(a) PCA using breeding birds

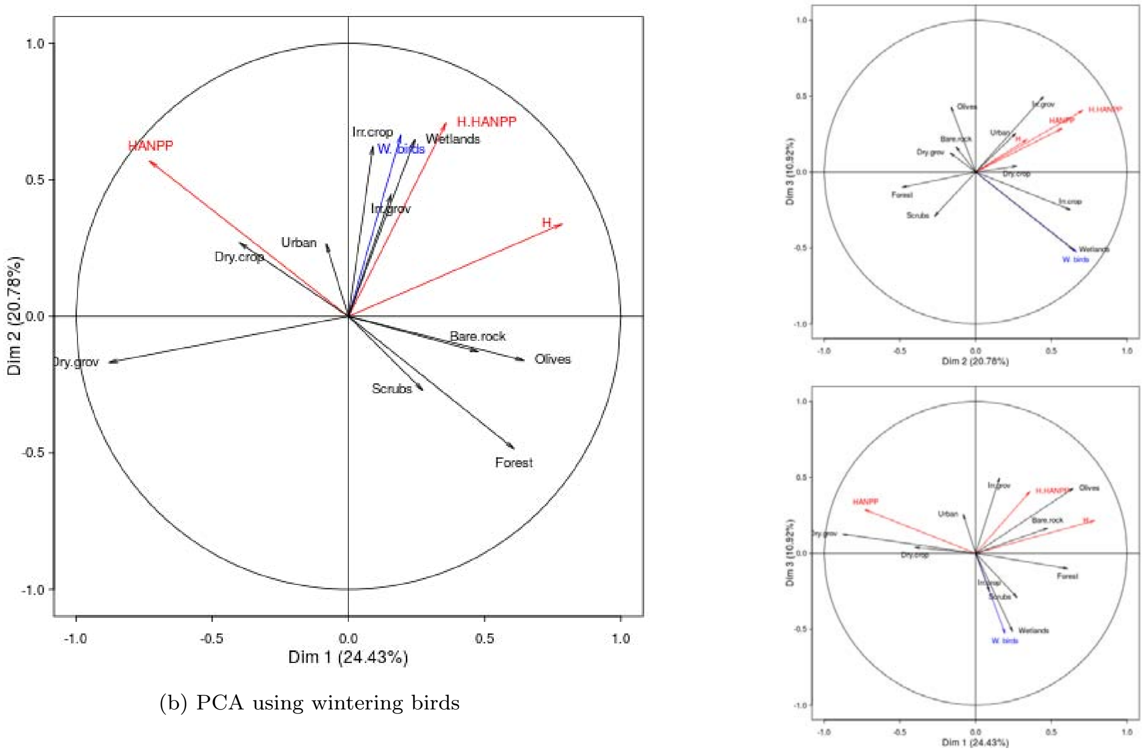

(b) PCA using wintering birds

Figure 2.5: Principal Component Analysis (PCA) applied to breeding (a) and wintering (b) bird species richness, Shannon-Wiener Index (H), Human Appropriation of Net Primary Production ($HANPP$), and land covers of Mallorca (SF-1; 5x5 km^2 sample cells).

2.3.3 Socio-metabolic change and landscape dynamics (landscape scale -SF2)

Figure 2.6 shows the results for three time points (1956, 1989, 2011) of the eight scenes at landscape scale (SF-2). For the three years we have 13 different land use types with a particular w_i. A perfect mosaic is understood as the one with $p_i = \frac{1}{n},\ i = 1, \ldots, n,\ n < k$. In 1956 possible perfect agro-forest mosaics comprise up to five land uses in a cell (the maximum value of H is $\log_k 5$) while in 1989 and 2011 the number of possible land uses in a cell increased up to seven (the maximum value of H is $\log_k 7$). This may be due to forest regrowth in abandoned cropland that became intermingled with the rest within the selected areas. In addition, it becomes apparent that rural abandonment has taken place over the years: point density shifted to the left and concentrated on agricultural or semi-natural land uses (i.e., forest w_1, shelterbelts w_2, scrubland w_3, and rain-fed groves mixed with scrubs w_4). These trends can be seen looking at the landscape scene of 'Esporles' and 'Santa Maria'.

On the whole, we can say that all areas are moving to the left, with a decrease in $HANPP$, except 'Sa Pobla' that stays fairly constant on the axis corresponding to intensive irrigated cropland w_{11} (Figure 2.6). At the same time values of H grow up due to a wider diversity of land uses, pointing at more agro-forest mosaic. Although 'Albocàsser' and 'Santanyí' practically remain at the same values, there appears to be a slight tendency towards a H increase and a $HANNP$ decrease. Similarly but stronger, a trend can be observed in the landscape scenes 'Calicant' and 'Sant Joan'. Only 'Marina' breaks off this tendency in relation to H due to a loss of land use diversity driven by tourist urbanization. We conclude from these results that the main prevailing trends in land use change in Mallorca (1956-2011) were towards rural abandonment and forest transition on the one hand, and urban development on the other.

2.3.4 Testing the 'resilience assumption'

Finally, we calculate the resilience capacity paying attention to the displacements of the points ($HANPP$, H) from 1956 to 2011, at SF-2. Figure 2.7 shows the relationship between

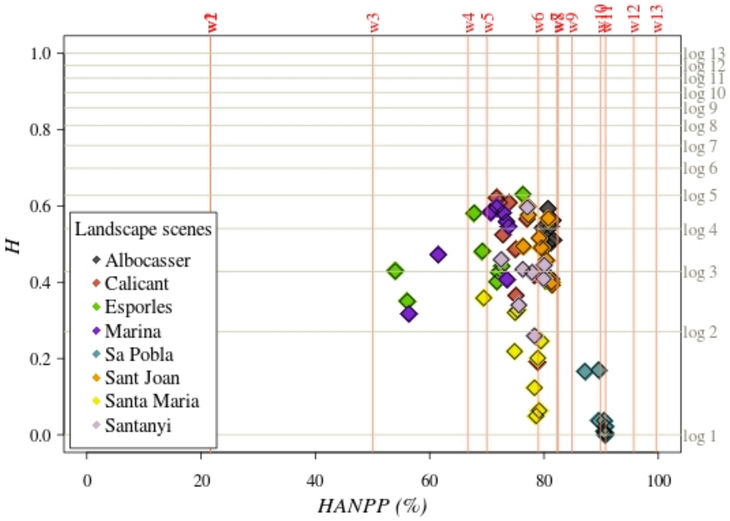

(a) 1956.

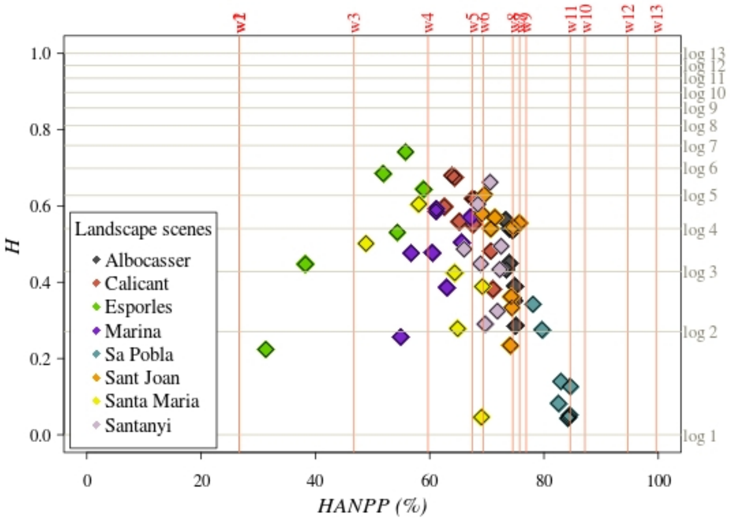

(b) 1989.

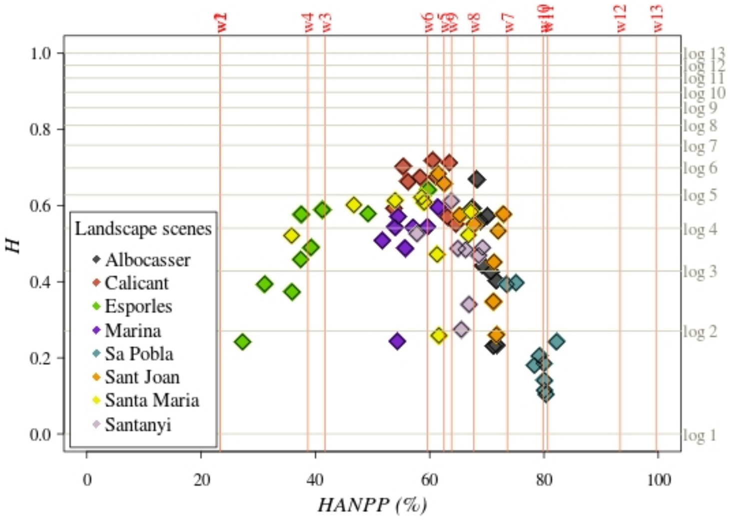

(c) 2011.

Figure 2.6: Applying the Shannon-Wiener Index (H) - Human Appropriation of Net Primary Production ($HANPP$) model to eight Mallorca Landscape Study Areas (SF-2) at three time points (1956, 1989 and 2011; using a 1x1 km^2 sample cell scale).

H_{1956}, in the vertical axis, and S in the horizontal axis, where $\Delta H = H_{2011} - H_{1956}$ and $\Delta HANPP = HANPP_{2011} - HANPP_{1956}$. For higher values of H we find a smaller slope for the vector of displacement at any point ($HANPP$, H) from 1956 to 2011, while the steepest slopes are observed for smaller values of H. These results can be interpreted as the higher socio-ecological resilience that landscape mosaics provide. A particular case is observed for the points corresponding to the scene of 'Sa Pobla', which despite having low values of H does not show large variations in slope. This is explained by the fact that 'Sa Pobla' is an intensive irrigated landscape that has evolved towards monocultures, and is strongly affected by the decrease of w associated to the main land cover (w_{11}). The same explains why there are no high variations of $\frac{\Delta H}{|\Delta HANPP|+1}$.

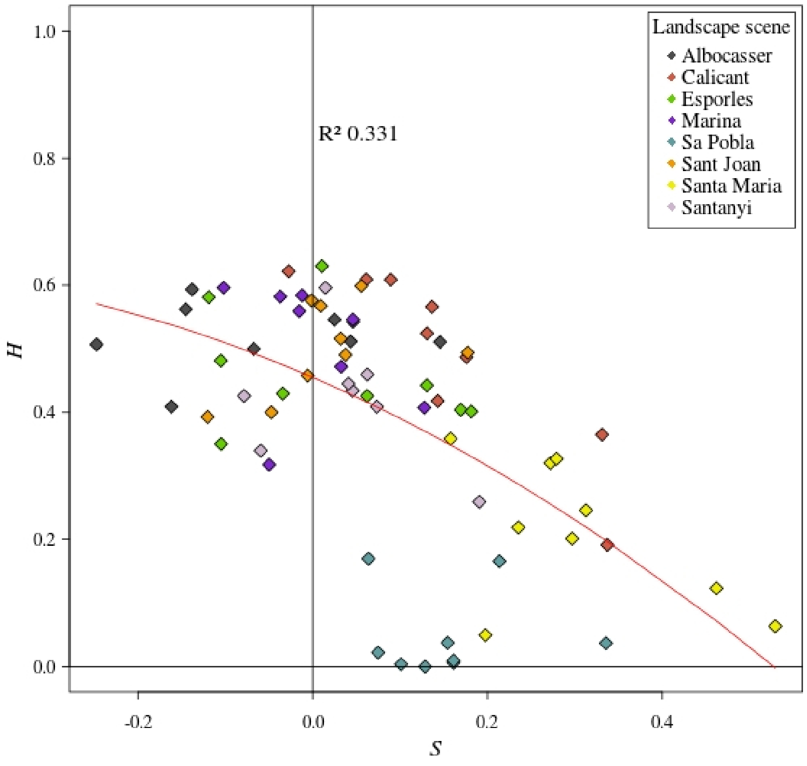

Figure 2.7: Long-term change (1956-2011) of Shannon-Wiener Index (H) and Human Appropriation of Net Primary Production ($HANPP$) in eight Mallorca Landscape Study Areas (SF-2). Resilience (inverse of S) is measured by the product of the slope of the movements from a time period to the next one (see Figure 2.6) by the intensity of the change.

In future research, when we could work with larger database, a type of quadratic curve with a maximum at $H = 0$ (i.e., decreasing when S has negative values) is expected to be found.

2.4 Conclusion

We have built a spatial-explicit model that accounts for the joint behaviour of human appropriation of photosynthetic capacity ($HANPP$), and Shannon-Wiener index (H) of land cover diversity in cultural landscapes, aimed at bringing to light the thresholds and shapes of this interplay that can enhance the biodiversity associated to a wildlife-friendly farming. The empirical results found by applying the model to Mallorca show that H peaks at intermediate-high levels of $HANPP$ —i.e. around 60%, similar to the trend obtained by Wrbka et al. (2004) when $HANPP$ is correlated with species richness in an Austrian case study. This was no surprise given the shape of all possible $HANPP$ – H values adopted in the model. The really important result is the $HANPP$ - H dynamics found when a long-term perspective is adopted. In 1956, at the very end of traditional organic farm systems existing before the onset of the Green Revolution, most land units were clustered around those intermediate levels of $HANPP$ that kept highest levels of H —except in some inner dry cereal growing areas, and in some intensively watered lands. On the contrary, in 1989 and even more in 2011, many land units were moved towards lower levels of H either in reforested and abandoned lands with much lesser levels of $HANPP$, or in intensively monocultures with stronger levels of $HANPP$. This means that the model captures the vanishing of landscape mosaics or, conversely, to what extent they are still in place. Additionally, a measure of Land Cover Land Use Change (LCLUC) resilience obtained from the model has allowed analysing the resistance to spatial change and shedding some light on how the fact of having reached low entropy levels may affect the following changes in landscape functional structure. Knowing these long-term dynamics behind current LCLUC proves to be helpful for a better biological conservation policy, particularly once biodiversity is no longer identified with wilderness.

These results point out that agro-forest mosaics still existing in Mallorca allow maintaining the kind of heterogeneous landscapes that are increasingly acknowledged as being able to keep complex ecological patterns and processes, to host great species richness, and to provide high socio-ecological resilience. They give support to the hypothesis that most of the Mediterranean biodiversity appears to be located in cultural landscapes created by traditional organic farm systems (Marull et al 2015a). Accordingly, actual species richness can be viewed as a resource for the future offered by a legacy of historically build farm systems that kept the agro-forest mosaics. Yet, these heterogeneous landscapes are currently disappearing due to industrial farm intensification, rural abandonment and urban sprawl. Our results clearly reinforce the land sharing approach that highlights the key role that a wildlife-friendly farming can play in biodiversity maintenance, at least in the Mediterranean hotspot. They also show the usefulness of transferring the concept of intermediate disturbance to the LCLUC dynamics, by using $HANPP$ and H as variables.

The $HANPP - H$ interplay has also been correlated with species richness of breeding and wintering birds, taken as a proxy of biodiversity. The statistical results obtained with an Exploratory Factor Analysis (EFA) corroborate the landscape functional structure assumption with breeding bird locations, while the wintering bird locations appear to be more linked to wetlands and irrigated cropland according to the positive correlation between biological productivity and animal species richness found in other studies (Cusens et al 2012). These preliminary statistical results highlights the need of further research, either in the relationships between $HANPP$ and H, or by using other variables that would allow higher spatial resolution, like the interplay between anthropogenic energy loops and land use complexity (Marull et al 2015b). If this energy–landscape integrated analysis prove to be consistent and fruitful, it may offer a very useful tool to make robust assessments of the impact of land management on ecological landscape functioning and help to design better land use policies.

2.5 Bibliography

[1] Agnoletti M (ed) (2006) The Conservation of Cultural Landscapes. CABI Pub, Wallingford

[2] Agnoletti, M (2014) Rural landscapes, nature conservation and culture. Some notes on research trends and management approaches from a (southern) European perspective. Landscape Urban Plan 126:66-73

[3] Altieri M. (1999) The ecological role of biodiversity in agroecosystems. Agr Ecosyst Environ 74:19-31

[4] Antrop M (2006) Sustainable landscapes: contradiction, fiction or utopia? Landscape Urban Plan 75:187-197

[5] Barnes B, Sidhu HS, Roxburgh SH (2006) A model integrating patch dynamics, competing species and the intermediate disturbance hypothesis. Ecol Model 194:414-420

[6] Bengston J, Angelstam P, Elmqvist T et al (2003) Reserves, Resilience and Dynamic Landscapes. Ambio 32(6):389-396

[7] Benton TG, Vickery JA, Wilson JD (2003) Farmland biodiversity: is habitat heterogeneity the key? Trends Ecol Evol 18:182-8

[8] Berkes F (2007) Community-based conservation in a globalized world. P Natl Acad Sci USA 104(39):15188–15193

[9] Bianchi FJJA, Booij CJH, Tscharntke T (2006) Sustainable pest regulation in agricultural landscapes: a review on landscape composition, biodiversity and natural pest control. P Roy Soc Lond B Bio 273:1715-1727

[10] Blitzer EJ, Dormann CF, Holzschuh A et al (2012) Spillover of functionally important organisms between managed and natural habitats. Agr Ecosyst Environ 146:34-43

[11] Blondel J, Aronson J, Bodiou J-Y, Boeuf G (2010) The Mediterranean region. Biological diversity though time and space. Oxford University Press, Oxford.

[12] Buckling A, Kassen R, Bell G, Rainey PB (2000) Disturbance and diversity in experimental microcosms. Nature 408:961-964

[13] Cardinale BJ, Duffy JE, Gonzalez A et al (2012) Biodiversity loss and its impact on humanity. Nature 486:59-67

[14] Cattell RB (1966) The scree test for the number of factors. Multivariate Behavioural Research 1: 245-276

[15] Chesson P, Huntly N (1997) The roles of disturbance, mortality, and stress in the dynamics of ecological communities. Am Nat 150:519-553

[16] Collins SL, Glenn SM (1997) Intermediate disturbance and its relationship to within and between-patch dynamics. New Zeal J Ecol 21(1):103-110

[17] Connell JH (1978) Diversity in Tropical Rain Forest and Coral Reefs. High diversity of trees and corals is maintained only in a nonequilibrium state. Science 199:1302-1309

[18] Costello AB, Osborne JW (2005) Best Practices in Exploratory Factor Analysis: Four Recommendations for Getting the Most From Your Analysis. Practical Assessment, Research & Evaluation 10 (7): 1-9

[19] Cusens J, Wright SD, McBride PD, Gillman LN (2012) What is the form of the productivity– animal-species-richness relationship? A critical review and meta-analysis. Ecology 93(10):2241–2252

[20] Dale VH, Efroymson RA, Kline KL (2011) The land use-climate change-energy nexus. Landscape Ecology 26:755-773

[21] Darlington RB, Weinberg SL, Walberg HJ (1973) Canonical Variate Analysis and Related Techniques. Review of Educational Research 43 (4): 433-454.

[22] De Groot R (2006) Function-analysis and valuation as a tool to assess land use conflicts in planning for sustainable, multi-functional landscapes. Landscape Urban Plan 75:175-186

[23] Dial R, Roughgarden J (1998) Theory of marine communities: the intermediate disturbance hypothesis. Ecology 79:1412-1424

[24] Donald RF, Green RE, Heath MF (2001) Agricultural intensification and the collapse of Europe's farmland bird populations. P Roy Soc Lond B Bio 268:25-29

[25] Elmqvist T, Folke C, Nyström M, Peterson G, Bengtsson J, Walker B, Norberg J (2003) Response diversity, ecosystem change, and resilience. Front Ecol Environ 1:488–494

[26] Farina A (1997) Landscape structure and breeding bird distribution in a sub-Mediterranean agroecosystem. Landscape Ecol 12:365-378

[27] Farina A (2000) The Cultural Landscape as a Model for the Integration of Ecology and Economics. BioScience 50:313-20

[28] Fahrig L, Jonsen I (1998) Effect of habitat patch characteristics on abundance and diversity of insects in an agricultural landscape. Ecosystems 1(2):197-205

[29] Firbank LG, Petit S, Smart S et al (2008) Assessing the impacts of agricultural intensification on biodiversity: a British perspective. Philos T Roy Soc B 363:777-787

[30] Fischer J, Brosi B, Daily GC et al (2008) Should agricultural policies encourage land sparing or wildlife-friendly farming? Front Ecol Environ 6(7):380-385

[31] Fischer-Kowalski M, Haberl H (eds) (2007) Socioecological Transitions and Global Change. Trajectories of Social Metabolism and Land Use. Edward Elgar, Cheltenham

[32] Folke C (2006) Resilience: The emergence of a perspective for social-ecological systems analyses. Global Environ Chang 16(3):253-267

[33] Forman RTT (1995) Some general principles of landscape and regional ecology. Landscape Ecol 10:133-142

[34] Fox WF (2013) The intermediate disturbance hypothesis should be abandoned. Trends Ecol Evol 28(2):86-92

[35] Gabriel D, Roschewitz I, Tscharntke T, Thies C (2006) Beta diversity at different spatial scales: plant communities in organic and conventional agriculture. Ecol Appl 16:2011-2021

[36] Gerard F, Petit S, Smith G, Thomson A. et al (2010) Land cover change in Europe between 1950 and 2000 determined employing aerial photography. Prog Phys Geog 34:183-205

[37] Gliessman SR (ed.) (1990) Agroecology: Researching the Ecological Basis for Sustainable Agriculture. Springer, New York

[38] GOB 2008. Atles dels Aucells Nidificants de Mallorca i Cabrera 2003-2007. Grup Balear d'Ornitologia i Defensa de la Naturalesa, Palma de Mallorca

[39] Godfray HCJ, Beddington JR, Crute IR et al (2010) Food Security: The Challenge of Feeding 9 Billion People. Science 327:812-818

[40] Gomiero T, Paoletti MG, Pimentel D (2008) Energy and environmental issues in organic and conventional agriculture. Crit Rev Plant Sci 27:239-254

[41] Green RE, Cornell SJ, Scharlemann JPW, Balmford A (2005) Farming and the Fate of Wild Nature. Science 307:550-551

[42] Haberl H. (2001) The Energetic Metabolism of Societies. Part I: Accounting Concepts. J Ind Ecol 5:107-136

[43] Haberl H, Schulz, NB, Plutzar C, et al (2004) Human appropriation of net primary production and species diversity in agricultural landscapes. Agr Ecosyst Environ 102:213-218

[44] Haberl H, Erb KH, Krausmann F et al (2007) Quantifying and mapping the human appropriation of net primary production in earth's terrestrial ecosystems. P Natl Acad Sci USA 104(34):12942-12947

[45] Harper KA, MacDonald SE, Burton PJ et al (2005) Edge Influence on Forest Structure and Composition in Fragmented Landscapes. Conserv Biol 19:768-82

[46] Hawkins BA, Field R, Cornell HV et al (2003) Energy, water, and broad-scale geographic patterns of species richness. Ecology 84(12):3105-3117

[47] Heikkinen RK, Luoto M, Virkkala R, Rainio K (2004) Effects of habitat cover, landscape structure and spatial variables on the abundance of birds in an agricultural–forest mosaic. J Appl Ecol 41:824-835

[48] Helming K, Perez-Soba M, Tabbush P (eds.) (2007) Sustainability Impact Assessment of Land Use Changes. Springer, New York

[49] Huston MA (2014) Disturbance, productivity, and species diversity: empiricism vs. logic in ecological theory. Ecology 95(9):2382-2396

[50] Inger R, Gregory R, Duffy JP et al (2014) Common European birds are declining rapidly while less abundant species' numbers are rising. Ecol Lett doi:10.1111/ele.12387

[51] Kaiser HF (1960) The application of electronic computers to factor analysis. Educational and Psychological Measurement 20: 141-151

[52] Lambin EF, Geist H (eds.) (2006) Land-use and land-cover change: local processes and global impacts. Springer, New York

[53] Lang DJ, Wiek A, Bergmann M et al (2012) Transdisciplinary research in sustainability science: practice, principles, and challenges. Sustain Sci 7(1):25-43.

[54] Li B-L (2000) Why is the holistic approach becoming so important in landscape ecology? Landscape Urban Plan 50:27-41

[55] Lindenmayer D, Cunningham S (2013) Six principles for managing forests as ecologically sustainable ecosystems. Landscape Ecology 28:1099-1110

[56] Loreau M (2000) Are communities saturated? On the relationship between α, β and γ diversity. Ecol Lett 3:73-76

[57] Loreau M, Naeem S, Inchausti P, Bengtsson J, Grime JP, Hector A, Hooper DU, Huston MA, Raffaelli D, Schmid B, Tilman D, Wardle DA (2001) Biodiversity and Ecosystem Functioning: Current Knowledge and Future Challenges. Science 294:804-808

[58] Loreau M, Mouquet N, Gonzalez A (2003) Biodiversity as spatial insurance in heterogeneous landscapes. P Natl Acad Sci USA 100(22):12765-12770

[59] Margalef R (2006) Ecological Theory and Prediction in the Study of the Interaction between Man and the Rest of Biosphere. Medi Ambient.Tecnologia i Cultura 38:114-125

[60] Marull J, Mallarach JM (2005) A new GIS methodology for assessing and predicting landscape and ecological connectivity: Applications to the Metropolitan Area of Barcelona (Catalonia, Spain). Landscape Urban Plan 71:243-262

[61] Marull J, Pino J, Mallarach JM, Cordobilla MJ (2007) A land suitability index for strategic environmental assessment in metropolitan areas. Landscape Urban Plan 81:200-212.

[62] Marull J, Pino J, Tello E, Cordobilla MJ (2010) Social metabolism, landscape change and land- use planning in the Barcelona Metropolitan Region. Land Use Policy 27:497-510

[63] Marull J, Tello E, Wilcox P et al (2014) Recovering the landscape history behind a Mediterranean edge environment (The Congost Valley, Catalonia, 1854-2005): The importance of agroforestry systems in biological conservation. Appl Geogr 54:1-17

[64] Marull J, Tello E, Fullana N et al (2015 a) Long-term socio-ecological transition at different spatial scales: Exploring the intermediate disturbance hypothesis in cultural landscapes (Mallorca, 1856-2012). Biodiversity and Conservation (in press)

[65] Marull J, Font C, Padró R et al (2015 b) Energy–Landscape Integrated Analysis: A proposal for measuring complexity in internal agro-ecosystem processes (Barcelona Metropolitan Region, 1860-2000). Ecological Modelling (submitted)

[66] Matson PA, Parton WJ, Power AG, Swift MJ (1997) Agricultural Intensification and Ecosystem Properties. Science 277:504-509

[67] Matson PA, Vitousek PM (2006) Agricultural Intensification: Will Land Spared from Farming be Land Spred for Nature? Conserv Biol 20(3):709-710

[68] Matthews R, Selman P (2006) Landscape as a focus for integrating human and environmental processes. J Agr Econ 57:199-121

[69] McDonnell MJ, Pickett STA (eds) (1993) Humans as Components of Ecosystems. The Ecology of Subtle Human Effects and Populated Areas. Springer, New York.

[70] Miller A, Reilly D, Bauman S., Shea K (2012) Interactions between frequency and size of disturbance affect competitive outcomes. Ecol Res 27:783-791

[71] Myers N, Mittermeier RA, Mittermeier CG et al (2000) Biodiversity hotspots for conservation priorities. Nature 403:853-858

[72] Padisak J (1993) The influence of different disturbance frequencies on the species richness, diversity and equitability of phytoplankton in shallow lakes. Hydrobiologia 249:135-156

[73] Parcerisas L, Marull J, Pino J et al (2012). Land use changes, landscape ecology and their socioeconomic driving forces in the Spanish Mediterranean coast (El Maresme County, 1850-2005). Environ Sci Policy 23:123-32

[74] Perfecto I, Vandermeer J (2010) The agroecological matrix as alternative to the land- sparing/agriculture intensification model. P Natl Acad Sci USA 107(13):5786-5791

[75] Phalan B, Onial M, Balmford A, Green RE (2011) Reconciling Food Production and Biodiversity Conservation: Land Sharing and Land Sparing Compared. Science 333:1289- 1291

[76] Pickett STA, White PS (1985) The Ecology of Natural Disturbance and Patch Dynamics. Academic Press, London

[77] Pierce S (2014) Implications for biodiversity conservation of the lack of consensus regarding the humped-back model of species richness and biomass production. Funct Ecol 28:253-257

[78] Pino J, Marull J (2012) Ecological networks: Are they enough for connectivity conservation? A case study in the Barcelona Metropolitan Region (NE Spain). Land Use Policy 29:684-90

[79] Reynolds CS (1995) The intermediate disturbance hypothesis and its applicability to planktonic communities. Comments on the views expressed in Padisak—vs.—Wilson. New Zeal J Ecol 19:219–225

[80] Rindfuss RR, Walsh SJ. Turner BL et al (2008) Developing a science of land change: challenges and methodological issues. P Natl Acad Sci USA 101(39):13976-13981

[81] Roxburgh SH, Shea K., Wilson JB (2004) The intermediate disturbance hypothesis, patch dynamics and mechanisms of species coexistence. Ecology 85:359-371

[82] Sasaki T, Okubo S, Okayasu T. et al (2009) Management applicability of the intermediate disturbance hypothesis across Mongolian rangeland ecosystems. Ecol Appl 19(2):423-432

[83] Schröter D, Cramer W, Leemans R. et al (2005) Ecosystem service supply and vulnerability to global change in Europe. Science 310:1333-1337

[84] Schwarzlmüller E (2009). Human appropriation of aboveground net primary production in Spain, 1955-2003: An empirical analysis of the industrialization of land use. Ecol Econ 69(2):282-291

[85] Shea K, Chesson P (2002) Community ecology theory as a framework for biological invasions. Trends Ecol Evol 17:170-176

[86] Shea K, Roxburgh SH, Rauschert ESJ (2004) Moving from pattern to process: coexistence mechanisms under intermediate disturbance regimes. Ecol Lett 7:491-508

[87] Sheil D, Burslem D (2003) Disturbing hypotheses in tropical forests. Trends Ecol Evol 18:18-26

[88] Shreeve TG, Dennis RLH, Van Dick H. (2004) Resources, habitats and metapopulations— whither reality? Oikos 106:404-408

[89] Sirami C, Brotons L, Burfield I et al (2008) Is land abandonment having an impact on biodiversity? A meta-analytical approach to bird distribution changes in the north-western Mediterranean. Biol Conserv 141(2):450-459

[90] Svensson JR, Lindegarth M, Jonsson PR, Pavia H (2012) Disturbance-diversity models: what do they really predicst and how are tested? P Roy Soc Lond B Bio 279:2163-2170

[91] Swift MJ, Izac AMN, van Noordwijk M (2004) Biodiversity and ecosystem services in agricultural landscapes—are we asking the right questions? Agr Ecosyst Environ 104(1):113-134

[92] Tilman D. (1994) Competition and Biodiversity in Spatially Structured Habitats. Ecology 75(1):2-16

[93] Tilman D, Cassman KG, Matson PA et al (2002) Agricultural sustainability and intensive production practices. Nature 418:671-677

[94] Tischendorf L (2001) Can landscape indices predict ecological processes consistently? Landscape Ecol 16:235-254

[95] Tress B, Tress G, Décamps H, d'Hauteserre AM (2001) Bridging human and natural sciences in landscape research. Landscape Urban Plan 57:137-41

[96] Tscharntke T, Klein AM, Kruess A. et al (2005) Landscape perspectives on agricultural intensification and biodiversity-ecosystem service management. Ecol Lett 8:857-874

[97] Tscharntke T, Clough Y, Wanger TC et al (2012) Global food security, biodiversity conservation and the future of agricultural intensification. Biol Conserv 151:53-59

[98] Turner MG (2005) Landscape ecology: what is the state of the science? Annu Rev Ecol Evol S 36:319-344

[99] Turner BL, Lambin EF, Reenberg A (2007) The emergence of land change science for global environmental change and sustainability. P Natl Acad Sci USA 104(52):20666-20671

[100] Turner BL, Robbins P (2008) Land-change science and political ecology: similarities, differences, and implications for sustainability science. Annu Rev Env Resour 33:295-316

[101] Turner MG, Donato DC, Romme WH (2013) Consequences of spatial heterogeneity for ecosystem services in changing forest landscapes: priorities for future research. Landscape Ecology 28:1081-1097.

[102] Van der Maarel E (1993) Some remarks on disturbance and its relations to diversity and stability. J Veg Sci 4:733-736

[103] Verburg PH, van de Steeg J, Veldkamp A, Willemen L (2009) From land cover change to land function dynamics: a major challenge to improve land characterization. J Env Manage 90:1327-1335

[104] Wilkinson DM. (1999) The Disturbing History of Intermediate Disturbance. Oikos 84(1):145- 147

[105] Wilson JB (1994) The 'intermediate disturbance hypothesis' of species coexistence is based in on patch dynamics. New Zeal J Ecol 18:176-181

[106] Wrbka T, Erb K-H, Schulz NB et al (2004) Linking pattern and process in cultural landscapes. An empirical study based on spatially explicit indicators. Land Use Policy 21:289-306

[107] Wu JG (2013) Landscape sustainability science: ecosystem services and human well-being in changing landscapes. Landscape Ecology 28:999-1023.

Chapter 3

Relating landscape patterns and Human Appropriation of Net Primary Production from Land cover Data[1]

3.1 Introduction

The Net Primary Production (NPP) is the net amount of solar energy converted to plant organic matter through photosynthesis. The Human Appropriation of Net Primary Production (HANPP, see, for instance, [20], [11], [10]) is an indicator of the alterations produced by human activity on the NPP. These alterations include the degradation of the environment (which leads to differentiate between the potential NPP and the actual NPP) and the harvesting of photosynthetic products, which further reduces the actual NPP to a quantity sometimes denoted NPP_t. Thus, $\mathrm{HANPP} = \mathrm{NPP}_{pot} - \mathrm{NPP}_t$.

It is customary to measure the human appropriation as a percentage of the potential primary production: $\mathrm{HANPP\%} = 100 \times \mathrm{HANPP}/\mathrm{NPP}_{pot}$. One way to approximate the HANPP% of a given area is to assign a coefficient w_i to each of the n different land covers present in the area and compute the weighted average

$$\mathrm{HANPP\%} = \sum_{i=1}^{n} w_i p_i \ , \tag{3.1}$$

---

[1] This work has been done by Carme Font, Mercè Farré and Aureli Alabert

where p_i are the proportion of land devoted to each use. The weights w_i indicate the percentage of human appropriation for each specific land cover. We will speak more generally of *land covers* (forest, wetlands, crop, etc).

Ideally, we would like to relate human appropriation of NPP with some measure of the biodiversity in a given agroecosystem, in order to assess how human activity affects other species.

According to the so-called *species-energy hypothesis* (see e.g. the survey by Currie et al. [5] of this and other hypotheses, and the references therein), the richness on species is increasing as a function of the available energy in the system. This would explain, for example, the richness gradient from the poles to the tropics, as the energy provided by the sun is greater at lower latitudes.

At geographical (large) scales, it has been suggested that this is true at all energy levels, although there is still little empirical evidence in this generality. At local scales this is not at all clear, and Gaston [7], among others, suggests that "there is a marked tendency for a general hump-shaped relationship between species richness and available energy". In other words, that whereas when the available energy goes from low to moderate levels, richness indeed increase, from moderate to high levels the relation is reversed.

In terms of HANPP, which represents energy that humans take out of the natural system, Gaston's remark amounts to say that biodiversity, as a function of HANPP, increases at the beginning, peaks at a certain point, and then decrease again when HANPP is high. The empirical work of Haberl et al. [11], who measured the number of species for 9 families (vegetal and animal), on 38 small Austrian regions of similar characteristics, confirms that above 40-50% of total possible HANPP, species richness indeed decreases, and there are no data below these percentages. The authors adjust a linear decreasing relationship, although graphically the decrease seems to be more "concave" than linear in most cases.

The possibility that low values of HANPP lead to diversity values below the maximum seems to be related to the so-called *Intermediate Disturbance Hypotheses* (IDH), which states that moderate disturbances or fluctuations of any kind in an environment lead to more diversity than strong or weak disruptions. It should be remarked that IDH is controversial, as it is the species-energy hypothesis. For instance, the recent review article by Fox [6] is clearly against. In any case, the intermediate disturbance in natural systems should be understood as punctual interventions or catastrophes, whereas in an agro-cultural system it is the result of the continuous human intervention.

Numerous studies haven been done relating landscape heterogeneity with biodiversity. Tews et al. [18] contains a large review of articles on this subject; in most of them it is concluded that landscape diversity is positively correlated with species diversity.

It has been said in [19] that a high degree of biodiversity underlies in heterogeneous and well connected landscapes. So, we use Shannon index to measure landscape heterogeneity,

$$H = -\sum_{i=1}^{n} p_i \log p_i \tag{3.2}$$

The entropy H of (3.2) is in fact an indicator of the degree of mosaic structure of the use of a piece of land. It is not directly a measure of biodiversity. Marull et al [16] use a combination of H and the Ecological Connectivity Index to model biodiversity in cultural landscapes. In this sense, it is only one of the components of the landscape functionality that we are relating to HANPP.

3.1.1 Methodology Approach

In this chapter we try to relate human appropriation of net primary production as defined by (3.1) with the Shannon entropy index given by (3.2)

Both are functions of the land proportions p_i in a terrain cell, but we would like somehow to obtain a “function” yielding H from the appropriation alone, to assess the influence of humans in the potential biodiversity (approximated by the diversity of land covers). In the sequel we will denote the HANPP% measure defined in (3.1) simply by A in the formulae, and speak of (human) *Appropriation.*

The entropy H is not really a function of A because the same value of the appropriation may correspond to many values of the entropy, and vice-versa. We propose the following setup:

On a given terrain cell ω, the different land covers may appear in certain proportions $0 \leq p_i(\omega) \leq 1$. Suppose we observe a big number of such cells, while we are applying a fixed set of coefficients $w_1, \ldots, w_n$ to all of them.

Then, cell ω has a certain appropriation $A(\omega)$ and a certain entropy $H(\omega)$. We may think that ω is a random parameter, so that $p_i(\omega)$ are random proportions and also $A(\omega)$ and $H(\omega)$ are random. We would like to describe the probability distribution of H given a certain value $A(\omega) = a$ of the appropriation, for every possible a. It is therefore the probability distribution of H which is a function of A.

3.1.2 Case study

Our case study is *Mallorca*, a Mediterranean island with a total area of 3,603 km^2 of calcareous origin. The mountain range of *Serra de Tramuntana* runs parallel to the North coast and reaches 1,445 metres in the highest peak. Between this and the eastern mountains of *Serres de Llevant*, a plain occupies most of the island. Annual precipitation ranges from 300 mm (in the South) to 1,800 mm (in the North) with an average temperature of 16 °C. We work with land cover data based on land cover maps of Mallorca (figure 3.1) obtained from [8] at regional scale (1:50,000) for three time periods (1956, 1973, 2000). These data comprises a total of 3360 cells of size 1×1 km^2, once disregarded those with some part into the sea.

We have grouped land covers into four categories, namely 'semi-natural', 'croplands', 'groves' and 'urban'. Semi-natural land covers include forest, scrub, prairie and bedrock, and wetlands. Croplands land covers include both dry and irrigated croplands. Groves are composed of rain-fed arboricultural groves, irrigated groves and olive groves. Urban land covers are both urban and industrial areas.

3.1.3 Plan of the chapter

As already mentioned, our aim is to relate the Shannon entropy H, as an index of landscape patterns, with the appropriation A. The methodology proposed here can also be used with

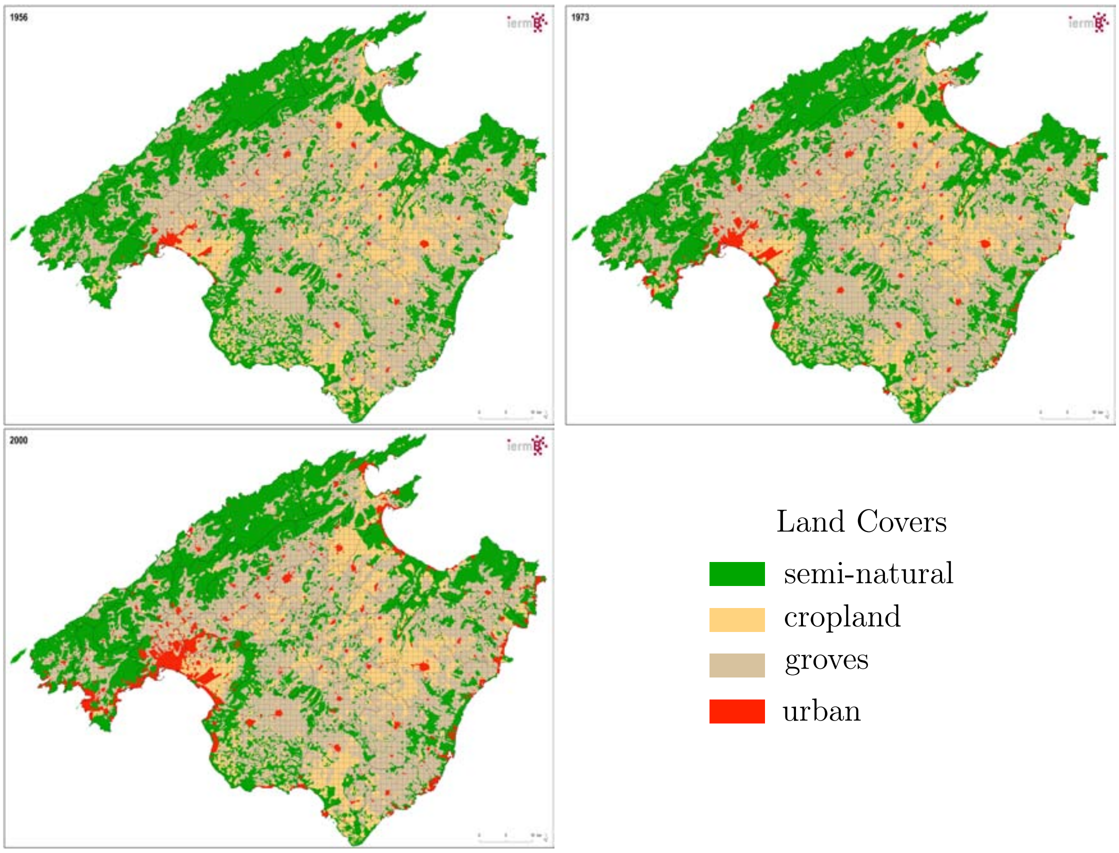

Figure 3.1: Mallorca land cover maps at regional scale (1:50,000) for 1956, 1973 and 2000. Source: from [8] in collaboration with the Barcelona Institute of Regional and Metropolitan Studies.

the other landscape metrics (or with other functions of land cover proportions). The human appropriation is either a random variable whose distribution is determined by a given theoretical distribution of land covers (case treated in Section 3.2), or a function of empirically obtained data (case of Section 3.3, with our case study in mind).

In Section 3.2, we assume a simple uniform probability distribution of proportions of land covers and

a) show how to deduce (by simulation) the distribution of the entropy H, and to compute exactly its expected value;

b) compute the distribution of the appropriation A and its expectation; and

c) deduce a formula for the expectation of H for any given fixed value of the appropriation.

In Section 3.3, we estimate the conditional expectation of H given A using real sample data. This involves estimating the probability distribution from which the data has been (ideally) originated, and produce a very large sample following the estimated distribution. The process has some difficulties which are explained at the beginning of the section, and developed in several subsections.

Finally, some specific data-related details and the results of the case study are presented in Section 3.4.

3.2 Uniform distribution of land covers

Given a set of cells Ω, and a set of $n+1$ possible land covers, we have defined the appropriation and Shannon indices of each cell $\omega \in \Omega$, by

$$\begin{aligned} A(\omega) &= \sum_{i=1}^{n+1} w_i p_i(\omega) \\ H(\omega) &= -\sum_{i=1}^{n+1} p_i(\omega) \log_{n+1} p_i(\omega) \end{aligned} \tag{3.3}$$

where $p_i(\omega)$ is the proportion of cover i in cell ω, and we arbitrarily take $n+1$ as the base of the logarithm, so that the maximal value that H can achieve is normalised to 1. Working in dimension $n+1$ instead of n simplifies the notation later.

We study the relation between these two quantities by postulating some probability distribution of the random vector $p(\omega) = \big(p_1(\omega), \dots, p_n(\omega)\big)$. Notice that this vector takes values on the so-called *standard n-simplex in $\mathbb{R}^{n+1}$*, i.e. the n-dimensional surface

$$\Delta = \{(p_1, \dots, p_{n+1}) \mid p_i \geq 0,\ p_1 + \dots + p_{n+1} = 1\} \ .$$

We are thus working with *compositional data* (see e.g. [2]).

In this section we will assume that p follows the uniform distribution on the simplex. In particular, this assumption implies that all covers are actually present in all cells, but otherwise it is a natural choice if no other information is present, and it is invariant by permutations of the indices.

The volume of the standard n-simplex is $\frac{\sqrt{n+1}}{n!}$, whence the density of the uniform distribution is given by

$$f(p_1, \ldots, p_{n+1}) = \begin{cases} \frac{n!}{\sqrt{n+1}} & \text{if } p \in \Delta \\ 0 & \text{otherwise .} \end{cases}$$

The marginal distribution of the first n coordinates is also uniform, on the projected simplex

$$\Delta' = \{(p_1, \ldots, p_n) \mid p_i \geq 0,\ p_1 + \ldots + p_n \leq 1\} \ ,$$

with the density

$$f(p_1, \ldots, p_n) = \begin{cases} n! & \text{if } p \in \Delta' \\ 0 & \text{otherwise .} \end{cases}$$

We can easily obtain the marginal density function of p_i integrating f with respect to p_j, $j \neq i$. For p_1,

$$\begin{aligned} f(p_1) &= n! \int_0^{1-p_1} \ldots \int_0^{1-\sum_{i=0}^{n-1} p_i} dp_n \ldots dp_2 \\ &= n(1-p_1)^{n-1}. \end{aligned} \tag{3.4}$$

Since p_1, $\ldots$, p_n are identically distributed, we have an analogous formula for all p_i.

It is better to work in the projected simplex, since f is then a true density with respect to Lebesgue measure in $\mathbb{R}^n$, whereas on the standard simplex the support of the probability has zero measure as a subset of $\mathbb{R}^{n+1}$. We will in general avoid to write explicitly the random parameter ω from which the land covers depend.

In the next subsections we study the probability distribution of the random variables H and A, and the conditional expectation of H given A.

3.2.1 The distribution of H

It is not possible to find analytically the probability distribution of H from the law of p. However it is trivial to generate random samples of p according to the uniform distribution

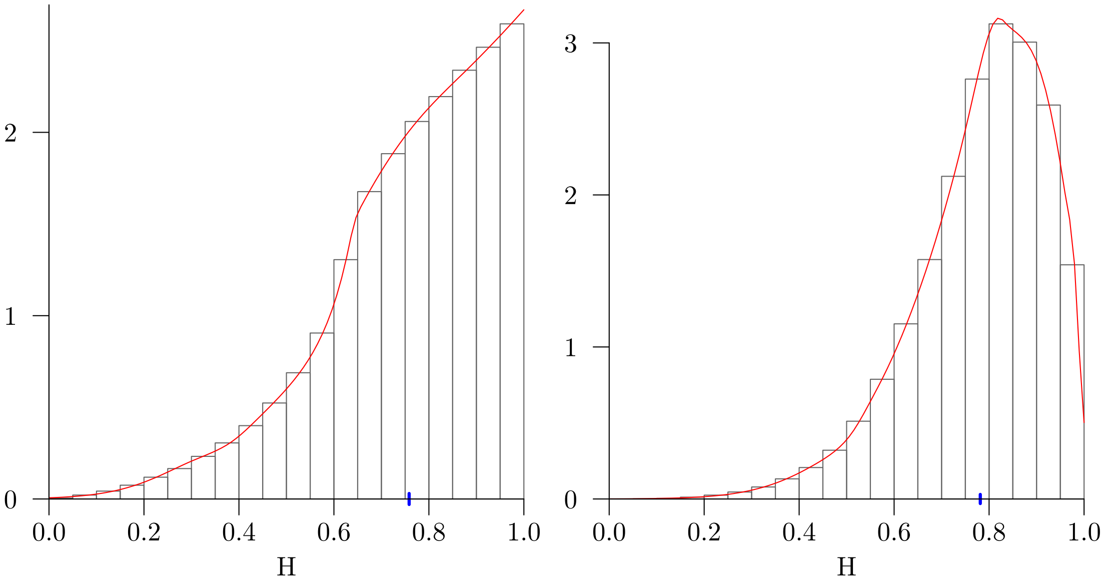

(a) With 3 land covers

(b) With 4 land covers

Figure 3.2: Histogram and density approximation for the random Shannon index H with 3 and 4 land covers. The blue line corresponds to the mean of the sample data. H has been calculated from a simulated uniform sample of p of size 10^6.

on the simplex and draw a histogram of values of H using (3.3). In Figure 3.2, we show such histograms for 3 and 4 land covers, with a sample size of one million. We have also added to the Figure an estimation of the density function of H and the position of the sample mean.

The density estimation has been carried out using the logsplines method implemented in the R package `logspline` [12]. The usual kernel methods to estimate densities are not suitable here because H is a bounded random variable.

The base uniform sample on the simplex has been generated using the algorithm explained in [17]: If $Y_1, \ldots, Y_{n+1}$ are independent unit-exponential random variables, and

$$E_i = \frac{Y_i}{\sum_{j=1}^{n+1} Y_j} \ , \tag{3.5}$$

then the random vector $(E_1, \ldots, E_{n+1})$ is uniformly distributed on Δ.

In fact, one does not need to estimate the theoretical mean of the distribution of H by simulation, since it can be computed exactly. Indeed, the integral of $x \log_{n+1} x$ against the density (3.4), yields

$$\frac{-1}{\ln(n+1)} \left[\frac{\Psi(n+1) + \gamma - 1}{n+1} + \frac{1}{(n+1)^2} \right] ,$$

where Ψ is the digamma function, and γ is Euler's constant. Therefore, the expectation of the Shannon index H of (3.3), under the hypothesis of uniform distribution of the proportions p_i in the simplex, can be represented as

$$\mathrm{E}[H] = \frac{1}{\ln(n+1)}\left[\Psi(n+1)+\gamma-1+\frac{1}{n+1}\right] .$$

This expectation tends to 1 as $n \to \infty$, as it is easily seen from the inequalities $\ln n \leq \Psi(n+1) \leq \ln(n+1)$.

3.2.2 The distribution of A

For A it is possible, on the contrary, to deduce an analytical formula for its probability distribution, because it is a simple linear function of the proportions p.

Without loss of generality, assume that the vector of weights $w = (w_1, \ldots, w_{n+1})$ is sorted: $0 < w_1 < \ldots < w_{n+1}$. We can write

$$\begin{aligned} A &= \sum_{i=1}^{n} w_i p_i + w_{n+1}\Big(1 - \sum_{i=1}^{n} p_i\Big) \\ &= w_{n+1} - \sum_{i=1}^{n}(w_{n+1} - w_i)p_i \\ &= w_{n+1} - \sum_{i=1}^{n} s_i p_i, \end{aligned}$$

where $s_i := w_{n+1} - w_i$, and clearly $0 < s_n < s_{n-1} < \ldots < s_1 < w_{n+1}$.

We want to compute the distribution of A when p is uniform on Δ'. Let us compute first the probability density of $\sum_{i=1}^{n} s_i p_i = w_{n+1} - A$. We use a change of variable by means of the bijective linear transformation $T\colon \Delta' \longrightarrow B \subset \mathbb{R}^n$ given by

$$\begin{cases} v_1 = \sum_{i=1}^{n} s_i p_i \\ v_j = s_j p_j\ , \quad j = 2, \ldots, n \end{cases}$$

where

$$B = \left\{ v \in \mathbb{R}^n : \ \sum_{i=1}^{n} \frac{v_i}{s_i} - \sum_{i=2}^{n} \frac{v_i}{s_1} \leq 1,\ \sum_{i=2}^{n} v_i \leq v_1,\ v_i \geq 0 \text{ for } i > 1 \right\} ,$$

as can be easily checked.

The inverse mapping $T^{-1}\colon B \longrightarrow \Delta'$ is defined by

$$\begin{cases} p_1 = \frac{1}{s_1}\left(v_1 - \sum_{i=2}^{n} v_i\right) \\ p_j = s_j v_j \ , \quad j = 2, \ldots, n \end{cases}$$

with Jacobian determinant equal to $\prod_{i=1}^{n} \frac{1}{s_i}$.

Therefore, the density of the vector $v = (v_1, \ldots, v_n)$ is given by

$$f(v_1, \ldots, v_n) = \begin{cases} n! \prod_{i=1}^{n} \frac{1}{s_i} & \text{if } v \in B \\ 0 & \text{otherwise .} \end{cases} \tag{3.6}$$

To obtain the density of v_1, we integrate (3.6) with respect to $v_2, \ldots, v_n$. For fixed $v_1, \ldots, v_{k-1}$, the variable v_k ranges from 0 to m_k, with

$$m_k = \min\left\{ v_1 - \sum_{i=2}^{k-1} v_i, \ \frac{s_1 s_k}{s_1 - s_k}\left(1 - \frac{v_1}{s_1} - \sum_{i=2}^{k-1} v_i \frac{s_1 - s_i}{s_1 s_i}\right) \right\} .$$

Hence,

$$f(v_1) = \int_0^{m_2} \cdots \int_0^{m_n} n! \prod_{i=1}^{n} \frac{1}{s_i} \, dv_n \cdots dv_2 \ ,$$

which can be exactly computed for given values of $s_1, \ldots, s_n$.

Finally, the density function of A is simply

$$f_A(a) = \begin{cases} f(w_{n+1} - a) & \text{if } a \in [w_1, w_{n+1}] \\ 0 & \text{otherwise .} \end{cases}$$

The graph of this function of a is depicted in Figure 3.3 for three and four land covers and some given values of w.

The expected value of A is easily computed using (3.4) directly, or reasoned by symmetry:

$$E[A] = \sum_{i=1}^{n+1} \frac{w_i}{n+1}.$$

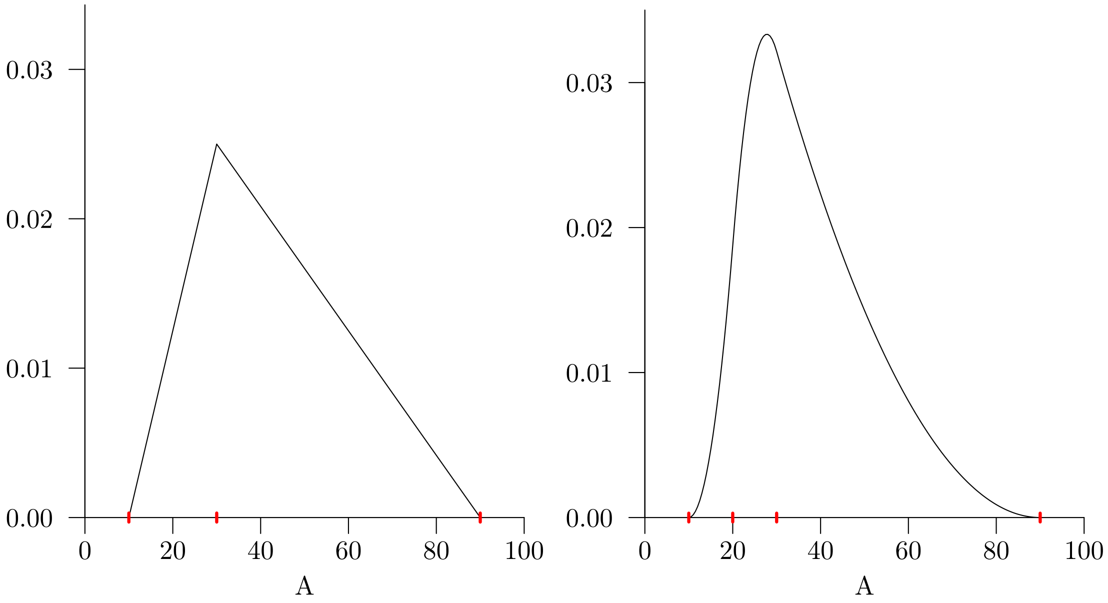

(a) With 3 land covers and $w = (10, 30, 90)$

(b) With 4 land covers and $w = (10, 20, 30, 90)$

Figure 3.3: Density of the appropriation A for 3 and 4 land covers, and for a particular vector of weights w, with values indicated by the red marks.

3.2.3 Expected value of H for a given appropriation

We show in this subsection that a closed formula can be derived for the expected value of the Shannon index H for a given level of appropriation A. Specifically, we want to compute the function

$$a \mapsto E[H \mid A = a] \tag{3.7}$$

Since both H and A are functions of the vector of land covers $p = (p_1, \ldots, p_n) \in \Delta'$, the conditional expectation can be computed by means of the conditional law of p given $A(p) = a$.

Lemma. *Let $X = (X_1, \ldots, X_n)$ be a random vector following a continuous uniform distribution with support on a set Borel set $\Gamma \subset \mathbb{R}^n$ and let $Y := \alpha_0 + \alpha_1 X_1 + \cdots + \alpha_n X_n$, for some constants $\alpha_i \in \mathbb{R}$.*

Then, the conditional distribution of X given $\{Y = a\}$ is uniform in $\mathbb{R}^{n-1}$ with support on the intersection $I_a := \Gamma \cap \{\alpha_0 + \alpha_1 x_1 + \cdots + \alpha_n x_n = a\}$, for almost all a with respect to the law of Y.

The fact stated in the lemma seems intuitive and it is indeed straightforward to prove. Notice, however, that the fact that $\{\alpha_0 + \alpha_1 x_1 + \cdots + \alpha_n x_n = a\}$ is a bundle of parallel lines is crucial, and that the result does not say anything about a particular value a, but should be understood with respect to the set of values a as a whole.

We apply the lemma to $X = (p_1, \ldots, p_n)$, $\Gamma = \Delta'$, and $Y = A = w_{n+1} - \sum_{i=1}^{n}(w_{n+1} - w_i)p_i$.

The intersection of the simplex Δ' with the line $\{A = a\}$ is given by

$$I_a = \{(p_1, \ldots, p_{n-1}) \in \mathbb{R}^{n-1} : \ m_{k,a} \leq p_k \leq M_{k,a}, \ \forall k\} \ ,$$

where

$$m_{k,a} := \max\left\{0, \frac{w_{k+1} - a - \sum\limits_{i=1}^{k-1}(w_{k+1} - w_i)p_i}{w_{k+1} - w_k}\right\}$$

$$M_{k,a} := \frac{w_{n+1} - a - \sum\limits_{i=1}^{k-1}(w_{n+1} - w_i)p_i}{w_{n+1} - w_k} \ .$$

Taking into account that, on I_a, we can write p_n and p_{n-1} as a function of the other coordinates, namely,

$$p_n = \frac{w_{n+1} - a - \sum_{i=1}^{n-1}(w_{n+1} - w_i)p_i}{w_{n+1} - w_n}$$

and

$$p_{n+1} = 1 - \sum_{i=1}^{n} p_i = \frac{a - w_n + \sum_{i=1}^{n-1} p_i(w_n - w_i)}{w_{n+1} - w_n} \ ,$$

we have that the conditional expectation (3.7) is in fact a function of $n-1$ coordinates of p, and can be expressed as

$$E[H \mid A = a] = \int_{I_a} C_a^{-1}\Big[- \textstyle\sum_{i=1}^{n+1} p_i \log_{n+1} p_i\Big] \, dp \ ,$$

where

$$C_a := \int_{m_{1,a}}^{M_{1,a}} \cdots \int_{m_{n-1,a}}^{M_{n-1,a}} dp_{n-1} \cdots dp_1$$

is the volume of I_a.

The integral can be computed exactly as a piecewise function that depends on the value of a. The result is given in Figures 3.4 i 3.5, for $n+1 = 3$ and $n+1 = 4$ and two sets of weights w. In all cases and dimensions the function (3.7) is continuous, piecewise concave, and non-smooth at the points w_i.

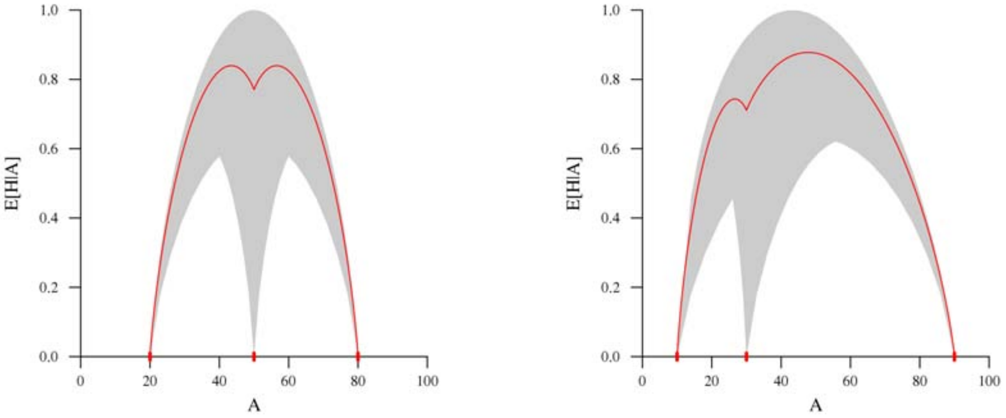

(a) With weights $w = (20, 50, 80)$

(b) With weights $w = (10, 30, 90)$

Figure 3.4: The red curve is the expected value of the Shannon index H as a function of the human appropriation A, for $n+1 = 3$ covers. The shaded area corresponds to the set of possible pairs of values (A, H), and has been drawn by simulating one million points from their joint probability distribution, for uniform p.

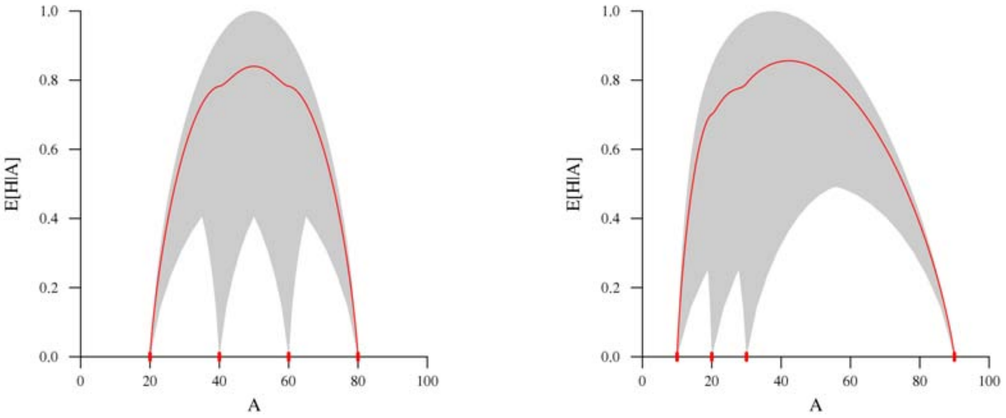

(a) With weights $w = (20, 40, 60, 80)$

(b) With weights $w = (10, 20, 30, 90)$

Figure 3.5: The analogues of Fig. 3.4 for $n+1 = 4$ covers. Note that the set of possible points and the conditional expectation curves are symmetrical when the weights are equally spaced.

3.3 Shannon index and appropriation with real data

For the sake of simplicity we change $n + 1$ to n and hereinafter the simplex will be

$$\Delta = \{(p_1, \ldots, p_n) \mid p_i \geq 0,\ p_1 + \cdots + p_n = 1\} \ .$$

Given a wide region, divided in small cells, the proportion of land covers in each cell will rarely be well represented by the uniform distribution. Not only some land covers can take more surface than others in the region, but also not all covers will be present in all cells.

To apply the method of the previous section with sample data, we need first to estimate from the data the probability distribution of land covers for the target region.

Then, a large sample will be drawn from that distribution, and the conditional expectation $E[H \mid A = a]$ will be estimated from that sample. The analytical exact computation is of course no longer possible, since there is no a closed analytical expression for the distribution of A, unlike the uniform case. However, the estimated distribution of the proportions p allows to simulate as many values of H and A as desired, and these in turn allow to approximate $\mathrm{E}[H \mid A = a]$. The quality of the result depends on the quality of the estimation of the distribution of p and the number of simulations used.

This programme has some difficulties, that will be addressed in different subsections below. First, we develop the estimation of a density on a simplex by means of Dirichlet kernels. (Another option is to employ the log-ratios $y_i = \log(p_i/p_{n+1})$, see [1], or symmetric and isometric log-ratios, see [3], and then use kernels with unbounded domain, but these methods have serious drawbacks with samples whose points can very well be on the boundary of the simplex, as is in our case.) This estimation has numerical difficulties, that we solve in the second subsection. Next, we consider the global sampling strategy, taking into account the many points that lie in the facets of the simplex, which are themselves simplices of lower dimensions. Finally, we explain our procedure to choose the bandwidth parameter of the kernels, which was a detail postponed from the first subsection.

3.3.1 Kernel density estimation on the simplex

The estimation of probability distributions from data can be done in two ways: Either postulating a parametric family of distributions and estimating the parameters from the data, or by letting the data directly shape the distribution. In the second case, a probability *density function* is usually assumed to exist, and we speak of *non-parametric density estimation.*

We dismiss the first method due to the following reason: the only standard family of distributions with bounded support is the so-called *Dirichlet family* (see [1]), but we found that our data was far from being well represented by any of its members, since bimodality is present in our sample data. Nevertheless we will use the Dirichlet family in a different way, as kernels to apply the *kernel density estimation* method. For the reader convenience, we recall here the definition of the Dirichlet family and the kernel method:

The density function of the Dirichlet distribution of dimension $n > 1$ and positive parameters $\alpha = (\alpha_1, \ldots, \alpha_n)$ is

$$f(x_1, \ldots, x_n) = \frac{1}{B(\alpha)} \prod_{j=1}^{n} x_j^{\alpha_j - 1} \ , \tag{3.8}$$

supported by the simplex Δ, where B is the multivariate Beta function:

$$B(\alpha) = \frac{\prod_{j=1}^{n} \Gamma(\alpha_j)}{\Gamma(\sum_{j=1}^{n} \alpha_j)} \ , \quad \text{and} \quad \Gamma(t) = \int_0^\infty x^{t-1} e^{-x} dx \ .$$

The kernel method, in general, consists of estimating the true density function f by

$$\hat{f}(x) = \frac{1}{N} \sum_{i=1}^{N} K(x, z_i, \Lambda)$$

where K is the *kernel function*, which is a probability density function in x depending on the sample points z_i, $i = 1, \ldots, N$, and an $n \times n$ symmetric and positive-definite matrix Λ, called the *smoothing* or *bandwidth* matrix. As a function of x, K attains its maximum at $x = z_i$. Parameters out of the diagonal in Λ define the grade of covariance between the kernel marginal laws and its eigenvalues size are related to the kernel spread, that is, the greater the eigenvalues, the larger the spread in the corresponding eigenvector direction. In general, the kernel methods have good asymptotic properties.

In the absence of any relevant additional information, we will take Λ as a diagonal matrix with the same intensity λ in all coordinate directions, and the kernel will be the Dirichlet density (3.8) with

$$\alpha_j = 1 + \frac{z_{ij}}{\lambda} \ ,$$

where z_{ij} is the j-th coordinate of z_i.

Using a kernel supported on the simplex Δ ensures that the estimation is also supported on Δ.

The choice of the bandwidth parameter λ is crucial for an accurate estimation of the density. We have spent a considerable effort to get it right, and this is the contents of Subsection 3.3.4.

According with the assumptions above, our estimated density of the proportions p, assuming it exists on the simplex Δ, is given by

$$\hat{f}(x) = \frac{1}{N} \sum_{i=1}^{N} \frac{\Gamma\left(n + \frac{1}{\lambda}\right)}{\prod\limits_{j=1}^{n} \Gamma\left(1 + \frac{z_{ij}}{\lambda}\right)} \prod_{j=1}^{n} x_j^{z_{ij}/\lambda} \; . \tag{3.9}$$

As we will see, in the search of the optimal value of λ, we need to evaluate (3.9) with λ in the order of 10^{-3}. That means, the gamma functions in both numerator and denominator will have a very large argument, with a subsequent precision loss in the division. For that reason, in Subsection 3.3.2, we look for an approximation of the gamma function to simplify the quotient before evaluating each part.

All of the above can be applied under the assumption that there exists a density on the simplex. In our case this is in fact not true, because there are data points in the lower dimensional facets of the simplex, corresponding to the cells on which not all land covers are present. We explain the solution in Subsection 3.3.3.

3.3.2 Numerical approximation of the estimated density

To get an appropriate numerical approximation of the quotient of gammas in (3.9). We use Weierstrass' formula

$$\Gamma(t+1) = e^{-\gamma t} \prod_{k=1}^{\infty} (1 + t/k)^{-1} e^{t/k} \; ,$$

where γ is the Euler constant again. Denoting

$$C := \prod_{j=1}^{n-1} (n - j + \tfrac{1}{\lambda}) \; ,$$

the quotient in (3.9) can be written

$$\begin{aligned}\frac{\Gamma(n+\frac{1}{\lambda})}{\prod\limits_{j=1}^{n}\Gamma(1+\frac{z_{ij}}{\lambda})} &= C\prod_{j=1}^{n}\frac{\Gamma(1+\frac{1}{\lambda})^{1/n}}{\Gamma(1+\frac{z_{ij}}{\lambda})}\\ &= C\prod_{j=1}^{n}\Big[e^{-\frac{\gamma}{\lambda}(\frac{1}{n}-z_{ij})}\prod_{k=1}^{\infty}\frac{1+\frac{z_{ij}}{k\lambda}}{(1+\frac{1}{k\lambda})^{\frac{1}{n}}}e^{\frac{1}{k\lambda}(\frac{1}{n}-z_{ij})}\Big]\\ &= C\prod_{j=1}^{n}\Big[e^{-\frac{\gamma}{\lambda}(\frac{1}{n}-z_{ij})}\exp\Big\{\sum_{k=1}^{\infty}\Big[\frac{\frac{1}{n}-z_{ij}}{k\lambda}+\log\frac{1+\frac{z_{ij}}{k\lambda}}{\big(1+\frac{1}{k\lambda}\big)^{\frac{1}{n}}}\Big]\Big\}\Big].\end{aligned}$$

Now we replace the series by a finite sum, with a controlled error, by means of the Euler–MacLaurin formula. Denoting by $g(k)$ the expression in the internal square brackets (which depends also on z_{ij}),

$$\sum_{k=m}^{\infty} g(k) = \int_{m}^{\infty} g(x)dx + \frac{1}{2}g(m) - \sum_{r=1}^{s}\frac{B_{2r}}{(2r)!}g^{(2r-1}(m) + R_s,$$

with the remainder term satisfying

$$|R_s| \leq \frac{|B_{2s+2}|}{(2s+2)!}|g^{2s+1}(m)| \ ,$$

and where B_r are the Bernoulli numbers, that can be defined recursively as

$$B_r = -\sum_{k=0}^{r-1}\frac{n!B_k}{k!(r+1-k)!} \ , \quad B_0 = 1 \ .$$

The formula is true under the conditions

(i) $g^{(2s+2}(x)g^{(2s+4}(x) > 0$, for $x \in [m,\infty]$,

(ii) $\lim_{x\to\infty} g^{(2s+1}(x) = 0$.

If we call $\bar{f}$ the approximation of the estimated density $\hat{f}$ when disregarding the remainder R_s, and $M := \exp\{\max_{i,j}|R_s|\}$, then

$$\bar{f}M^{-n} \leq \hat{f} \leq \bar{f}M^{n} \ .$$

Thus to obtain a final relative error η, we have to find an ε such that $\varepsilon \geq \max_{i,j}|R_s|$ and $\exp\{n\varepsilon\} \leq (1+\eta)$. This amounts to take

$$\varepsilon = \frac{1}{n}\log(1+\eta) \ ,$$

and to find natural numbers s and m such that $\max_{i,j} |R_s| < \varepsilon$, and satisfying the conditions of the Euler-MacLaurin formula. In this way, we will finally get the approximation

$$\bar{f}(x) = \frac{C}{N}\sum_{i=1}^{N} \exp\Big\{\sum_{j=1}^{n}\Big[\frac{1}{\lambda}(-\gamma(\frac{1}{n} - z_{ij}) + z_{ij}\log(x_j)) + \sum_{k=1}^{m-1} g(k) \\ + \int_m^\infty g(x)dx + \frac{1}{2}g(m) - \sum_{r=1}^{s}\frac{B_{2r}}{(2r)!}g^{(2r-1}(m)\Big]\Big\}.$$

with

$$(1+\eta)^{-1} \leq \hat{f}/\bar{f} \leq (1+\eta) \ .$$

The conditions to apply the Euler-MacLaurin formula are in our case always fulfilled for some small values of m and s. The minimal ones are readily found by simple search.

3.3.3 Sampling strategy

Our real dataset contains many cells in which one or more land covers are not present. Hence, the theoretical distribution from which they are taken does not actually possess a density on the simplex Δ. However, we can assume the existence of a density on the subsimplices obtained by restricting some of the coordinates to be zero. Indeed, the resolution of our data is sufficient to estimate the density on each subsimplex, using the points that lie on it.

If f_δ is the theoretical density on the subsimplex δ, and $q_\delta := P\{p \in \delta\}$ is the theoretical probability that one random point of Δ lie on the subsimplex δ, the overall probability distribution can be described as

$$\begin{aligned} P\{p \in A\} &= \sum_\delta q_\delta \cdot P\{p \in A \cap \delta \mid p \in \delta\} \\ &= \sum_\delta q_\delta \cdot \int_{A\cap\delta} f_\delta(x)\, dx \ , \end{aligned}$$

for any Borel set $A \subset \Delta$.

To estimate the distribution of the whole dataset we can therefore proceed in the following way: The probabilities q_δ can be estimated by the sample proportion $\hat{q}_\delta$ of points lying in δ; the densities on each subsimplex δ can be estimated and approximated as $\bar{f}_\delta$ by the method just described on Subsection 3.3.2. One obtains the estimate

$$P\{p \in A\} \sim \sum_{\delta} \hat{q}_\delta \cdot \int_{A \cap \delta} \bar{f}_\delta(x)\, dx \ .$$

Although there is no a explicit form for the densities $\bar{f}_\delta$, we can evaluate them at arbitrary points x and apply the acceptance/rejection method to simulate a large sample following this density.

1. Choose randomly a subsimplex δ with probability $\hat{q}_\delta$.
2. Generate a random vector x with uniform distribution on δ, with the method of Section 3.2.
3. Generate a random number u with uniform distribution on $[0, 1]$ and evaluate

   $$uC_\delta \leq \bar{f}_\delta(x) \ .$$

   If the inequality holds true, accept x as a new point of the sample; otherwise, reject it and go back to step 2.
4. Go back to step 1 until the desired sample size is reached.

In step 3, C_δ is any constant satisfying

$$C_\delta \geq \max\{\bar{f}_\delta(x)\} \ .$$

Ideally, this constant must be as tight as possible an upper bound of the density function $\bar{f}_\delta$, in order to reject as few generated points as possible. However, we only know this density in a big, but finite, number of points. If, during the run of the acceptance/rejection method, a value of $\bar{f}_\delta$ greater than the chosen C_δ is found, then some of the already accepted points must have been actually rejected. From the practical point of view, we have preferred in our case study to take a safe upper bound, so that none of the accepted points have to be discarded later, despite the larger running times incurred.

The absolute error in the probability of accepting a point x based in the approximate density $\bar{f}$ in step 2 above, when it must be rejected if $\hat{f}$ could be used, it is bounded by the constant η. Indeed, the difference in the probabilities to accept the point in the two cases is

$$\begin{aligned}0 &\leq \frac{1}{C_\delta}\big(\bar{f}(x) - \hat{f}(x)\big) \leq \frac{1}{C_\delta}\big(\bar{f}(x) - \bar{f}(x)(1+\eta)^{-1}\big)\\ &= \frac{\bar{f}(x)}{C_\delta}\big(1-(1+\eta)^{-1}\big) \leq 1 - \frac{1}{1+\eta} \leq \eta \ .\end{aligned}$$

Analogously, one can show that the difference in the probability of rejecting a point is less than the same constant η.

3.3.4 Choosing the bandwidth parameter

As mentioned before (see Subsection 3.3.1) the goodness of the estimation of a density by a kernel method depends heavily on the choice of the bandwidth (or smoothing) parameter λ. In general, the larger the sample size, the smaller the bandwidth should be, or, in other words, the less influence each sample point must have on the final estimation.

In our case, the initial sample size is $N = 3360$. Although we have to work independently on each subsimplex, the bandwidths will tend to be small anyway, as this is what creates the numerical problem that we have addressed in Section 3.3.2.

In the frequently cited paper by Habbema et al. [9], and in Aitchison [1], the authors propose to choose the smoothing parameter λ that maximises the pseudo-likelihood

$$\prod_{i=1}^{N} \frac{1}{N-1} \sum_{j \neq i} K(x_i, x_j, \lambda) \ ,$$

where x are the sample points and N is the sample size.

Instead, we will adjust λ according to the use that we will make of the estimated density. Namely, we want to approximate the function that maps appropriation levels to the conditional expectation of the Shannon index given that level:

$$a \overset{\phi}{\mapsto} E[H \mid A = a] \ . \tag{3.10}$$

To this end, we proceed with the following steps, on each subsimplex:

1. Assume the points in the subsimplex follow a Dirichlet distribution.
2. Estimate the parameters α of the distribution (3.8). We have used the maximum likelihood method implemented in the function `dirichlet.mle` of the R package `sirt`.
3. Generate a large number of points (e.g. 10^6) Y with the estimated distribution. These data plays the role of 'synthetic population' in this process.
4. Sample a subset Z of Y of the same size as the part of the real sample that lies on the subsimplex. These data Z is used as the 'synthetic sample' for the next steps.
5. For a given value of λ, apply the procedure explained in 3.3.3 to simulate a sample X_λ of the estimated density (say, of size 10^4).
6. Measure the fit of the simulated data with the 'synthetic population' Y using the integrated square error
$$\int_{w_1}^{w_n} \left(\phi_Y(a) - \phi_{X_\lambda}(a)\right)^2 \, da \ , \tag{3.11}$$
where ϕ_Y and ϕ_{X_λ} are the functions (3.10) for ϕ corresponding respectively to the population Y, and to the sample X_λ.
7. Repeat steps 5–6 to choose λ that minimises (3.11).

Some remarks are in order about the scheme above:

a) In our case study, it is possibly not true that the data can be well represented by a Dirichlet distribution; if we knew it were, then we would be better off adopting directly the density that results from the maximum likelihood estimate. However, we use it at this point as a proxy because of its support on the simplex, and only to obtain a plausible bandwidth; using the uniform distribution on the subsimplices for the same purpose will be even more inadequate.

b) The sample sizes of Y and X_λ are arbitrary. They should simply look like a (big) population and an (also big) sample from it. On the contrary, we think that it is realistic to make the size of Z equal to the size of the real data at hand. The integral in (3.11) cannot be computed exactly, because the function (3.10) cannot be either. We discretise the values of A to obtain a stepwise approximation of ϕ, so that the integral is in fact approximated by a finite sum. But this is fine, since the final result will necessarily be given as a discretised function.

c) Finally, the integrated square error is not the only possible criterion for the choice of λ; others can be used, depending on the application sought.

3.4 Results

In this section we present the results of the procedures proposed in Sections 3.2 and 3.3 when applied to the data of the case study described in the Introduction. The four types of land covers are: the semi-natural land covers, with lowest human appropriation (forest, scrubland, prairie and bedrock, and wetland), p_1; the cropland, both irrigated and dry crops, p_2; the land covers with groves, p_3; and the urban and industrial surfaces, p_4.

The weights w for each land cover type have been obtained as the average of the weights of the original ten land covers, the latter taken from [15] (see Table 3.1). There are different values of weights for each year, due to the changes in the exploitation of land covers over time. From 1956 to 2000 there is a general reduction in the values of w. It is known that in the last decades of the twentieth century there has been in Mallorca a progressive abandonment of the arable land, inducing a expansion of forests, from which humans extract little profit [15].

year	w_1	w_2	w_3	w_4
1956	51.042	78.880	89.993	95.730
1973	43.958	76.200	85.322	94.792
2000	48.542	74.978	81.837	93.958

Table 3.1: w values for each year.

The real data is distributed in subsimplices as described in Table 3.2. As we can see in this table, the dominant subsimplex in 1956 and 1973 is the one comprising 'semi-natural', 'cropland' and 'groves' covers. Such combinations are usually referred as *mosaic* *landscapes.* Their frequency clearly declines in 2000, where the combination of 'semi-natural' and 'cropland' prevails.

In Figure 3.6, a scatter plot of the joint values of H and A is shown, for each of the three times periods (1956, 1973 and 2000). Recall that the support of the feasible pairs has the irregular greyed shape that we saw in Figure 3.5, with the 'legs' of the region resting over the weight values in the horizontal axis; hence the white empty zones in the scatter plot. Dots are plotted with some degree of transparency; the apparently solid lines describing arcs between the legs are points whose corresponding proportions p lie in the edge joining two vertices of the simplex. Some of these edges are more populated than others, or more evenly distributed, and those arcs are therefore more noticeable in the figure.

Subsimplices δ	1956		1973		2000	
	N_δ	λ	N_δ	λ	N_δ	λ
1 0 0 0	228	-	224	-	226	-
0 1 0 0	30	-	27	-	240	-
1 1 0 0	109	0.007	98	0.029	1094	0.001
0 0 1 0	84	-	78	-	24	-
1 0 1 0	787	0.003	766	0.002	199	0.039
0 1 1 0	489	0.013	454	0.026	212	0.009
1 1 1 0	1311	0.006	1208	0.006	532	0.004
0 0 0 1	1	-	3	-	7	-
1 0 0 1	3	-	12	-	28	-
0 1 0 1	8	-	14	-	144	0.008
1 1 0 1	8	-	13	-	298	0.007
0 0 1 1	39	0.027	51	0.05	24	-
1 0 1 1	59	0.032	111	0.015	29	-
0 1 1 1	105	0.014	141	0.011	136	0.015
1 1 1 1	99	0.035	160	0.03	167	0.031

Table 3.2: Subsimplex typologies δ, corresponding to different combinations of land covers (1 indicates presence, 0 absence); size N_δ of each subsimplex, and chosen values of λ.

In Figure 3.7, the same scatter plot of the pairs (A, H) is depicted, for the enlarged dataset obtained by the sampling method of Subsection 3.3.3, and the three corresponding time periods. Table 3.2 shows the λ values fitted on each subsimplex obtained following the optimisation procedure of Subsection 3.3.4. Of course, vertices of the simplex does not have a density. Also, we have not estimated a density for subsimplices with less than 30 data points; instead, we have sampled them as a discrete equally probable population. The threshold of 30 is arbitrary.

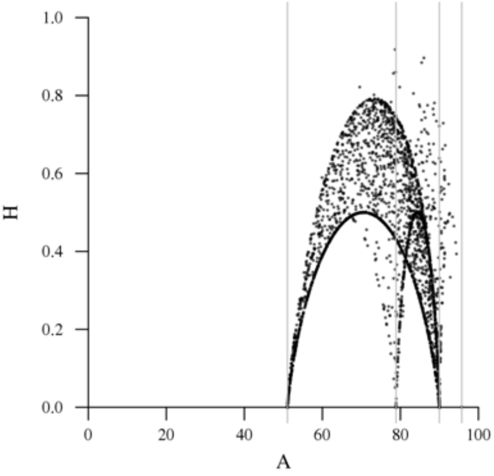

(a) 1956

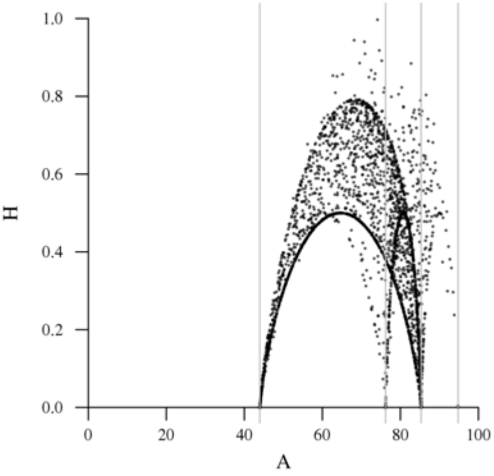

(b) 1973

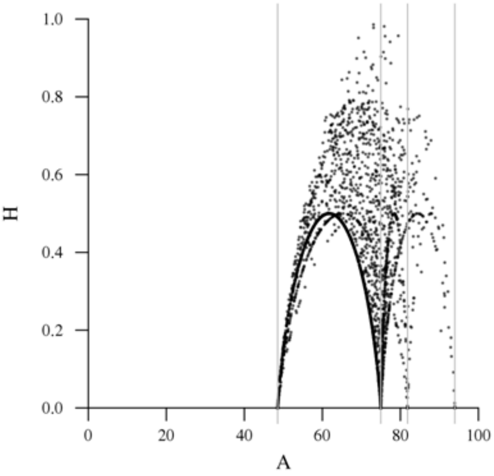

(c) 2000

Figure 3.6: Values (A, H) of the real data from Mallorca Island (four land covers, 3360 points).

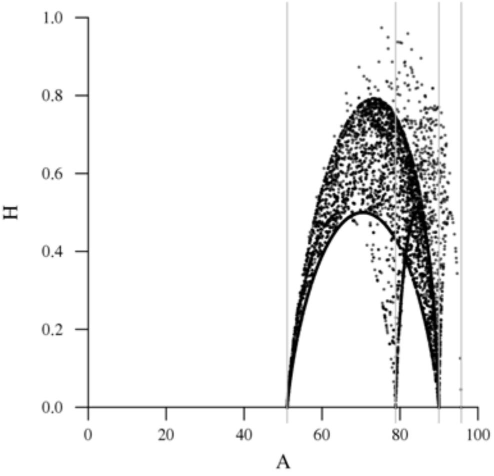

(a) 1956

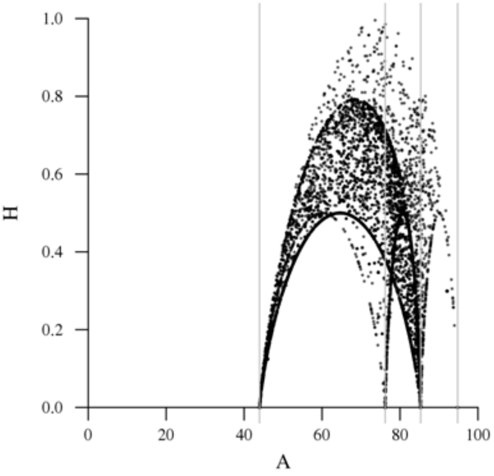

(b) 1973

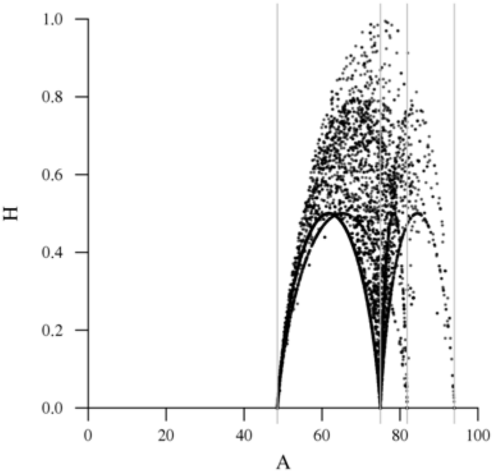

(c) 2000

Figure 3.7: Simulated values (A, H) generated from the estimated distribution, and a sample size of 10^4 points.

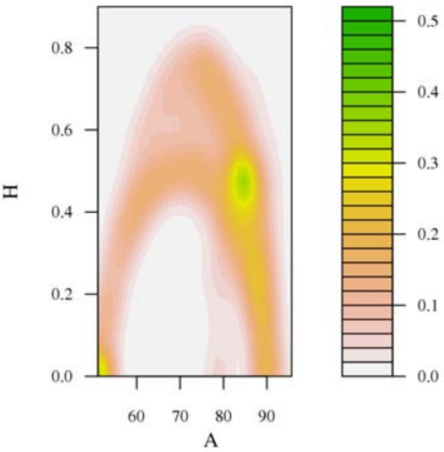

(a) 1956

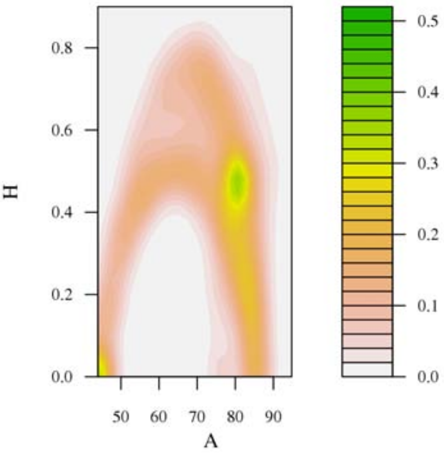

(b) 1973

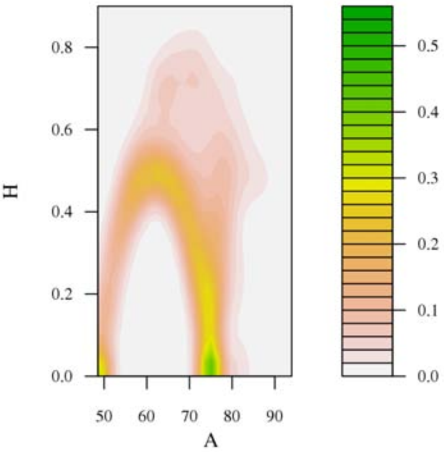

(c) 2000

Figure 3.8: 'Filled-contour plot' of the two-dimensional of (A, H), estimated from real data.

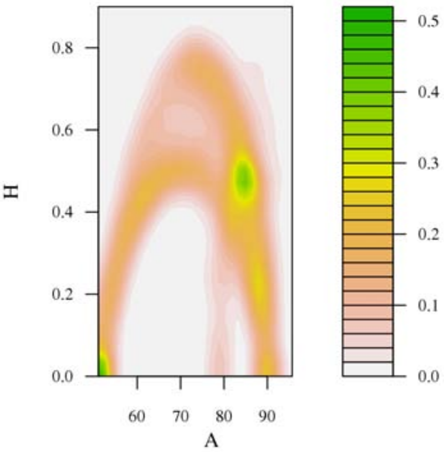

(a) 1956

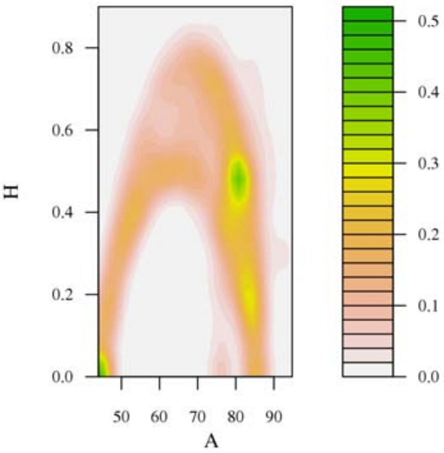

(b) 1973

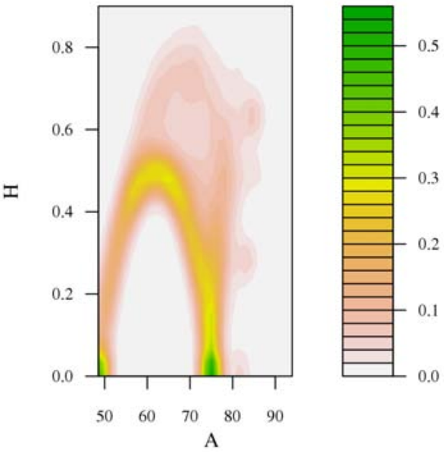

(c) 2000

Figure 3.9: Analogue of Figure 3.8 for the simulated data.

Figures 3.6 and Figure 3.7 look indeed quite similar, except for the number of points, which speaks in favour of our method of estimation of the probability distribution of the proportions in the simplex. To reinforce this impression, in Figures 3.8 and 3.9 we compare estimations of the join density of A and H both from the initial data and for the enlarged sample. In these figures we have used a simple Gaussian kernel density estimation in the plane, just to have a visual quick idea of the similarity of the large synthetic sample with the original one, in order to validate the whole computation of the conditional expectations in Section 3.3.

3.4.1 Shannon index conditioned to the appropriation

In Figure 3.10 we can see superimposed the plots of $a \mapsto E[H|A = a]$, with the assumptions of both sections 3.2 and 3.3. The red curve is the analytic result obtained assuming a uniform distribution of covers, whereas the blue points are the ones we have obtained with the real data of our case study and the procedure of Section 3.3. The vertical grey lines indicate the values w.

Real data produce, for all time periods and for practically all values of appropriation, an expected value of the Shannon index H lower than with the uniform distribution. This was absolutely expected, because in the real dataset rarely all types of cover appear in a single cell (only 99 over 3360 cases, see Table 3.2), nor the appearing ones look like evenly distributed. Recall that the Shannon index is maximal when all proportions coincide.

Concerning the annual evolution, figures show a strong similarity in the expected H for 1956 and 1973, whereas there are noticeable differences in 2000. First, there is a high decrease around $a = w_2$, motivated by the intensification of p_2 (see table 3.2). Secondly, the expectation after w_2 increases due to the growth of urban areas combined with other land covers. The maximum of the expectation, in fact, jumps to the interval $[w_3, w_4]$.

3.4.2 A variant of Shannon index

At the scale we are working, one may consider that the urban cover is not a real habitat for living species (except humans). It has been proposed in [14] to use a variation of the

Shannon index that penalises the presence of urban land cover as indicator of habitat diversity:

$$L := (1 - p_u)\Big(- \sum_{i=1}^{n} p_i \log_n p_i \Big) ,$$

where p_i are the proportions of non-urban covers, inside the total of non-urban surface, and p_u is the proportion of urban surface in the cell. With the obvious notation,

$$p_i = \frac{S_i}{S_{\text{Cell}} - S_u} , \quad p_u = \frac{S_u}{S_{\text{Cell}}} .$$

The maximum of L is 1 and it corresponds to $p_i = \frac{1}{n}$, $p_u = 0$, and $A = \frac{1}{n}\sum_{i=1}^{n} w_i$.

In Figure 3.11 one can see the relation between the appropriation A and the conditional expectation $E[L|A]$. Again, the red curve corresponds to the expectation of the index L for each value of A when the land covers, including p_u, are uniformly distributed. In contrast with the case of H, this conditional expectation is in some region smaller than the value derived from the real data (with the procedure of Section 3.3), and represented by the blue dots. This is due to the fact that the urban land cover has the same weight in the uniform case, whereas for the real data the urban cover has a smaller presence than the other.

Figure 3.11 shows the temporal evolution of $E[L|A]$. The shape of the blue curve is clearly affected by the mosaic loss and the urban growth. The use of index L instead of the Shannon index H helps to interpret, in this case, the evolution of the land cover. Furthermore, we want to point out with this variation that our methodology is not particularly tied to the Shannon index.

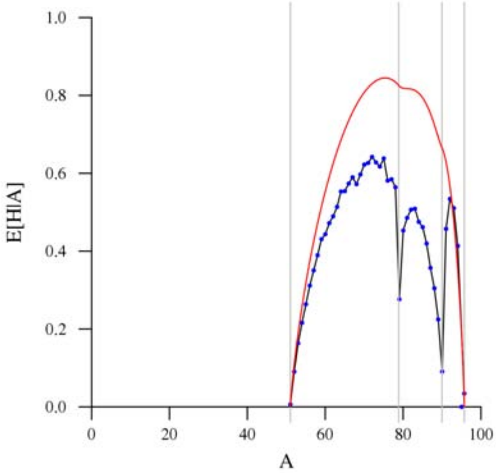

(a) 1956

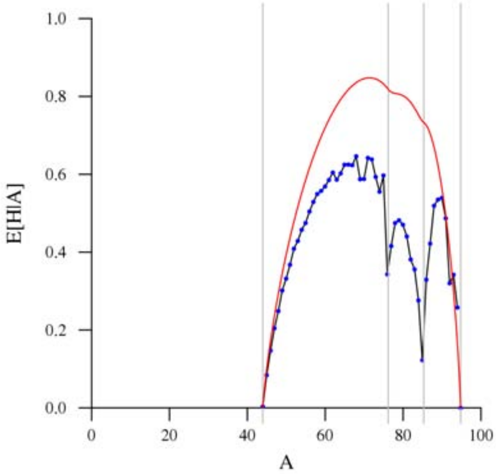

(b) 1973

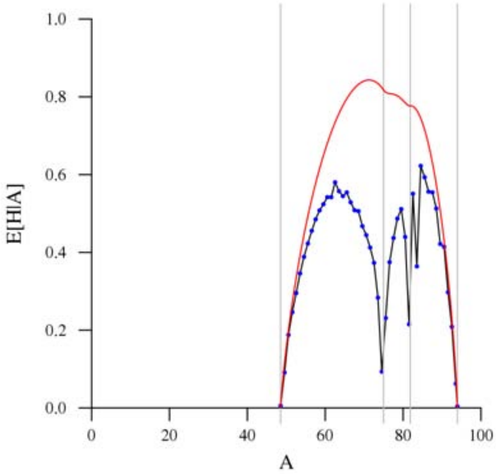

(c) 2000

Figure 3.10: Conditional expectation $E[H|A = a]$ with the uniform distribution of covers (red curve) and starting form the data of the case study (blue dots).

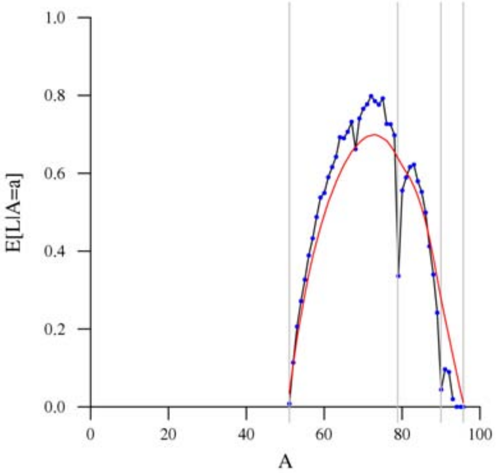

(a) 1956

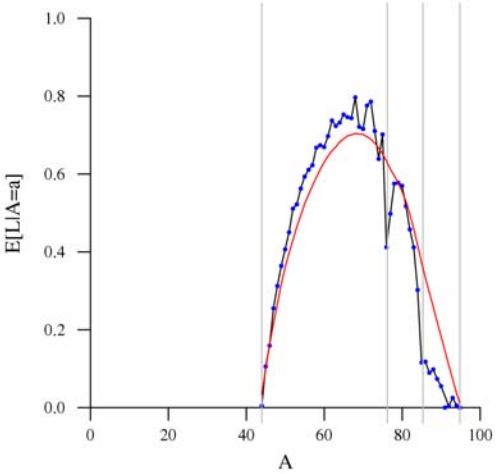

(b) 1973

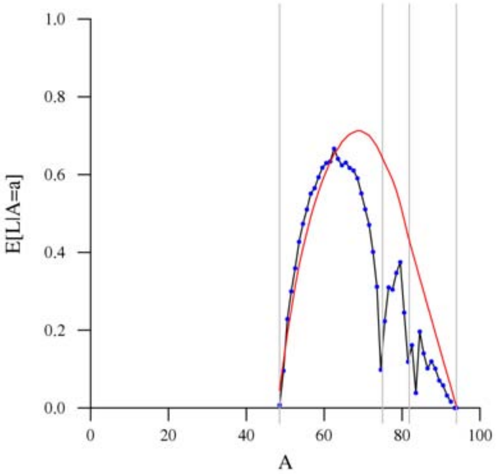

(c) 2000

Figure 3.11: Analogue of Figure 3.10 with the indicator L.

3.5 Conclusions

The contribution of this work goes beyond the analysis of Shannon entropy and human appropriation; it is also studied the dirichlet distribution for land cover data. A methodology to choose the bandwidth parameter for the dirichlet distribution is provided, as well as a sampling strategy to obtain large new samples according to a given real data set. The procedure of generating new samples is computationally intensive. Due to this fact, we grouped the original ten land covers of the Mallorca case of study into four classes.

This model allows to evaluate, in a simplified way, the relationship between landscape patterns, H, (or some other landscape metrics) and human appropriation, A, reducing the entire dataset to a curve $f(A) = E[H|A]$. The curve behaviour shows the change of land covers combinations. Furthermore, this can be used to compare some sample data with a fixed pattern, in our case the uniform distribution of land covers. It is also possible to observe the historical evolution of a territory, or compare several cases of study.

3.6 Computational notes

The computations have been done in R with the following setup:

- R version 3.3.1 (2016-06-21), `x86_64-pc-linux-gnu`
- Base packages: base, datasets, graphics, grDevices, methods, stats, utils
- Other packages: CDM 5.0-0, knitr 1.13, logspline 2.1.9, mvtnorm 1.0-5, sirt 1.12-2, TAM 1.995-0

The whole procedure of Section 3.3 is computationally intensive, due to the optimisation step to choose the right value of the parameter λ for each subsimplex, including an acceptance/rejection simulation for each tentative value. It is not a prohibitive load, though. The computational complexity is of course exponential as a function of the number of different covers, since there are $2^{n+1} - 1$ subsimplices in the n-dimensional standard simplex Δ in $\mathbb{R}^{n+1}$. For this reason, and to have enough sample size in most of the subsimplices, we grouped together the original data of ten different covers into four classes, using a similarity criterion.

3.7 Bibliography

[1] J. Aitchison. A general class of distributions on the simplex. *J. Roy. Statist. Soc. Ser. B*, 47(1):136–146, 1985.

[2] A. Buccianti, G. Mateu-Figueras, and V. Pawlowsky-Glahn, editors. *Compositional Data Analysis in the Geosciences.* Geological Society of London, 2006.

[3] J.E. Chacón, G. Mateu-Figueras, and J.A. Martín-Fernández. *Gaussian kernels for density estimation with compositional data. Computers & Geosciences*, 37(5):702–711, 2006.

[4] Robert K. Colwell. Biodiversity: Concepts, patterns, and measurement". In Simon A. Levin, Stephen R. Carpenter, H. Charles J. Godfray, Ann P. Kinzig, Michel Loreau, Jonathan B. Losos, Brian Walker, David S. Wilcove, and Christopher G. Morris, editors, *The Princeton Guide to Ecology*, chapter III.1, pages 257–263. Princeton University Press, 2009.

[5] David J. Currie, Gary G. Mittelbach, Howard V. Cornell, Richard Field, Jean-Francois Guégan, Bradford A. Hawkins, Dawn M. Kaufman, Jeremy T. Kerr, Thierry Oberdorff, Eileen O'Brien, and J. R. G. Turner. Predictions and tests of climate-based hypotheses of broad-scale variation in taxonomic richness. *Ecology Letters*, 7(12):1121–1134, 2004.

[6] Jeremy W. Fox. The intermediate disturbance hypothesis should be abandoned. *Trends in Ecology & Evolution*, 28(2):86–92, 2016/01/13 XXXX.

[7] Kevin J. Gaston. Global patterns in biodiversity. *Nature*, 405(6783):220–227, May 2000.

[8] GIST. Mapes de cobertes del sòl de les illes balears (1:25.000): 1956(1973), 1995, 2000. *Universitat de les Illes Balears, Departament de Ciències de la Terra, Grup d'Investigació de Sostenibilitat i Territori, Palma de Mallorca*, 2009.

[9] J. D. E Habbema, J. Hermans, and K. van den Broek. A stepwise discriminant analysis program using density estimation. In *COMPSTAT 1974: Proceedings in Computational Statistics*, pages 101–110. Physica-Verlag, 1974.

[10] Helmut Haberl, K. Heinz Erb, Fridolin Krausmann, Veronika Gaube, Alberte Bondeau, Christoph Plutzar, Simone Gingrich, Wolfgang Lucht, and Marina Fischer-Kowalski. Quantifying and mapping the human appropriation of net primary production in earth's terrestrial ecosystems. *Proceedings of the National Academy of Sciences*, 104(31):12942–12947, 2007.

[11] Helmut Haberl, Niels B. Schulz, Christoph Plutzar, Karl Heinz Erb, Fridolin Krausmann, Wolfgang Loibl, Dietmar Moser, Norbert Sauberer, Helga Weisz, Harald G. Zechmeister, and Peter Zulka. Human appropriation of net primary production and species diversity in agricultural landscapes. *Agriculture, Ecosystems & Environment*, 102(2):213 – 218, 2004.

[12] Charles Kooperberg and Charles J Stone. Logspline density estimation for censored data. *Journal of Computational and Graphical Statistics*, 1(4):301–328, 1992.

[13] Tom Leinster and Christina A. Cobbold. Measuring diversity: the importance of species similarity. *Ecology*, 93(3):477–489, 2006.

[14] Joan Marull, Carme Font, Roc Padró, Enric Tello, and Andrea Panazzolo. Energy–landscape integrated analysis: A proposal for measuring complexity in internal agroecosystem processes (barcelona metropolitan region, 1860–2000). *Ecological Indicators*, 66:30–46, 2016.

[15] Joan Marull, Carme Font, Enric Tello, Nofre Fullana, Elena Domene, Manel Pons, and Elena Galán. Towards an energy–landscape integrated analysis? exploring the links between socio-metabolic disturbance and landscape ecology performance (mallorca, spain, 1956–2011). *Landscape Ecology*, 31(2):317–336, 2015.

[16] Joan Marull, Enric Tello, Nofre Fullana, Ivan Murray, Gabriel Jover, Carme Font, Francesc Coll, Elena Domene, Veronica Leoni, and Trejsi Decolli. Long-term bio-cultural heritage: exploring the intermediate disturbance hypothesis in agro-ecological landscapes (mallorca, c. 1850–2012). *Biodiversity and Conservation*, 24(13):3217–3251, 2015.

[17] RY Rubinstein and Benjamin Melamed. *Modern simulation and modeling.* Number 04; T57. 62, R8. Wiley, 1998.

[18] J Tews, U Brose, V Grimm, K Tielbörger, MC Wichmann, M Schwager, and F Jeltsch. Animal species diversity driven by habitat heterogeneity/diversity: the importance of keystone structures. *Journal of biogeography*, 31(1):79–92, 2004.

[19] Teja Tscharntke, Yann Clough, Thomas Wanger, Louise Jackson, Iris Motzke, Ivette Perfecto, John Vandermeer, Anthony Whitbread. Global food security, biodiversity conservation and the future of agricultural intensification. *Biological conservation*, 151(1), 53–59, 2012.

[20] Peter M. Vitousek, Paul R. Ehrlich, Anne H. Ehrlich, and Pamela A. Matson. Human appropriation of the products of photosynthesis. *BioScience*, 36(6):368–373, 1986.

Chapter 4

Energy-Landscape Integrated Analysis: A proposal for measuring complexity in internal agroecosystem processes (Barcelona Metropolitan Region, 1860 - 2000)[1]

4.1 Introduction

4.1.1 Sustainable farm systems: the global food-biodiversity dilemma

Farm systems are facing a global challenge amidst a socio-metabolic transition (Muradian et al., 2012; Scheidel and Sorman, 2012; Schaffartzik et al., 2014) that places them in a dilemma between increasing land use intensity to meet the growing demand of food, feed, fibres and fuels (Godfray et al., 2010; Lambin and Meyfroidt, 2011), while trying to avoid a dangerous biodiversity loss (Tilman, 1999; Schröter et al., 2005; Cardinale et al., 2012). The industrialization of agriculture through the 'green revolution' spread from the 1960s onwards has been a major driver of this loss (Matson et al., 1997; Tilman et al., 2002). However, it is increasingly acknowledged that well-managed agroecosystems can play a

---

[1] This work has been published in the journal Ecological Indicators with the participation of Joan Marull, Carme Font, Roc Padró, Enric Tello, Andrea Panazzolo

key role in biodiversity maintenance (Bengtsson et al., 2003; Tscharntke et al., 2005). From a land sharing approach to biological conservation (Perfecto and Vandermeer, 2010; Tscharntke et al., 2012), there is a claim for a wildlife-friendly farming liable to provide complex agroecological matrices. An heterogeneous and well connected land matrix could maintain high species richness in cultural landscapes (Tress et al., 2001; Agnoletti, 2006, 2014; Jackson et al., 2007). Depending on land use intensities and the type of farming, agricultural systems may either enhance or decrease biodiversity (Altieri 1999; Swift et al 2004). In turn, the adaptive capacities to farming disturbances and agroforestry land usages vary across species and biomes (Gabriel et al., 2013; Balmford et al., 2014).

Solving the global food-biodiversity dilemma requires a deeper research to know how species richness is kept or lost in different land use patterns, according to the level (quantity) and character (spatiotemporal scale and quality) of the ecological disturbances that farmers carry out across the landscape (Fischer et al., 2008; Phalan et al., 2011). If human society wants to ensure all sorts of ecosystem services in the future, we need better operative criteria and indicators in order to assess when, where and why the energy throughput driven by farmers increases or decreases the mosaic pattern of cultural landscapes and their capacity to hold biodiversity (Gliessman, 1990; Pierce, 2014). This calls for an integrated research of coupled human-natural systems aimed at revealing complex structures and processes which are not apparent when studied by social or natural scientists separately (Liu et al., 2007; Marull et al., 2015a).

4.1.2 Aim and scope of this study

A growing consensus in conservation biology points to landscape heterogeneity as being a key mechanism that generates a dynamic biodiversity peak at intermediate levels of ecological disturbance in agroecosystems, thanks to the interplay between spatial diversity, ecosystem complexity and dispersal abilities of colonizing species either coming from less disturbed patches or the survivors in the most disturbed ones (Tilman, 1994; Elmqvist et al., 2003; Roxburgh et al., 2004; Harper et al., 2005; Perfecto and Vandermeer, 2010; Loreau et al., 2010). This opens a research field on how the complexity of energy flows driven by farmers shapes these types of heterogeneous landscapes that can offer a great deal of habitats, food chains and ecological connectivity required by the associated biodiversity of farm systems. The Energy–Landscape Integrated Analysis (ELIA) of agroecosystems proposed in this work aims to contribute to this task by bringing to light the link between the anthropogenic energy carriers flowing among the components of a farm system, the information held within this energy network, and the land cover diversity of cultural landscapes that arises with the spatial imprint of these farming energy flows.

4.2 Theory

4.2.1 Towards an energy-landscape integrated analysis

Living systems are capable of using metabolic energy carriers in order to maintain or even increase their organization (Schrödinger, 1944), when they attain a far-from-thermodynamic equilibrium set up with the organized information that allows transferring energy while maintaining their complexity, reproducing themselves, and evolving (Ho, 1998; Gladyshev, 1999; Ulanowicz, 2003). Applying this approach to agroecosystems requires analysing 1) the energy throughput and closure degree of socio-metabolic cycles; 2) the information carried by the spatially differentiated shape of these energy fluxes flowing across the land matrix; and 3) the land cover diversity of the landscape to which the species are adapted (Ho and Ulanowicz, 2005). Like any other ecosystem, in agroecosystems the energy dissipated in space also leads to the emergence of self-organized structures that experience historical successions ruled by adaptive selection (Morowitz, 2002). Thanks to the internal biophysical cycles that link organisms one another, these agroecosystems can enhance their own complexity, increase temporal energy storage and decrease entropy. This set of emergent properties translates into integrated spatial heterogeneity and biodiversity of landscapes (Ho, 2013; Ulanowicz, 1986). Their sustainability is directly related to the information-complexity interplay, and inversely related to energy dissipation (Prigogine, 1996; Ulanowicz, 1997).

In this vein, agroecosystems are seen as the historically changing outcome of the interplay between sociometabolic flows (Haberl, 2001), the land use patterns set up by farmers, and ecological functioning (Farina, 2000; Wrbka et al., 2004). Despite the long-lasting work done on energy analysis of farm systems, which revealed a substantial decline in energy returns of agro-industrial management brought about by the massive consumption of cheap fossil fuels (Odum, 1984, 2007; Giampietro and Pimentel, 1991; Pelletier et al., 2011; Giampietro et al., 2011, 2013), the role played by sociometabolic energy throughput as a driving force of contemporary Land Cover and Land-Use Change (LCLUC) is not yet well understood (Peterseil et al., 2004). ELIA intends to link these two lines of research, the agroecological accounting of energy flows (Guzmán and González de Molina, 2015; Tello et al., 2016) and the study of LCLUC from a landscape ecology standpoint (Marull et al., 2015a). This requires specifying and measuring the pattern of energy flows and the information held in agroecosystems.

4.2.2 Cultural landscapes as socio-metabolic imprint

Traditional organic farm systems with a solar-based metabolism, like the ones existing in Europe before the massive spread of the green revolution from the 1960s onwards, tended to organize their land usages according to different gradients of intensity, keeping an integrated management of the landscape because their whole subsistence depended on this. In order to offset the energy lost in the inefficient human exploitation of animal bioconversion –on which they had to depend to obtain the internal farm services of traction and manure (Guzmán and González de Molina, 2009)—, traditional organic farming kept livestock breeding carefully integrated with cropland, pasture and forest spaces (Krausmann, 2004). While the organic farm management strategy of closing cycles within an agroecosystem led to landscape mosaics, the socio-ecological transition to agro-industrial farm systems that rely on external flows of inputs coming from underground fossil fuels has enabled society to overcome the age-old energy dependency on bioconverters (Krausmann et al., 2003; Schaffartzik et al., 2014). As a result, integrated land use management at a local or regional scale was no longer necessary—and overcoming this former necessity also led to losing its agroecological virtue (Cussó et al., 2006a, 2006b). The environmental damage caused worldwide by this lack of integrated management between energy flows and land usages urges societies to recover the former 'landscape efficiency' (the socioeconomic satisfaction of human needs while maintaining the healthiest landscape ecological patterns and processes) at present (Marull et al., 2010). Since the lack of an integrated management of energy flows and land uses at different scales is part of the current global ecological crisis, its recovery becomes crucial for a more sustainable foodscape.

This line of research involves a wider and more complex approach to agroecosystems' energy efficiency. It requires not only accounting for a single input-output ratio between the final product and the external energy consumed, but looking at the harnessing of energy flows that loop within the system as well. The cyclical nature of these flows is important in order to grasp the emergent complexity and the information held within the agroecosystem, given that they involve an internal maximization of less-dissipative energy carriers—in the same vein as Ho and Ulanowicz (2005) explain the 'loopy' character of any living system. The temporal energy storage that these loops allow becomes a foundation for all sustainable systems (Ho, 2013). Hence, the usual methodology of energy flow analysis of social metabolism needs to be adapted and enlarged in order to give account of the cyclical character of agroecosystems' processes (Giampietro, 2004, 2011, 2013; Guzmán and González de Molina, 2015).

4.3 Method

4.3.1 Energy flows of an agroecosystem as a graph

Graph modelling is a well-known mathematical structure that allows us to chart natural phenomena as a set of 'nodes' and 'edges' (Urban et al., 2009). ELIA treats the pattern of flows in an agroecosystem as a graph where energy carriers are 'nodes' whose 'edges' represent their interaction. Fig. 4.1 shows how the total amount of phytomass obtained from solar radiation through the autotrophic production by plants, that accounts for the actual Net Primary Production (NPP_{act}) (Vitousek et al., 1986; Smil, 2011; Krausmann et al., 2013; Guzmán et al., 2014), is the natural energy source for all heterotrophs living there. From this starting point, we analyse the pattern adopted by the subsequent energy processes carried out, the internal loops they generate, the final product extracted or the external inputs introduced from outside the agroecosystem.

The whole biomass included in NPP_{act} that becomes available for all species is split into Unharvested Biomass (UB) and the share of Net Primary Production harvested (NPP_h) (Fig. 4.1). The UB remains in the same place where it has been primary produced to feed the populations of the farm-associated biodiversity. It becomes a source of the whole Agroecosystem Total Turnover (ATT) that closes the first cyclical subsystem called 'Natural' in Fig. 4.1a, because it allows for the production of NPP_{act} again through the trophic net of non-domesticated species either in the edaphic processes of the soil or aboveground. This does not mean, however, that the entire NPP_h which has been appropriated by farmers goes out of the agroecosystem. In turn, NPP_h is subdivided into Biomass Reused (BR) inside the agroecosystem and Farmland Final Produce (FFP) that goes outside to be consumed by humans (Fig. 4.1). The BR share is an important flow that remains within the agroecosystem as a farmer's investment addressed to maintain two basic renewable funds: livestock and soil fertility. Hence, BR closes the second basic loop called 'Farmland' subsystem in Fig. 4.1b.

Then BR is split into the share that goes to feed the domesticated animals as Livestock Biomass Reused (LBR), which is added to the whole amount of Livestock Total Inputs (LTI), whereas another share of BR is Farmland Biomass Reused (FBR) which adds up to Farmland Total Inputs (FTI) as seeds, green manure and other vegetal fertilizers (Fig. 4.1). In this way the 'Farmland' subsystem, which comes from the NPP_{act} in the 'Natural' one, becomes linked to the third 'Livestock' subsystem (Fig. 4.1c). These energy linkages in the graph enable us to make apparent how they relate to an integrated land use management.

Afterwards, LBR flows to domestic animal bioconversion and then it splits into Livestock Final Produce (LFP) and internal Livestock Services (LS) obtained by farmers as draft power and manure (both make up Livestock Produce and Services LPS). In this way the two subsequent loops called 'Farmland' and 'Livestock' subsystems are partially closed within the agroecosystem, while offering a Final Produce (FP) to be consumed outside—as well as receiving a lower or higher amount of External Inputs (EI). Therefore, the amount of UB, BR and LS provide the internal flows that lead to a stronger or weaker ‘loopiness’ in the pattern of energy networks of agroecosystems (Fig. 4.2). Notice that when only the ‘Natural’ subsystem is in place, but some Final Produce (FP) is extracted, we are looking at a very simple gathering or forestry systems. If all the human-appropriated NPP_{act} is diverted towards livestock bioconversion, we are facing a purely pastoral system. In an agro-industrial monoculture of grains, almost all NPP_{act} would be appropriated, except some weeds or herbivores that survive pesticide application, while the greatest share of the energy carriers would flow from outside as EI or would go outside as FP, except some remnant BR like the stubble ploughed in the soil.

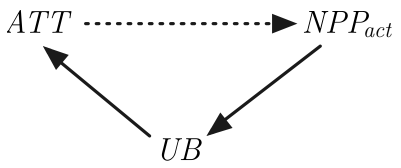

(a) ’Natural’ subsystem

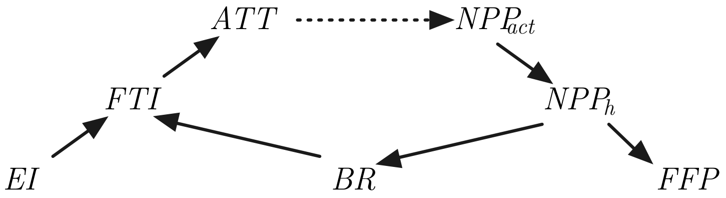

(b) ’Farmland’ subsystem

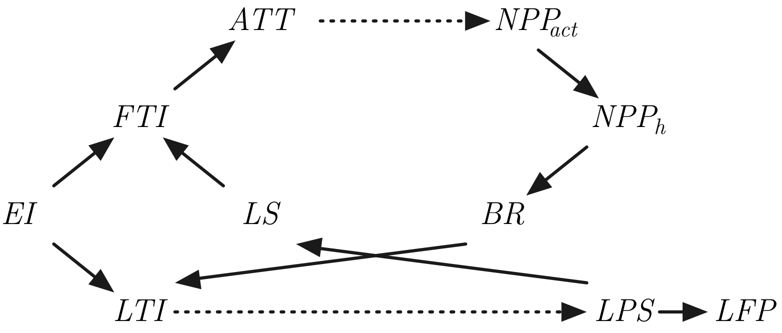

(c) ’Livestock’ subsystem

Figure 4.1: Graph model of energy carriers into three subsystems of an agroecosystem.

Once we have dissected the agroecosystem, Fig. 4.2 shows the three subsystems coupled in one that becomes an outline of a mixed farming that integrates cropping and forestry with livestock breeding. It goes without saying that the complexity reached and the information needed to run an integrated mixed farming like this is much higher than with forestry exploitation, a monoculture or a pastoral system carried out separately. This explains why we are going to use this graph model (Fig. 4.2) to calculate the level of energy storage within the agroecosystem provided by its 'loopiness', as well as the information embedded in this network of flows.

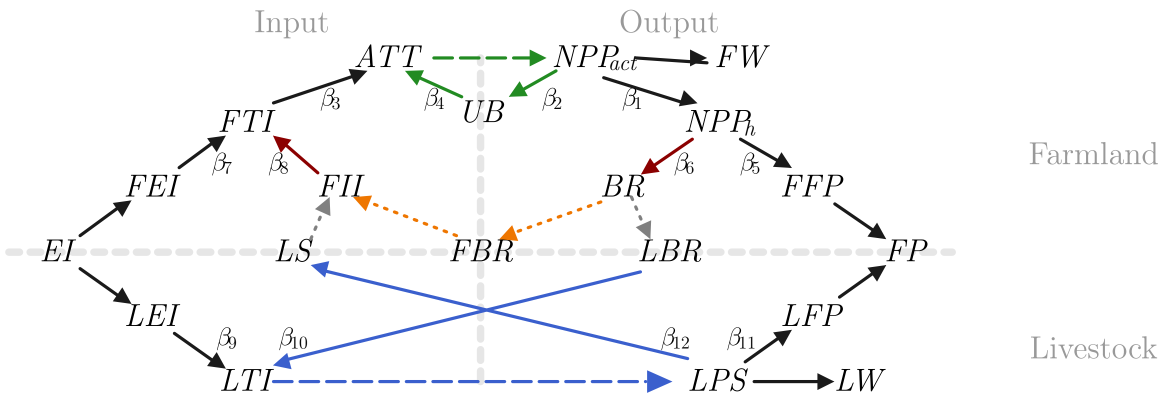

Figure 4.2: Graph model of interlinked energy carriers flowing in a mixed-farming agroecosystem.

4.3.2 Energy carriers stored within agroecosystems

The agroecosystem can behave in a cyclical manner because the outputs of one subsystem (Fig. 4.1) become the inputs of the next one (Fig. 4.2). This, in turn, provides the base for its 'loopiness' that allows storing energy carriers and information within the dissipative structure (Ho and Ulanowicz, 2005). There is an exception to this rule though, when some energy carriers circulating inside the agroecosystem are turned into what Odum (1993) named a 'resource out of place'. As seen in Fig. 4.2, sometimes a fraction of NPP_{act} can be wasted. The same may happen with a fraction of the LPS, such as dung slurry coming from agro-industrial feedlots that are spread in excess into cropland and end up contaminating the water table. If they exist, these Farmland Waste (FW) and Livestock Waste (LW) do not contribute to the renewal of the agroecosystem's funds, neither to enhance its internal complexity, nor to meet human needs. Accordingly, the enthalpy of these energy carriers cannot be taken into account in our graph modelling as fluxes that contribute to keeping up the agroecosystem reproduction—although they have to be included as cost.

In the integrated graph (Fig. 4.2) we can identify six main subprocesses. In all of them the flow that exits from a node can be differentiated between the portion that remains within the agroecosystem and the other which goes to other subsystems or out of the system. Accordingly, there is always a pair of incoming-outgoing flows for each subprocess of the agroecosystem. Hence, we propose twelve coefficients (β_i) along the edges of the graph.

$$\beta_1 = \frac{NPP_h}{NPP_{act}},\ \beta_2 = \frac{UB}{NPP_{act}},\ \beta_3 = \frac{FTI}{ATT},\ \beta_4 = \frac{UB}{ATT},\ \beta_5 = \frac{FFP}{NPP_h},\ \beta_6 = \frac{BR}{NPP_h},$$
$$\beta_7 = \frac{FEI}{FTI},\ \beta_8 = \frac{FII}{FTI},\ \beta_9 = \frac{LEI}{LTI},\ \beta_{10} = \frac{LBR}{LTI},\ \beta_{11} = \frac{LFP}{LPS},\ \beta_{12} = \frac{LS}{LPS}.$$

These β_i's account for the proportion in which every flow is split into two in each crossroads within the network. Then, we can differentiate between even and odd β_i's, where the even ones account for the energy carriers looping inside the agroecosystem. Any pair of the same subprocess sum 1, except for those processes that have a third direction (waste). This is the case of NNPact and LPS, which affects β_1, β_2, β_{11} and β_{12}. Another advantage of using β_i's is that they are bounded (between 0 and 1), which allows comparing different case studies or historical examples.

In Fig. 4.2 we differentiate between three shapes of arrows. Solid arrows show the energy flows we are most interested in, as they represent the internal and external exchange of energy carriers. Dashed arrows indicate fluxes that require biological conversion (i.e. photosynthesis). Finally, point-line arrows show energy carriers that are not diverted inside or outside but remain as 'resources out of place' (i.e. waste). Tables 4.1 and 4.2 give a complete description of an agroecosystem's energy carriers and coefficients.

4.3.3 Turning agroecosystems' energy graphs into spatially-explicit ones

Once we have the agroecosystem's energy network graph (Fig. 4.2), we are interested in the relationships of the evolving complexity of the internal energy loops with the information they contain and the diachronic LCLUC. The next step is converting the incoming-outgoing coefficients (β_i's) to their land matrix expressions, by calculating the mean estimated values of energy fluxes flowing across each land use (in MJ·ha-1).

In most of fluxes there are no difficulties when assigning a value for each land use if they form part of the first two subsystems ('natural' and 'farmland'; Figs. 4.1a and 4.1b). In the 'livestock' subsystem the key point is to set the weight of the whole internal loop which corresponds to each land use, by taking into account that part of the animal bioconversion that goes to each type of farmland (see Tables A1 and A2 in the Appendix). In order to allocate the full energy cost of livestock to different land uses, we not only weighted the values of LS (manure and traction), but LW (dung wasted) as well. Moreover, we have to solve the problem of the energy carriers that flow from one land use to another within farmland when we calculate spatially-specific values of biomass reuses included in FBR and LBR. We may have, e.g. a biomass flow coming from forest clearing that is buried into cropland, or the pruning of vineyards that is burnt and added to the soil of cereal-growing areas, etc. Although these fluxes cancel one another when they are accounted at aggregated level, for the land usages involved in these inter-farmland flows the values for FBR and LBR have to be differentiated depending on whether we are considering a flow entering or going out from each spatial unit of analysis.

Then, in order to link this network of energy flows with the land matrix, we have to correlate both types of data (ingoing and outgoing flows) measured in the same spatial unit of analysis (sample cell). This also requires specifying and measuring the variables we are going to study. Recall that our aim is to analyse the agroecosystem's energy pattern of flows, as a dissipative structure (Prigogine, 1996). Hence, what is relevant here is not only the magnitude of each energy flow as such but two other things captured by our graph modelling: i) the specific part of this network of flows that provides negentropy by storing energy carriers within the agroecosystem and allows for the enhancement of its complexity; and ii) the increasing information embedded in this energy network. According to Ho and Ulanowicz (2005), the most relevant fluxes are the loop producers that have to be detached from the entropy producing flows. For this reason we will use as a first variable β_i^j defined as the quotient of the energy flow relation i associated with the land use j.

$$\beta_1^j = \frac{npp_{h\ j}}{npp_{act\ j}},\ \beta_2^j = \frac{ub_j}{npp_{act\ j}},\ \beta_3^j = \frac{fti_j}{att_j},\ \beta_4^j = \frac{ub_j}{att_j},\ \beta_5^j = \frac{ffp_j}{npp_{h\ j}},\ \beta_6^j = \frac{br_j}{npp_{h\ j}},$$

$$\beta_7^j = \frac{fei_j}{fti_j},\ \beta_8^j = \frac{fii_j}{fti_j},\ \beta_9^j = \frac{lei_j}{lti_j},\ \beta_{10}^j = \frac{lbr_j}{lti_j},\ \beta_{11}^j = \frac{lfp_j}{lps_j},\ \beta_{12}^j = \frac{ls_j}{lps_j}.$$

Here lowercase letters indicate we refer to coefficients, not to variables like was done previously. All the variables of the energy flow graph (Fig. 4.2) are expressed for each land use j. Thus, for each sample cell we have β_i.

$$\beta_i = \sum_{j=1}^{k} \beta_i^j p_j,$$

where p_j is the proportion of the land use j in the corresponding sample cell, and k is the number of different land uses. Starting from this spatially-explicit β_i's we can then calculate the complexity and information carried by energy flows, so as to analyse its relationship with landscape patterns.

4.3.4 From the complexity of energy flows to landscape patterns through information

Once we have defined how to account for spatially-explicit energy flows, we can introduce the three indicators that we are going to use in ELIA. They are ordered hierarchically, according to the logical string that goes from the interplay between energy and information to landscape patterns. Energy storage can be seen as the harnessing of dissipation thanks to the farmers' efforts to generate and enhance energy loops (Ulanowicz, 2003). The intervention of farmers' labour also means that the looping of these biomass reuses is not produced randomly through space, because it is driven by information. Owing to the information delivered by farmers' labour the energy fluxes are directed in one or another way across the land matrix with different intensities. It is precisely because energy carriers flow across different land covers following a deliberate pattern that they imprint a specific mosaic that we recognize as a cultural landscape.

	Energy carriers	Formula	GJ year	
			1860	2000
Single variables	Farmland External Input (FEI)	-	5553	193,383
	Unharvested Biomass (UB)	-	294,693	561,462
	Farmland Waste (FW)	-	0	11,150
	Farmland Biomass Reused (FBR)	-	146,555	12,424
	Livestock Biomass Reused (LBR)	-	96,308	129,822
	Farmland Final Produce (FFP)	-	259,890	73,562
	Livestock External Input (LEI)	-	6657	1,060,277
	Livestock Waste (LW)	-	0	256,502
	Livestock Services (LS)	-	36,980	36,997
	Livestock Final Produce (LFP)[a]	-	2954	238,765
Composed variables	Actually Net Primary Production (NPP_{act})	$NPP_{act} = UB + NPP_h + FW$	797,446	788,421
	Harvested Net Primary Production (NPP_h)	$NPP_h = BR + FFP$	502,753	215,808
	Agroecossytem Total Turnover (ATT)[b]	$ATT = FTI + UB$	483,781	804,267
	Livestock Total Input (LTI)	$LTI = LEI + LBR$	102,965	1,190,098
	Livestock Produce and Services (LPS)	$LPS = LS + LFP$	39,934	532,264
	Farmland Total Input (FTI)	$FTI = FII + FEI$	189,088	242,805
	Farmland Internal Input (FII)	$FII = LS + FBR$	183,535	49,421
	Biomass Reused (BR)	$BR = FBR + LBR$	242,864	142,246
	Final Produce (FP)	$FP = FFP + LFP$	262,843	312,327
	External Input (EI)	$EI = FEI + LEI$	12,209	1,253,660

Table 4.1: Agroecosystem energy carriers taken into account and their values in the Valles case study (1860s, 2000s).

[a] The concept of land produce is the same that Vitousek et al. (1986) used for the Harvested Net Primary Production.

[b] We use the ecological term of 'turnover' adapted from Dettmann (2008) meaning all the energy flow-through in an agroecosystem; in this specific case it refers to all the incoming energy carriers that go to the farmland. For the terminology used, and the set of EROIs obtained from the energy balances, see Tello et al. (2015, 2016) and Galán et al. (2016).

Therefore, energy reinvestement and storage driven by farmers' knowledge produces an effect on landscape patterns and processes. ELIA correlates the following three indicators: i) the complexity attained through the energy storage of loops (E); ii) the information embedded in the energy network of flows (I); and iii) the landscape functional structure (L). Acknowledging from the onset that to collect all the necessary data to analyse the whole environmental impact of the agroecosystem's energy cycles is not possible, we think that the use of the previously explained β_i's is a valuable proxy to give account of a looping rather than a linear set of energy transformations (Giampietro et al., 2011).

The 'loopiness' of energy carriers driven by farmers through UB, BR and LS flows (Fig. 4.2) can be adopted as a measure of E that expresses the energy potentially available for all food chains taking place in the agroecosystem. We are going to start measuring E as the quantity of energy remaining in the system, and then we will measure I that allows the farmers to reproduce the agricultural metabolism thanks to the information embedded in the system. I can be measured taking into account how evenly distributed

Energy coefficients		Formula	Case study values	
			1860	2000
Incoming or outcomming flows	β_1	$\beta_1 = NPP_h/NPP_{act}$	0.630	0.274
	β_2	$\beta_2 = UB/NPP_{act}$	0.370	0.712
	β_3	$\beta_3 = FTI/ATT$	0.391	0.302
	β_4	$\beta_4 = U/ATT$	0.609	0.698
	β_5	$\beta_5 = FFP/NPP_h$	0.517	0.341
	β_6	$\beta_6 = BR/NPP_h$	0.483	0.659
	β_7	$\beta_7 = FEI/FTI$	0.029	0.796
	β_8	$\beta_8 = FII/FTI$	0.971	0.204
	β_9	$\beta_9 = LEI/LTI$	0.065	0.891
	β_{10}	$\beta_{10} = LBR/LTI$	0.935	0.109
	β_{11}	$\beta_{11} = LFP/LPS$	0.074	0.449
	β_{12}	$\beta_{12} = LS/LPS$	0.926	0.070
Information-loss	γ_F	$\gamma_F = (UB + NPP_h)/2NPP_{act}$	0.500	0.493
	γ_L	$\gamma_L = (LS + LFP)/2LPS$	0.500	0.259
Subsystems-contribution	k_1	$k_1 = UB/(UB + BR + LS)$	0.513	0.758
	k_2	$k_2 = BR/(UB + BR + LS)$	0.423	0.192
	k_3	$k_3 = LS/(UB + BR + LS)$	0.064	0.050
	k'_2	$k'_2 = BR/(BR + LS)$	0.868	0.794
	k'_3	$k'_3 = LS/(BR + LS)$	0.132	0.206
Energy Storage	E	$E = \frac{\beta_2+\beta_4}{2}k_1 + \frac{\beta_6+\beta_8}{2}k_2 + \frac{\beta_{10}+\beta_{12}}{2}k_3$	0.618	0.622
Energy Reinvestment Effort	Ee	$Ee\frac{\beta_6+\beta_8}{2}k'_2 + \frac{\beta_{10}+\beta_{12}}{2}k'_3$	0.754	0.361
Energy Information	I	$I = \left(-\frac{1}{6}\sum_{i=1}^{12}\beta_i \log_2 \beta_i\right)(\gamma_F + \gamma_L)$	0.639	0.587

Table 4.2: Agroecosystem energy coefficients, complexity of internal energy loops (E), information held by energy flows (I), and their values in the Valles case study (1860s, 2000s).

the set of pairwise incoming-outgoing fluxes of the graph are. Both indicators, E and I, are assessing characteristics of human-made structures that allow us to dissect energy flows of agroecosystems and bring to light the energy-information interplay. These variables can then be related with L, considering them as the landscape 'imprint' of social metabolism.

4.3.5 Measuring Energy Storage (E) as the complexity of internal energy loops

We understand agroecosystem complexity as the differentiation of dissipative structures that allows for diverse potential ranges in their behaviour (Tainter, 1990). At the same time, the more complex the space-time differentiation is, the more coherent energy is stored within a system (Ho and Ulanowicz, 2005). Hence, higher mean values of even β_i's entail that agroecosystems are increasing in complexity because the different cycles are all coupled together and the residence time of the stored energy is enlarged thanks to a greater interlinked number of transformations looping inside. Accordingly, our way of calculating complexity is as follows:

$$E = \frac{\beta_2 + \beta_4}{2} k_1 + \frac{\beta_6 + \beta_8}{2} k_2 + \frac{\beta_{10} + \beta_{12}}{2} k_3,$$

$$k_1 = \frac{UB}{UB + BR + LS},\ k_2 = \frac{BR}{UB + BR + LS},\ k_3 = \frac{LS}{UB + BR + LS}.$$

Where the coefficients k_1, k_2, k_3 account for the share of reusing energy carriers that are looping through each of the three subsystems (Fig. 4.2).

The formula used implies that E remains within the range $[0, 1]$. E close to 0 implies low reusing of energy carriers—a behaviour that usually corresponds to an agro-industrial management highly dependent on external inputs and with maximum levels of Human Appropriation of Net Primary Production ($HANPP$). E close to 1 implies more internal energy loops, meaning that a high share of energy carriers harvested are reused within the agroecosystem—a behaviour usually associated with organic farming with lower dependence on external inputs, lower biomass extraction as FP, and also moderate levels of $HANPP$.

E assesses the amount of energy flows that go inside, relative to the whole energy flowing across each one of the three subsystems of the network structure of an agroecosystem. Hence E measures the proportion of energy stored on the land coming from each loop considered sequentially. That is, taking into account that a share of the flow stemming from the first loop can still be redirected inside again when flowing across the two subsequent loops. When we account for the three loops nested within one another, we are adopting a landscape standpoint that is focused on what happens with the energy flowing across different land units driven by farmers, and we name this value Energy Storage (E). For some purposes it is also useful focusing the standpoint on what driving these energy throughputs means in terms of human labour allocation. Notice that from a labour cost point of view the ingoing flow of UB is the result of not doing anything (Tello et al., 2015), whereas BR and LS always require investing a farmer's labour. If we calculate this process of energy harnessing by adopting a labour-cost standpoint, we obtain Ee:

$$Ee = \frac{\beta_6 + \beta_8}{2} k_2' + \frac{\beta_{10} + \beta_{12}}{2} k_3',$$

$$k_2' = \frac{BR}{BR + LS},\ k_3' = \frac{LS}{BR + LS}.$$

Indeed, what Ee accounts is only that part of the agroecosystem's energy throughput that involves a labour investment, leaving UB aside. Thus Ee expresses as a coefficient the reinvestment effort made by farmers relative to the energy flowing only across the agricultural and livestock subsystems (Fig. 4.2), and we name this value Energy Reinvestment Effort (Ee).

4.3.6 Measuring Energy Information (I) as shown in the energy flow pattern

The measuring of the information held in the network of energy flows draws on Information Theory (IT)—despite some common misunderstandings that we will try to avoid (Georgescu-Roegen, 1971; Ulanowicz, 2001; Vranken et al., 2014; Cushman 2014). In ELIA, IT is applied to the graph model of the network of energy fluxes that cross an agroecosystem (Figs. 4.1 and 4.2). The equidistribution of the energy carriers flowing across the binary strings that link the nodes of this graph assumes that the information they carry cannot be known beforehand. In this vein information can be seen as a measure of uncertainty, or the degree of freedom for the system to evolve (Prigogine, 1994). When energy flows concentrate in a specific sector of our graph model, the defined pattern tends to vanish. Conversely, the information embedded is the highest in an equidistributed pattern of energy fluxes.

This kind of 'information' is often called structuring information-message that only registers the likelihood of the occurrence of a pair of events (Passet, 1996; Ulanowicz, 2001). It differs from the meaningful content of the information farmers use to direct the fluxes of energy carriers according to a defined purpose, and also from the spatially organized information that can be measured in the land cover diversity of a farmland mosaic—or even from the auto-reflexive information loop of considering the latter as an imprint of the former.

The information quantified in I has an important feature, though: It is always site-specific for the unit of analysis observed, which is a very important trait from a bio-cultural standpoint (Cocks, M., 2004; Robson and Berkes, 2011; Jackson et al., 2011; Gómez-

Baggethun et al., 2012; Barthel et al., 2013; Agnoletti, 2014). When ELIA registers a decrease on I, we wonder to what extent the information running the system has been lost or transferred from the traditional agroecological knowledge of farmers located at landscape level towards higher hierarchical scales, where other people outside the place have taken control over some important parts of the agroecosystem functioning after being linked to increasingly globalized food chains (Johns and Sthapit, 2004; McMichael, 2011; Muradian et al., 2011). Accordingly, we use a Shannon index (Shannon, 1948) adapted to be applied over each pair of β_i's, so that this indicator shows whether the β_i's pairs are evenly distributed or not. This measure of energy information (I) accounts for the equiproportionality of pairwise energy flows that exit from each node in every sub-process:

$$I = -\frac{1}{6}\left(\sum_{i=1}^{1} 2\beta_i \log_2 \beta_i\right)(\gamma_F + \gamma_L), \tag{4.1}$$

$$\gamma_F = \frac{NPP_{act} - FW}{NPP_{act}} = \frac{UB + NPP_h}{UB + NPP_h + FW},$$
$$\gamma_L = \frac{LPS - LW}{LPS} = \frac{LS + LP}{LS + LP + LW}.$$

Base 2 logarithm is applied as probability is dichotomous. Keeping in mind the definition of β_i's, we know that the pairs $\beta_1 - \beta_2$ and $\beta_{11} - \beta_{12}$ don't sum 1, as the rest of the pairs of β_i's do. This is because waste (FW and LW) can also be understood as a lack of information of the system. The introduction of γ_F and γ_L ensures that I remains lower than 1 when the system presents this information loss.

I values close to 1 are those with an equidistribution of incoming or outgoing flows of the agroecosystem's network structure where the structuring information-message is high, whereas values close to 0 means patterns of probability far from equidistribution. I values close to 0 correspond to a low site-specific information content in agroecosystem functioning, which may be related to an industrialized farm system with high $HANPP$ and low relevance of traditional peasant knowledge; or, by contrast, to an almost 'natural' turnover with slight $HANPP$ that may also correspond to rural abandoned forest or pastoral areas at present. Conversely, agroecosystems with I equal to 1 are the ones with equidistributed incoming and outgoing energy flows in each sub-process, as well as with intermediate levels of $HANPP$ (Marull et al., 2015a), that correspond to an organic mixed farming deeply embedded in local knowledge.

4.3.7 Measuring Energy Imprint (L) in the landscape functional structure

In order to correlate the above explained energy-information interplay with landscape functional structure we need to introduce a landscape metric (L) as proxy of biodiversity. A focus on landscape functionality stresses the spatial dimension of biodiversity, focuses on the interplay between disturbances and land cover heterogeneity, and the role of agro-ecological land management in ecosystem service provision (Tscharntke et al., 2005). This perspective relies on the interplay between patch disturbance and land cover diversity as the key mechanism that actually matters in biodiversity maintenance (Loreau et al., 2010). This also brings to light the capacity of agro-forest mosaics to offer a range of habitats that sustain many species (Harper et al., 2005). Much of this biological diversity is apparent at scales larger than plot or farm level, and depends on landscape-wide heterogeneity of land covers.

We use a modification of the Shannon index commonly used in ecology to account for landscape heterogeneity (Vranken et al., 2014). In this land cover dimension, Shannon index is not used for looking at agroecosystems as dissipative structures, but as the spatial 'imprint' of their social metabolism—therefore, without any thermodynamic meaning. We calculate L to capture the equidiversity of land covers into sample cells:

$$L = \left(-\sum_{i=1}^{k} p_i \log_k p_i \right) (1 - p_u).$$

Where k is the number of different land covers (potential habitats) (Fig. 4.1). We consider that the existence of urban land cover p_u results in a loss of potential habitats. Thus, p_i is the proportion of non-urban land covers i into every cell. L can be improved, when data is available, i.e. using the following algorithm:

$$Le = \left(aL + b\frac{ECI}{10} \right) \frac{1}{(a+b)}.$$

In this way we obtain a new indicator Le as proxy of biodiversity (Marull et al., 2015c), capturing landscape patterns (L, heterogeneity) and landscape processes (ECI, connectivity), using Principal Component Analysis –PCA (where a and b are the empirical PCA coeffitients).

After having defined all the ELIA indicators (E, I and L), we are going to analyse their relationship. We surmise that the interplay between E and I jointly leads to complexity, understood as a balanced level of intermediate self-organization (Gershenson and Fernández, 2012). Finally, we assume that the complexity of socio-metabolic fluxes and L are related to landscape ecological processes and biodiversity (Giampietro, 1997; Marull et al., 2015a).

4.3.8 Interplay of energy storage with information

Which configuration is adopted by the whole set of possible values that the interaction between E and I can take? As a first option, we compute some possible combinations of β_i's, and then perform the values of E and I for them, supposing $\gamma_F = \gamma_L = \frac{1}{2}$, $k_1 = k_2 = k_3 = \frac{1}{3}$ (see in Table 4.2 a complete description of energy coefficients). But E differentiates between the different distribution of β_i's values into the system, while I does not.

$$I(\beta_1, \beta_2, \ldots, \beta_{12}) = I(\beta_{\sigma(1)}, \beta_{\sigma(2)}, \ldots, \beta_{\sigma(12)}),$$

where σ is a permutation of β_i's. I provides seven types of zeros. To study these zeros we must look at each pair β_i and β_{2i} (see Fig. 4.2), for $i = 1, 3, 5, 7, 9, 11$, as $I(\beta_i, \beta_{2i}) = 0$ both when $\beta_i = 1$ or $\beta_{2i} = 1$. So we find seven possible combinations that imply $I = 0$, these are: $(\beta_2,\ \beta_4,\ \beta_6,\ \beta_8,\ \beta_{10},\ \beta_{12}) = (0,0,0,0,0,0)$, $(1,0,0,0,0,0)$, $(1,1,0,0,0,0)$, $(1,1,1,0,0,0)$, $(1,1,1,1,0,0)$, $(1,1,1,1,1,0)$, $(1,1,1,1,1,1)$ and any permutation over them. Furthermore, some of these β_i's combinations are unlikely, due to the fact that they do not maintain any equilibrium among loopiness.

Following Tello et al. (2015, 2016), we assume that if the energy amount of BR in an agroecosystem is greater than the energy content of its EI ($BR > EI$), then the ratio of FP over the Total Inputs Consumed (TIC) grows more for any improvement of FP/BR

than for FP/EI (i.e. if we wish a greater FP/TIC, we can to some extent increase EI in order to reduce BR taking advantage of their substitutability, given that $TIC = BR + EI$). Hence we can argue, from the above example, that any increase of EI will imply the corresponding increase of 'non loop-producers' β_i's relations. Accordingly, we suppose that some coherence can be established between the loop-producing β_i's (i.e. not all possible beta-combinations are equally likely).

Fig. 4.3 shows the theoretical representation of interactions between E and I components. $c_i = (i-1)/6$, represent the E values corresponding to (β_2, β_4, β_6, β_8, β_{10}, β_{12}) configurations that make I=0 and all its permutations. We can see an arc that reaches its maximum value on the vertical axis (I) for intermediate values of E, in the horitzontal axis—a figure that can suffer some variances for other β_i's. This figure highlights that our way of measuring the interplay between the information held in agroecosystems fluxes and the complexity of their internal energy loops makes sense. We have maximum information (I) for an intermediate level of complexity provided by the storage of energy carriers looping inside—which for the sake of simplicity we will call henceforth a 'sustainable' agroecosystem.

In the peak point of I (Fig. 4.3) we found an equi-proportionality of incoming and outgoing energy flows, a property that not only is coherent with our way of capturing the information embedded in agroecosystems but also fits with the vector directions of optimal paths found by Tello et al. (2015, 2016) for improving their joint energy efficiency (FP/TIC), depending on whether $BR > EI$ or the opposite. Low levels of site-specific information are found in the landscape either when the agroecosystem tends towards an agro-industrial management by increasingly relying on EI, or towards rural abandonment when farmers' labour and knowledge are withdrawn from it (i.e. either in highly 'intensive-industrialized' farm systems, or in former agroecosystems that presumably are being 'renaturalized'). More information embedded in cultural landscapes becomes a key resource for the future of sustainable farming that seeks to balance agricultural production with biodiversity conservation.

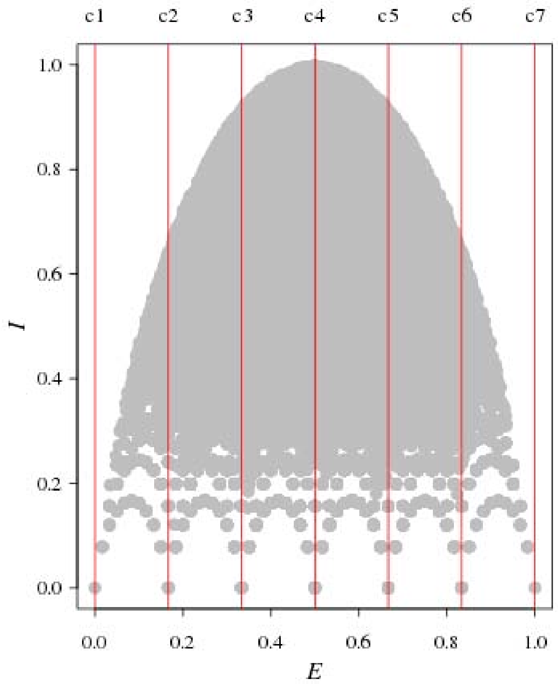

Figure 4.3: Theoretical relationship between complexity of internal energy loops (E) and information held in the network of energy flows (I) of an agroecosystem.

4.3.9 Energy imprint and landscape pattern modelling

The relationship between E, I and L is shown in Fig. 4.4. The values have been obtained from theoretical coefficients for two extreme agroecosystems' typologies (from 'natural' to 'intensive-industrialized' scenarios) listed above (Table 4.3). We propose β_i's for 'natural' (T1), 'balanced' (T3) and 'intensive-industrialized' (T5) agroecosystems. T1 is similar to an ecosystem (i.e. low or null $HANPP$; even β_i's are equal to one, while odd β_i's are equal to zero). T3 has been defined as one with equal proportion of incoming or outgoing energy flows (i.e. intermediate $HANPP$; all β_i's are 1/2). T5 is defined as having given up internal reuses (i.e. high $HANPP$; odd β_i's are equal to one and even β_i's to zero). In the three typologies waste has not been considered, so $\gamma_F = \gamma_L = 0.5$. Regarding (k_1, k_2, k_3), in the case of T1 $k_1 = 1$ and $k_2 = k_3 = 0$, which means that all the reuse comes from UB; in T2 it is considered that $k_1 = k_2 = k_3 = \frac{1}{3}$; and in T3 $k_2 = 1$ and $k_1 = k_3 = 0$.

In addition, two other agroecosystems' typologies have been introduced to show the results for intermediate values between the two extreme scenarios taken into account. Lastly, the points shown in Fig. 4.4 come from a probabilistic approximation by considering all possible land use combinations in a cell. The first form is obtained using the values of the 'natural', 'balanced' and 'intensive-industrialized' agroecosystems (T1, T3 and T5), while in the second also the intermediate agroecosystems have been considered (T1, T2, T3, T4 and T5). As a result Fig. 4.4 reveals the relationship between complexity of energy flows (E), the information carried in them (I), and their joint spatial imprint in agroecosystems (L). This ELIA modelling allows us to test the relationship we deem to exist between the simultaneous loss in energy throughput and landscape efficiency (Marull et al., 2010), going a step forward from previous explorations of the links between intermediate levels of sociometabolic disturbance as assessed with $HANPP$ and ecological functioning of cultural landscapes (Marull et al., 2015a).

ELIA is the energy–landscape integrated analysis resulting from the model. In order to improve its application, we propose a simplified indicator that combines the landscape functional structure with the complexity of the interlinking pattern of energy flows and the information carried by them, as a proxy of biodiversity in agroecosystems:

$$ELIA = 2(E \cdot I)L,$$

where E is the energy storage, I is the information carried by the network structure of energy flows and L is the energy imprint in the landscape structure (L can be substituted by Le; i.e. including functional attributes of the landscape).

4.3.10 Case study application

Many traditional Mediterranean agroecosystems had kept complex land use mosaics, which were later turned into homogeneous land covers –increasingly polarized between intensive monocultures and spontaneous afforestation of abandoned lands— as a result of the industrialization of farm systems fuelled by cheap fossil fuels that began in the 1960s (Gerard et al., 2010; Parcerisas et al., 2012; Marull et al., 2014). This historical process can be taken as a natural experiment for comparative analysis (Odum, 1984; Gliessman, 1990; Tscharntke et al., 2005). At the same time, the conservation of cultural landscapes has to take into account the human role in shaping their present ecological features (Gustavsson et al., 2007; Henle et al., 2008). ELIA looks at these landscape changes as the 'imprint'

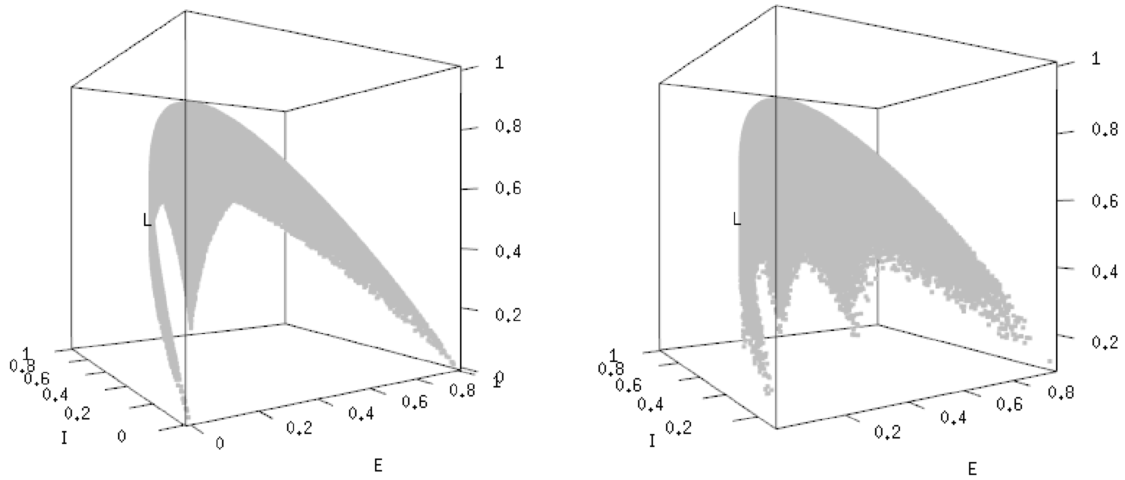

(a) 3 Agroecosystem typologies

(b) 5 Agroecosystem typologies

Figure 4.4: Theoretical relationship between complexity of internal energy loops (E), information held in the network of energy flows (I) and landscape functional structure (L), taking three (a) and five (b) agroecosystems typologies (Table 4.3).

Coefficients		T1	T2	T3	T4	T5
Incoming or outcomming flows	β_1	0	0.25	0.5	0.75	1
	β_2	1	0.75	0.5	0.25	0
	β_3	0	0.25	0.5	0.75	1
	β_4	1	0.75	0.5	0.25	0
	β_5	0	0.25	0.5	0.75	1
	β_6	1	0.75	0.5	0.25	0
	β_7	0	0.25	0.5	0.75	1
	β_8	1	0.75	0.5	0.25	0
	β_9	0	0.25	0.5	0.75	1
	β_{10}	1	0.75	0.5	0.25	0
	β_{11}	0	0.25	0.5	0.75	1
	β_{12}	1	0.75	0.5	0.25	0
Information - loss	γ_F	0.5	0.5	0.5	0.5	0.5
	γ_L	0.5	0.5	0.5	0.5	0.5
Subsystems contribution	k_1	1	0.33	0.33	0.33	0
	k_2	0	0.33	0.33	0.33	1
	k_3	0	0.33	0.33	0.33	0

Table 4.3: Theoretical energy coefficients for five agroecosystems typologies (T_i). T_1 corresponds to the most ‘natural’ agroecosystem, T_3 refers to a ‘balanced’ agroecosystem, T_5 refers to an ‘industrial-intensive’ agroecosystem. Then, T_2 and T_4 correspond to intermediate values.

of the energy carriers driven by farmers, and highlights the bio-cultural role performed by the changing complexity-information interplay in the energy profiles of agroecosystems.

ELIA is applied to a case study that comprises four municipalities (Caldes de Montbui, Castellar del Vallès, Polinyà and Sentmenat) in the Vallès County of the Barcelona Metropolitan Region (Fig. 4.5), located westward in the Mediterranean biodiversity hotspot

(Myers et al., 2000). Some authors have been studying this site from a long-term socio-ecological perspective (from c.1860 to the 2000s), by reconstructing the energy balances of farm systems (Cussó et al., 2006a, 2006b) and the ecological functioning of cultural landscapes (Marull et al., 2010). This led us to integrate the study of sociometabolic profiles of energy flows with the landscape ecology performance that existed in past organic farming, or characterize agro-industrial systems at present.

In mid-nineteenth century the Vallès County (Fig. 4.5) reached a population density of 65 inhab./km^2 close to the highest level that an organic rain-fed farming system could maintain in the Mediterranean bioregion in past times. This challenge drove peasants to combine as a response an export-led winegrowing specialization with traditional agro-forest mosaics (Garrabou et al., 2010; Badia-Miró and Tello, 2014). Maintaining and reproducing this poly-cultural landscape entailed a tight integration between cropland and livestock breeding, by means of a labour-intensive mixed farming (Olarieta et al., 2008, 2011; Tello et. al., 2012). Fodder and feed crops occupied 14% of cropland area in the organic case study c.1860, while livestock was also grazing pastures in 7% of farmland area, or in the grass layers below open forests and other uncultivated land. While all these links between diverse land covers through livestock feeding helped to maintain agroforest mosaics, the energy flows of draught power and manure provided by these animals returned again to cropland. Especially in solar-based agroecosystems that practically only depend on a single type of external inputs (labour), this integration among cycles involves the well-known stiffness in societal land use patterns due to the simultaneous need for food (cropland), firewood (forest) and animal feeding (pasture) (Guzmán and González de Molina, 2009). These were common features of late organic farm systems at the eve of the socio-ecological transition towards industrial agricultures in Europe (Krausmann, 2004).

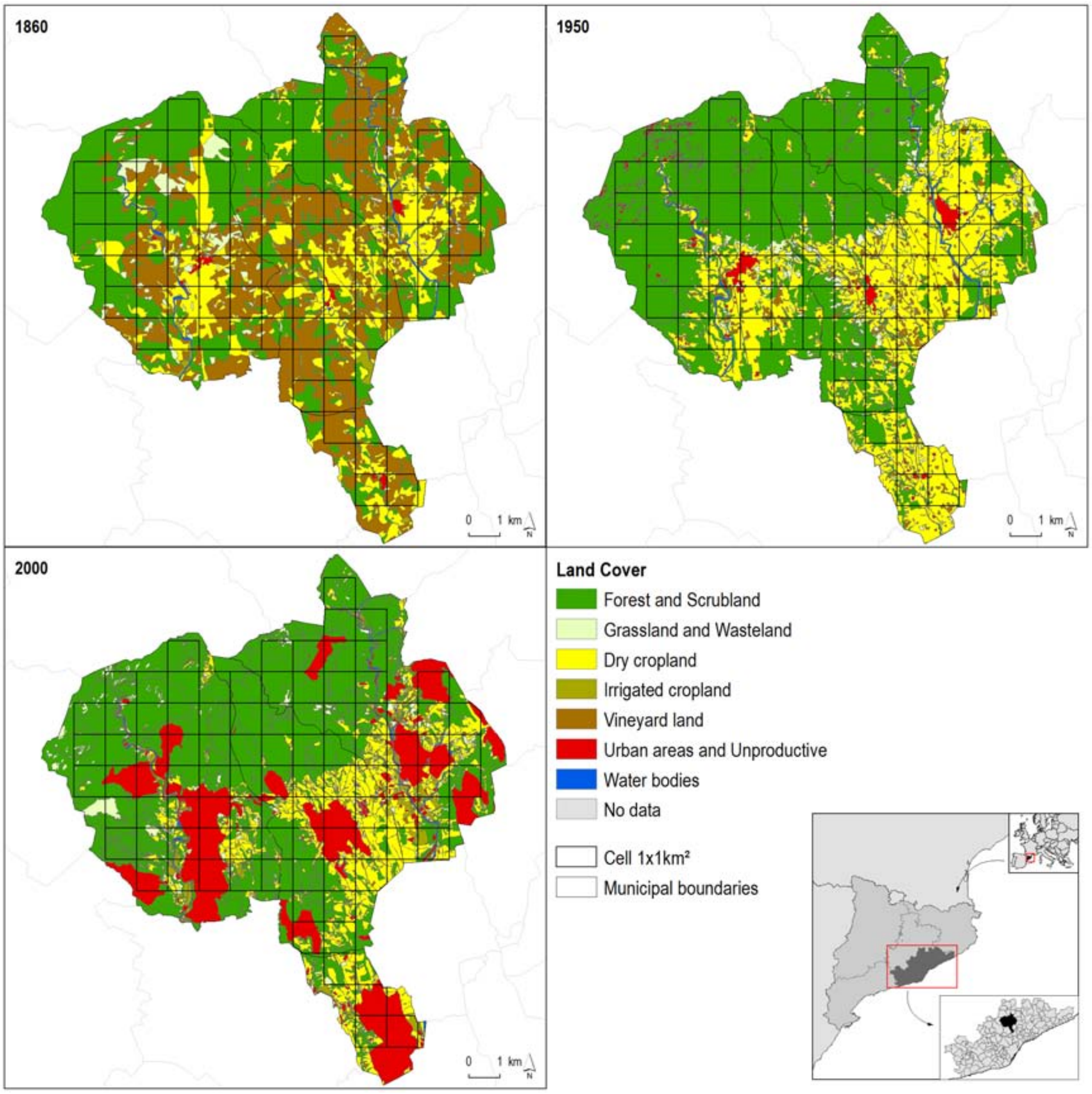

Figure 4.5: Land-cover maps of the Vallès case study (1860s, 1950s and 2000s).

4.4 Results

4.4.1 Land-use changes and landscape patterns from the 1860s to 2000s

Between the 1860s and 1950s the area allocated to vineyards was reduced in favour of cereals, hazelnut trees, irrigated orchards, woodland and pasture (Fig. 4.5). Cropland acreage fell from 58% to 34% of the total area, while urban expansion remained modest and the agrarian landscape mosaic was kept on the lowlands. Then, from the 1950s to the

Land covers	ha			%		
	1850	1950	2000	1850	1950	2000
Forest and Scrubland	3461.1	5556.9	5366.2	36.4%	58.5%	56.5%
Grassland and pastureland	273.9	282.8	257.3	2.8%	2.9%	2.7%
Dry cropland	1906.2	2966.8	1530.7	20.1%	31.2%	16.2%
Irrigated cropland	150.6	0	244.6	1.5%	0.0%	2.5%
Vineyard land	3452.7	227.6	16.1	36.4%	2.4%	0.1%
Water bodies	151.6	131.4	100.7	1.6%	1.3%	1.1%
Urban areas and Unproductive	55.0	320.0	1970.0	0.6%	3.3%	20.7%
No data	34.4	0	0	0.4%	0.0%	0.0%
Landscape structure $L = \left(-\sum_{i=1}^{k} p_i \log_k p_i \right) (1 - p_u)$	0.72	0.50	0.38	-	-	-

Table 4.4: Land-cover and landscape functional structure (L) in the Vallès case study (1860s, 1950s and 2000s). Land-covers into all 1 km x 1 km sample cells (see Fig. 4.5).

2000s, cropland area shrunk to 19% due to a wide-scale adoption of the 'green revolution'. On the one hand 1,947 ha were devoted to urban expansion (16% of the useful area, two thirds at the expense of arable land and the rest of woodland and pastures). On the other hand, 646 ha of abandoned cropland were reforested (5%). The former agro-forest mosaics tended to vanish, which led to a significant decrease of spatially organized heterogeneity: Land-cover diversity fell from $L = 0.72$ in the 1860s, to $L = 0.38$ in 2000s (Table 4.4). Hence, our study area underwent an important reduction in the kind of landscape hetrogeneity that it is increasingly related to farm- associated biodiversity worldwide (Perfecto and Vandermeer, 2010).

4.4.2 Energy transition of agroecosystems from the 1860s to 2000s

The metabolic profile of the case study in the 1860s shows a solar-based agriculture that followed the strategy currently known as Low External Inputs Technology (LEIT) with strong reuse of biomass addressed to maintain the underlying funds—mainly soil fertility, and also the associated biodiversity probably as a side effect (Marull et al., 2014, 2015b). Conversely, in the 2000s chemical fertilizers and tillage mechanization following the massive spread of the green revolution allowed land and labour productivity to increase, rendering the effort of keeping internal reuses unnecessary. This combined with huge imports of animal feed consumed in industrial livestock breeding. Meat became the main component of FP, and relegated arable land to the role of provider of fodder, feed and straw to feedlots. At the same time woodland grew with the withdrawal of farming and grazing in the steepest areas, while its human use shrunk due to the ongoing rural abandonment (Cussó et al., 2006a, 2006b).

The use of graph modelling as an analytical tool (Fig. 4.6) allows us to reveal how the agroecosystem c.1860 was indeed highly dependent on internal energy loops and relied on a low amount of external energy fluxes. To obtain FP with very few EI (a LEIT strategy), it had to bear a high 'sustainability cost' of BR while a significant amount of UB available for the farm-associated biodiversity was still kept (Guzmán and González de Molina, 2009). In turn, the graph model for the 2000s also reveals the deep transformation that has taken place in farming strategy, currently addressed to industrial livestock breeding as shown by the enormous amount of LTI, combined with a subsidiary monoculture of animal feeding crops.

A key component in agroecosystem analysis is to determine which part of the energy flowing is redirected again towards the land matrix, in order to keep the underlying renewable funds. Accordingly, we propose three indicators calculated from the graph modelling (E, Ee and I): E assesses the entire proportion of energy stored in the agroecosystem throughout the successive nested loops, either by means of farming activity or not, relative to its whole energy turnover ($E = 0.618$ in 1860 and $E = 0.622$ in 2000). Ee expresses as a coefficient, relative only to the agricultural and livestock turnover, the labour investment made by farmers to maintain the farm system ($Ee = 0.754$ in 1860 and $Ee = 0.361$ in 2000; Table 4.2). In turn, the network structure of these energy flows and loops provides us with a measure of the information (I) they contain ($I = 0.639$ in 1860 and $I = 0.587$; Table 4.4).

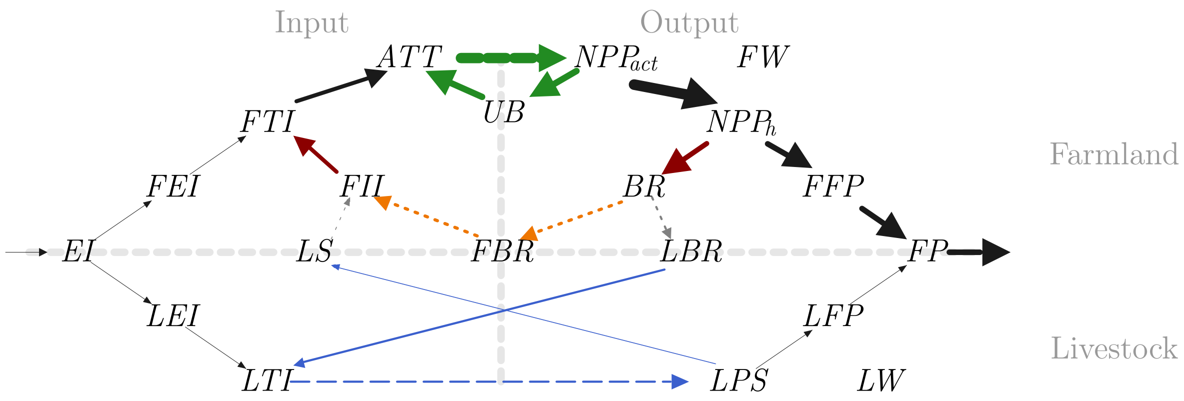

(a) 1860

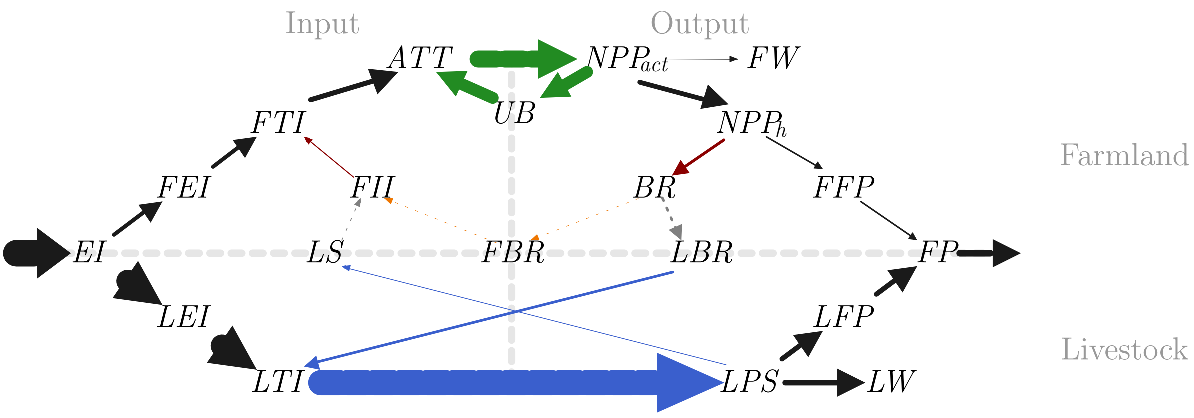

(b) 2000

Figure 4.6: Graph model of energy carriers flowing in the farm systems of the Vallès case study in the 1860s (a) and 2000s (b).

4.4.3 Complexity and information of energy flows in the 1860s and 2000s

We calculated E and I over energy carriers of agroecosystems' flows, and their specific coefficients (Tables 4.1 and 4.2). These results are consistent with what has been discussed in previous sections. Circa 1860 a traditional organic farm system was closer to what we have considered a 'balanced' agroecosystem typology than to the agro-industrial management adopted in the 2000s, which fits with what we have considered as 'industrialized-intensive' farm systems. We also expected that a LEIT strategy would have scored higher information (I) values combined with moderately high energy reinvestment (Ee) and storage (E) indices, as shown by the results. Conversely, resorting to industrial feedlots and cereal monocultures has led to a decrease of the information embedded in the local agroecosystem in the 2000s.

Seen at aggregate level the results show comparable energy storages for the two time-points, although these similar E values conceal that those ingoing energy flows followed very different paths across the three subsystems interlinked in the corresponding graph models (Fig. 4.6): c.1860 a great deal of them were biomass reused into farmland in a way that entailed many interconnections between cropland, forest and livestock, and showing an even distribution of energy flows among them; conversely, in 2000s these incoming energy flows turned out to be mainly unharvested biomass left in abandoned woodlands after forest transition. Ee values highlight these differences by showing that c.1860 the efforts that farmers made in energy reinvestment were much higher than in 2000s, while the energy storage that takes place in current industrial farm systems is an unintended result of the withdrawal of farmer's activity ensuing rural abandonment. Indeed, it concentrates in woodlands kept unexploited which have no bonds with cropland tillage and animal husbandry. Whereas in traditional organic farm systems the incoming flows were nesting all the three loops of the agroecosystem, in current industrial farm systems they stay either accumulated in forests, or they appear as dung slurry stemming from feedlots where animal intake comes from abroad (Table A2 in the Appendix). The splitting among subsystems that we observe in 2000s, and the disconnection between energy flows crossing land covers, is coherent with the decrease of the average farmers' energy reinvestment (Ee) and with the lower values of information (I) found in the agroecosystem's network structure compared with c.1860.

The disaggregated results in Table 4.1 also show a noteworthy decrease in NPP_h from 503 GJ in the 1860s to 216 GJ in the 2000s driven by rural abandonment and spontaneous reforestation of the study area (Table 4.4). Although this entailed an increase of UB, from 295 GJ to 561 GJ respectively, this did not translate into a potentially higher farm-associated biodiversity due to the simultaneous decrease in land use complexity and the loss of information embedded in the cultural landscape (Marull et al., 2015a; Tello et al., 2015;

Galán et al., 2015). Just making more biomass available to ecological food chains, while the number of habitats is reduced in a more homogeneous landscape, instead of enhancing biodiversity probably only increases the populations of some better adapted species (Tello et al., 2014; Marull et al., 2014).

4.4.4 Energy-landscape modelling applied in the 1860s and 2000s

To run the ELIA model we have to work with spatially-explicit energy carriers and coefficients (as measured in 1x1 km^2 sample cells, Fig. 4.5; see also Table A1 and Table A2). Looking at the relationships between land covers and the three variables $E - I - L$ (Fig. 4.7) we see that in the traditional organic agroecosystem E and I values ranged from 0.4 to 0.7, whereas in the current agro-industrial management there exists much more variability. Circa 1860 higher E and I can be found independently of the land cover type considered, which suggests that they were tightly interlinked with one another through sociometabolic energy fluxes. In the 2000s, E is clearly related to the role UB is playing in unmanaged woodland, while I is kept at intermediate-low levels only in dry cropland and some forests. The aggregated Energy-Landscape Integrated Analysis results show ELIA = 0.568 in 1860 and ELIA = 0.278 in 2000.

Fig. 4.8 shows both the theoretical and the empirical $E - I - L$ relationships in the Vallès County in a two dimensional projection of a three dimensional figure (see also Fig. 4.4). Lowest theoretical values of L correspond to lowest values of I for each E; furthermore, for intermediate values of E, I attains its maximum (Fig. 4.8a). This phenomenon is less evident in the empirical case of the 1860s, where points are closer than in 2000s (Fig. 4.8b). This is due to the fact that in the 1860s the cells' land cover distribution is similar, being tightly integrated to one another and having all of them higher energy complexity and higher information embedded. Conversely, in the 2000s there is more diversity among the cells' land cover distribution, owing to the simultaneous loss of landscape functional structure, energy complexity and site-specific information. This means that by applying ELIA to the selected size of cells we are capturing the socio-ecological role of the typical Mediterranean agro-forest mosaics that existed c.1860, and tended to vanish in the 2000s.

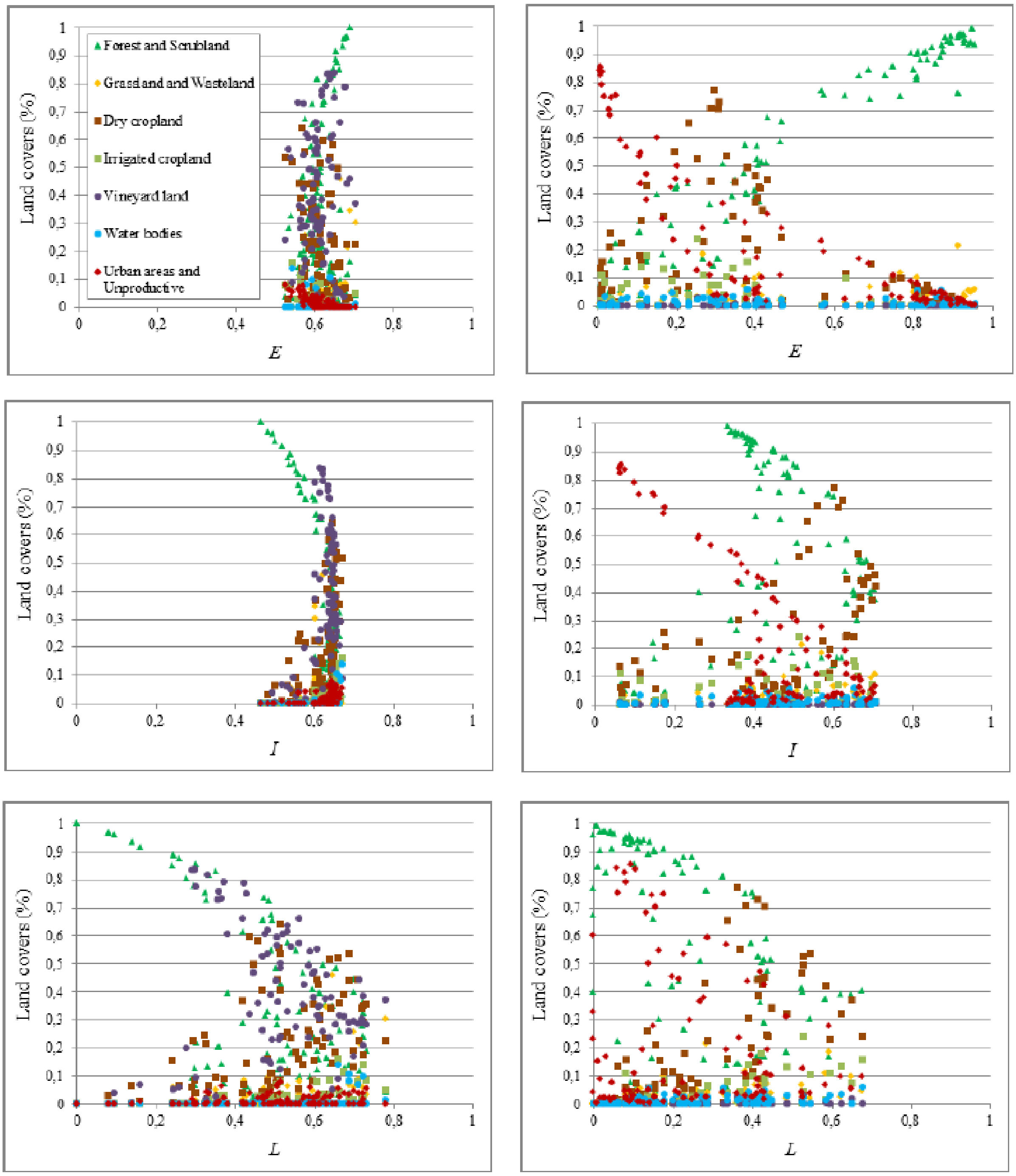

(a) (b)

Figure 4.7: Empirical relationship between the distribution of land covers in the Vallès case study in the 1860s (a) and 2000s (b), and the following indicators: complexity of internal energy loops (E), information held in the network of energy flows (I) and landscape functional structure (L).

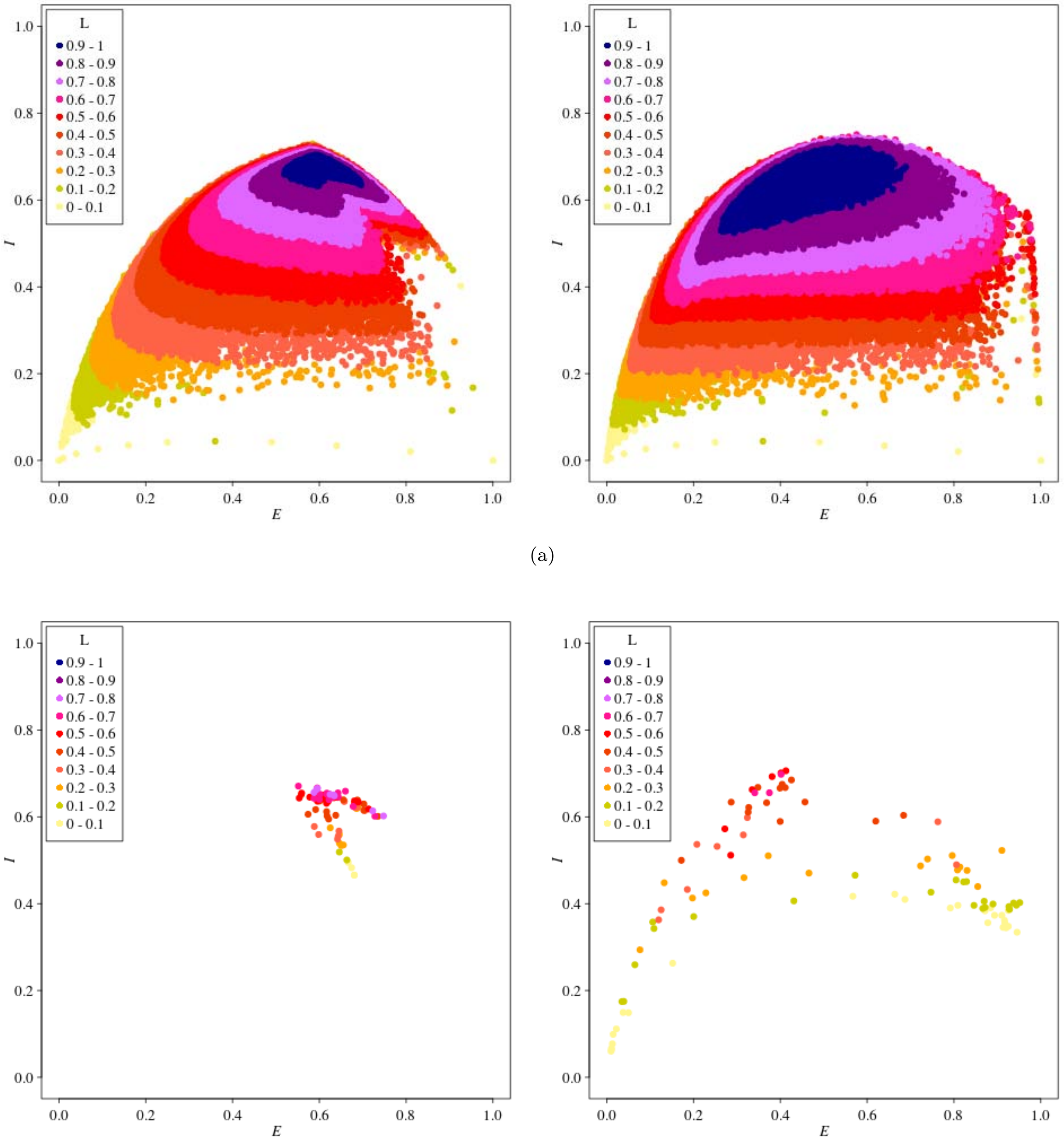

(a)

(b)

Figure 4.8: Relationship between complexity of internal energy loops (E), information held in the network of energy flows (I) and landscape functional structure (L). Theoretical values (a), and empirical results (b) in the Vallès case study (1860s and 2000s).

To sum up, the higher values found in ‘energy storage-reuse’ (E) and ‘energy message-information’ (I) in the 1860s (Fig. 4.8b) correspond to a lower dissipative structure, which was imprinted in the agro-ecological landscape (L) according to the typical mosaic shape of a ‘mixed-farming’ system. Instead of that, cells in the 2000s show a more polarized pattern, where some ‘natural’ landscapes (involved in forest transition) have low dissipative structures, while most ‘industrial-intensive’ landscapes (intensified cropland, feedlots that rely on imported feed and urbanized areas) are highly dissipative structures. These results highlight the bio-cultural role that the information embedded in the land matrix (I) plays as a crucial link between socio-metabolic energy looping fluxes (E) and landscape functioning (L) in agroecosystems (Marull et al., 2015c).

4.5 Conclusions

The main aim of this chapter has been to test the hypothesis that what lies behind the deterioration in the energy yield of agroecosystems, as a result of the current crisis of the rural world that is losing its age-old capacity to keep an integrated land use management, is a considerable decrease of landscape efficiency, related to a misplacing of information held by energy fluxes (local farmers’ knowledge) and its mutual interplay with energy-loop complexity. We have built an Energy-Landscape Integrated Analysis (ELIA) that allows us to measure both the energy storage as the complexity of internal energy loops, and the energy information held in the whole network of sociometabolic energy fluxes, in order to correlate both with the energy imprint in the landscape functional structure. The case study shows how landscape heterogeneity of Mediterranean land use mosaics, created by traditional organic mixed-farming, tended to vanish as a result of simultaneous reduction in the complexity of the interlinking pattern of energy carriers flowing across the land matrix and the quantity of information carried by them. From this case study we draw two main provisory conclusions, and a future research agenda:

Firstly, that the path followed by ‘industrialized-intensive’ agroecosystems which get rid of internal reuses to rely on increasing external fossil inputs has led to a loss of habitats in a simplified and monotonous landscape, in spite of the simultaneous ‘land sparing’ effect of steep land abandonment and forest transition that has taken place in the meantime. Land-use intensification and abandonment have been the joint outcome of giving up the former integrated multiple-use of farm systems. Both have entailed a reduction in land cover diversity and ecotones. Even if the amount of unharvested biomass free to feed ecological food chains has increased as a result of land abandonment, this has probably only enlarged the population of some species because of the lack of habitat differentiation in the land matrix. Recent studies in Mediterranean cultural landscapes reveal that the conservation of a heterogeneous and well-connected land matrix with a positive interplay between human disturbances and land cover/land use complexity are able to hold high species richness at regional scale (i.e. birds; Marull et al. 2015a), landscape scale (i.e. orchids; Marull et al. 2014) and local scale (i.e. butterflies; Marull et al. 2015b). Hence, the apparent land use polarization experienced in the 2000s (Fig 4.8b) has entailed an interlinked decrease in energy complexity, site-specific information held and land cover richness, leading to a likely loss of landscape capacity to host biodiversity.

Secondly, we infer that the opposite strategy of more 'sustainable' agroecosystems, which consists of saving external inputs by replacing them with internal reuses, also requires achieving a balance between human appropriation of net primary production and keeping high biodiversity in the landscape. By reinvesting as reuses a relevant share of the harvested biomass, and maintaining an integrated land use management, organic farmers seek to balance human pressure on the land with the increasing complexity, information and resilience of agroecosystems. This strategy will also have an upper limit though, given that up to a point increasing harvested phytomass, either reused by farmers or consumed outside, will decrease the unharvested share let free for the associated biodiversity. We deem that beyond a threshold land use intensification will no longer be 'sustainable' even in organic agriculture.

In the same vein, the capacity provided by organic agroecosystems able to shelter a high farm-associated biodiversity needs to be supplemented by natural protected spaces which offer refuge for the surviving populations of many species that recolonize the land matrix after each farming disturbance, as well as of sanctuaries for some rare highly-specialist species unable to withstand recurring disturbances (Tscharntke et al. 2012). By linking these protected sites one another, the heterogeneous cultural landscapes which host a rich α- and β-biodiversity may also provide suitable ecological connectors to ensure γ-biodiversity at the regional level—as argued by a land sharing approach (Gabriel et al. 2006). We deem that by combining landscape ecology metrics with a measure of the site-specific energy-information interplay exerted by farming, a useful assessment can be made to capture the underlying dynamics between land use patterns and species richness.

Confirming or rejecting these provisory hypotheses requires further research applying ELIA to more locations and time periods, and using large biodiversity datasets in order to find out where the abovementioned critical thresholds in energy throughputs and the information-complexity interplay are placed. This research agenda would help to reveal how and why different agroecosystem managements lead to key turning points in the relationship of the pattern of energy flows with landscape ecological functioning and biodiversity. No doubt, the results will be very useful for designing more sustainable farm systems worldwide in the future.

Appendix A

See Tables A1 and A2.

1860	Forest and scrubland	Grassland pastureland	Dry cropland	Irrigated cropland	Vineyard land	Water bodies	Urban areas unproductive
fei	61	61	814	5,091	556	0	0
ub	31,74	2,482	26,922	37,605	18,011	16,369	0
fw	0	0	0	0	0	0	0
fbr_1	1,756	0	8,235	8,539	27,418	0	0
fbr_2	0	0	10,257	26,728	27,418	0	0
lbr_1	2,893	15,05	24,618	20,842	4,387	0	0
lbr_2	1,795	9,263	10,593	13,23	13,629	0	0
ffp	35,784	0	14,597	27,184	12,616	0	0
lei	124	640	732	914	942	0	0
lw	0	0	0	0	0	0	0
ls	689	3,555	4,067	5,076	5,234	0	0
lfp	55	284	325	406	418	0	0
npp_{act}	72,174	17,532	74,372	94,17	62,432	16,369	0
npp_h	40,433	15,05	47,45	56,565	44,421	0	0
br	4,649	15,05	32,853	29,381	31,806	0	0
fti	750	3,616	15,137	36,895	33,209	0	0
fii	689	3,555	14,324	31,804	32,652	0	0
ei	185	701	1,546	6,005	1,498	0	0
lps	744	3,839	4,391	5,482	5,652	0	0
lti	1,919	9,903	11,325	14,144	14,57	0	0
att	32,49	6,098	42,059	74,5	51,219	16,369	0

Table A1: Spatially-explicit values of the energy carriers (GJ/km^2) flowing across the different land covers in the agro-ecological landscape of the Vallès case study (1860s, 2000s).

1860	Forest and scrubland	Grassland pastureland	Dry cropland	Irrigated cropland	Vineyard land	Water bodies	Urban areas unproductive
fei	2,448	0	73,698	128,311	80,618	0	0
ub	76,828	14,615	15,465	17,113	4,744	16,369	0
fw	0	0	1,418	23,504	76,109	0	0
fbr_1	0	0	2,469	26,979	0	0	0
fbr_2	0	0	2,469	26,979	0	0	0
lbr_1	139	139	62,307	42,592	0	0	0
lbr_2	255	255	62,744	31,351	71,876	0	0
ffp	3,537	0	18,908	47,181	22,431	0	0
lei	2,085	2,085	512,445	256,046	587,028	0	0
lw	0	0	120,798	102,724	40,655	0	0
ls	73	73	17,881	8,934	20,484	0	0
lfp	470	470	115,398	57,659	132,194	0	0
npp_{act}	80,504	14,754	100,567	157,369	103,284	16,369	0
npp_h	3,676	139	83,684	116,752	22,431	0	0
br	139	139	64,776	69,571	0	0	0
fti	2,521	73	94,048	164,225	101,102	0	0
fii	73	73	20,35	35,914	20,484	0	0
ei	4,534	2,085	586,143	384,357	667,646	0	0
lps	542	542	254,077	169,317	193,332	0	0
lti	2,341	2,341	575,189	287,396	658,905	0	0
att	79,349	14,687	109,513	181,338	105,846	16,369	0

Table A1: (Continued) Spatially-explicit values of the energy carriers (GJ/km 2) flowing across the different land covers in the agro-ecological landscape of the Vallès case study (1860s, 2000s).

Variables: Actual Net Primary Production (npp_{act}); Unharvested Biomass (ub); Harvested Net Primary Production (npp_h); Biomass Reused (br); Farmland Biomass Reused (fbr); Livestock Biomass Reused (lbr); Farmland Final Produce (ffp); External Inputs (ei); Farmland External Inputs (fei); Livestock External Inputs (lei); Livestock Total Inputs (lti); Livestock Produce and Services (lps); Livestock Final Produce (lfp); Livestock Services (ls); Final Produce (fp); Agro-ecosyten Total Turnover (att); Farmland Total Inputs (fti); Farmland Internal Inputs (fii).

1860	β_1	β_2	β_3	β_4	β_5	β_6	β_7	β_8	β_9	β_{10}	β_{11}	β_{12}	γ_F	γ_L	k_1	k_2	k_3	E	E_c
Forest and scrubland	0.56	0.44	0.02	0.98	0.89	0.11	0.08	0.92	0.06	0.94	0.07	0.93	0.50	0.50	0.86	0.13	0.02	0.69	0.57
Grassland and pastureland	0.86	0.14	0.59	0.41	0.00	1.00	0.02	0.98	0.06	0.94	0.07	0.93	0.50	0.50	0.12	0.71	0.17	0.90	0.98
Dry cropland	0.64	0.36	0.36	0.64	0.31	0.69	0.05	0.95	0.06	0.94	0.07	0.93	0.50	0.50	0.42	0.51	0.06	0.69	0.83
Irrigated cropland	0.60	0.40	0.50	0.50	0.48	0.52	0.14	0.86	0.06	0.94	0.07	0.93	0.50	0.50	0.52	0.41	0.07	0.58	0.73
Vineyard land	0.71	0.29	0.65	0.35	0.28	0.72	0.02	0.98	0.06	0.94	0.07	0.93	0.50	0.50	0.33	0.58	0.10	0.68	0.86
Water bodies	0.00	1.00	0.00	1.00	0.00	0.00	0.00	0.00	0.00	0.00	0.00	0.00	0.50	0.00	1.00	0.00	0.00	0.00	0.00
Urban and unproductive areas	0.00	0.00	0.00	0.00	0.00	0.00	0.00	0.00	0.00	0.00	0.00	0.00	0.00	0.00	0.00	0.00	0.00	0.00	0.00

2000	β_1	β_2	β_3	β_4	β_5	β_6	β_7	β_8	β_9	β_{10}	β_{11}	β_{12}	γ_F	γ_L	k_1	k_2	k_3	E	E_c
Forest and scrubland	0.05	0.95	0.03	0.97	0.96	0.04	0.97	0.03	0.89	0.11	0.87	0.13	0.50	0.50	1.00	0.00	0.00	0.96	0.06
Grassland and pastureland	0.01	0.99	0.00	1.00	0.00	1.00	0.00	1.00	0.89	0.11	0.87	0.13	0.50	0.50	0.99	0.01	0.00	0.99	0.70
Dry cropland	0.83	0.15	0.86	0.14	0.23	0.77	0.78	0.22	0.89	0.11	0.45	0.07	0.49	0.26	0.16	0.66	0.18	0.37	0.41
Irrigated cropland	0.74	0.11	0.91	0.09	0.40	0.60	0.78	0.22	0.89	0.11	0.34	0.05	0.43	0.20	0.18	0.73	0.09	0.32	0.37
Vineyard land	0.22	0.05	0.96	0.04	1.00	0.00	0.80	0.20	0.89	0.11	0.68	0.11	0.13	0.39	0.19	0.00	0.81	0.10	0.11
Water bodies	0.00	1.00	0.00	1.00	0.00	0.00	0.00	0.00	0.00	0.00	0.00	0.00	0.50	0.00	1.00	0.00	0.00	0.00	0.00
Urban and unproductive areas	0.00	0.00	0.00	0.00	0.00	0.00	0.00	0.00	0.00	0.00	0.00	0.00	0.00	0.00	0.00	0.00	0.00	0.00	0.00

Table A2: Spatially-explicit energy coefficients1 of the graph model of interlinked energy carriers flowing across the different land covers in the agro-ecological landscape of the Vallès case study (1860s, 2000s).

Note: 1 β_i's are the incoming-outgoing coefficients, β_i's are the information-loss coefficients, and k_i's the subsystem-contribution coefficients.

Appendix B

Supplementary data associated with this work can be found, in the online version, at http://dx.doi.org/10.1016/j.ecolind.2016. 01.015.

4.6 Bibliography

[1] Agnoletti, M., 2006. The conservation of cultural landscapes. CAB International, Cambridge.

[2] Agnoletti, M., 2014. Rural landscape, nature conservation and culture: Some notes on research trends and management approaches from a (southern) European perspective. Landscape and Urban Plan. 126, 66–73. doi:10.1016/j.landurbplan.2014.02.012

[3] Altieri, M., 1999. The ecological role of biodiversity in agroecosystems. Agr Ecosyst Environ 74, 19-31. doi:10.1016/S0167-8809(99)00028-6

[4] Badia-Miró, M. and Tello, E., 2014. Vine-growing in Catalonia: the main agricultural change underlying the earliest industrialization in Mediterranean Europe (1720–1939). Eur. Rev. Econ. Hist. 18(2), Volume 18, 203-226. doi:10.1093/ereh/heu006

[5] Balmford, A., Green, R. and Phalan, B., 2014. What conservationists need to know about farming. Proc. R. Soc. B.doi:10.1098/rspb.2012.0515

[6] Barthel, S., Crumley, C. and Svedin, U., 2013. Bio-cultural refugia—Safeguarding diversity of practices for food security and biodiversity. Global Environ Chang 23(5), 1142–1152.

doi:10.1016/j.gloenvcha.2013.05.001

[7] Bengtsson, J., Angelstam, P., Elmqvist, T., Emanuelsson, U., Folke, C., Ihse, M., Moberg, F. and Nyström, M., 2003. Reserves, Resilience and Dynamic Landscapes. Ambio 32(6), 389-396. doi:http://dx.doi.org/10.1579/0044-7447-32.6.389

[8] Cardinale, B. J., Duffy, J. E, Gonzalez, A., Hooper, D. U., Perrings, Ch., Venail, P., Narwani, A., Mace, G., Tilman, D., Wardle, D. A., Kinzig, A. P., Daily, G. C., Loreau, M., Grace, J. B., Larigauderie, A., Srivastava, D. S. and Naeem, S., 2012. Biodiversity loss and its impact on humanity. Nature 486, 59-67.doi:10.1038/nature11148

[9] Cocks, M., 2004. Biocultural Diversity: Moving Beyond the Realm of 'Indigenous' and 'Local' People. Hum. Ecol. 34(2), 185-200.doi:10.1007/s10745-006-9013-5

[10] Cushman, S. A., 2014. Thermodynamics in landscape ecology: the importance of integrating measurement and modeling of landscape entropy. Landscape Ecol. doi:10.1007/s10980-014-0108-x

[11] Cussó, X., Garrabou, R. and Tello, E., 2006a. Social metabolism in an agrarian region of Catalonia (Spain) in 1860–1870: Flows, energy balance and land use. Ecol. Econ. 58(1), 49–65. doi:10.1016/j.ecolecon.2005.05.026

[12] Cussó, X., Garrabou, R., Olarieta, J. R. and Tello, E., 2006b. Balances energéticos y usos del suelo en la agricultura catalana: una comparación entre mediados del siglo XIX y finales del siglo XX. Hist. Agrar. 40, 471–500. Retrieved from: http://hdl.handle.net/10459.1/31362 (accessed 21/12/2014)

[13] Dettmann, E. H., 2008. Encyclopedia of Ecology. Elsevier. doi:10.1016/B978-008045405-4.00140-3

[14] Elmqvist, T., Folke. C., Nyström, M., Peterson, G., Bengtsson, J., Walker, B. and Norberg, J., 2003. Response diversity, ecosystem change, and resilience. Front. Ecol. Environ. 1, 488–494. doi:http://dx.doi.org/10.1890/1540-9295(2003)001[0488:RDECAR]2.0.CO;2

[15] Farina, A., 2000. The cultural landscape as an example of integration of ecology and economics. BioScience 50, 313–320. doi:http://dx.doi.org/10.1641/0006-3568(2000)050[0313:TCLAAM]2.3.CO;2

[16] Fischer, J., Brosi, B., Daily, G. C., Ehrlich, P. R., Goldman, R., Goldstein, J., Lindenmayer, D. B., Manning, A. D., Mooney, H. A., Pejchar, L., Ranganathan, J. and Tallis, H., 2008. Should agricultural policies encourage land sparing or wildlife-friendly farming? Front Ecol Environ 6(7), 380-385. http://dx.doi.org/10.1890/070019

[17] Fischer-Kowalski, M.,and Haberl, H. (Eds.), 2007. Socioecological Transitions and Global Change. Trajectories of Social Metabolism and Land Use. Edward Elgar, Cheltenham.

[18] Gabriel D, Roschewitz I, Tscharntke T, Thies C., 2006. Beta diversity at different spatial scales: plant communities in organic and conventional agriculture. Ecol. Appl. 16, 2011-2021.

http://dx.doi.org/10.1890/1051-0761

[19] Gabriel, D., Sait, S. M., Kunin, W. E. and Benton, T. M., 2013. Food production vs. biodiversity: comparing organic and conventional agriculture. J. Appl. Ecol. 50, 355–364. doi:10.1111/1365-2664.12035

[20] Galán, E., Tello, E., Cunfer, G., Guzmán, G. I., González de Molina, M., Krausmann, F., Gingrich, S., Padró, R., Marco, I., Moreno-Delgado, D., forthcoming. The Energy Return On Investment (EROI) in agroecosystems: An analytical proposal to study socioecological transitions to industrialized farm systems (The Vallès County, Catalonia, in 1860 and 1999). Ecol Econ.

[21] Garrabou, R., Tello, E., and Cussó, X., 2010. Ecological and Socio-economic functioning of the Mediterranean agrarian systems in the middle of the nineteenth century. A Catalan case study (the Vallès county, 1850-70). In: Landsteiner, E. and Langthaler, E. (Eds.), Agrosystems and labour relations in European rural societies (Middle Ages-20th Century). Brepols Pubishing, Turnhout, 119-152.

[22] Georgescu-Roegen, N., 1971. The Entropy Law and the Economic Process. Harvard University Press, Cambridge MA.

[23] Gerard, F., Petit, S., Smith, G., Thomson, A., et al., 2010. Land cover change in Europe between 1950 and 2000 determined employing aerial photography. Prog Phys Geog 34:183-205.doi: 10.1177/0309133309360141

[24] Gershenson, C., and Fernández, N., 2012. Complexity and information: measuring emergence, self-organization, and homeostasis at multiple scales. Complexity 18(2), 29–44. doi:10.1002/cplx

[25] Giampietro, M., 1997. Socioeconomic constraints to farming with biodiversity. Agriculture, Ecosystems & Environment 62(2-3), 145-167.doi:10.1016/S0167-8809(96)01137-1

[26] Giampietro, M., 2004. Multi-Scale Integrated Analysis of Agroecosystems. CRC Press, Boca Raton.

[27] Giampietro, M., Pimentel, D., 1991. Energy Efficiency: assessing the interaction between humans and their environment. Ecol. Econ. 4(2), 117-144. doi:10.1016/0921-8009(91)90025-A

[28] Giampietro, M., Mayumi, K., and Sorman, A. H., 2011. The Metabolic Pattern of Societies: Where Economists Fall Short. Routledge, Oxon.

[29] Giampietro, M., Mayumi, K., and Sorman, A. H., 2013. Energy Analysis for Sustainable Future: Multi-Scale Integrated Analysis of Societal and Ecosystem Metabolism. Routledge, Oxon.

[30] Gladyshev, G. P., 1999. On Thermodynamics, Entropy and Evolution of Biological Systems: What Is Life from a Physical Chemist's Viewpoint. Entropy 1, 9–20.

[31] Gliessman, S. R. (Ed.), (1990) Agroecology: Researching the Ecological Basis for Sustainable Agriculture. Springer, New York

[32] Godfray H. C. J., Beddington, J. R., Crute, I. R. et al., 2010. Food Security: The Challenge of Feeding 9 Billion People. Science 327, 812-818.doi:10.1126/science.1185383

[33] Gómez-Baggethun, E., Reyes-García, V., Olsson, P. and Montes, C. 2012. Traditional ecological knowledge and community resilience to environmental extremes: A case study in Doñana, SW Spain. Global Environ Chang 22(3), 640–650.doi:10.1016/j.gloenvcha.2012.02.005

[34] González de Molina, M., 2010. A guide to studying the socio-ecological transition in european agriculture. Working Paper of the Sociedad Española de Historia Agraria, DT-SEHA n. 10-06.
Available on line: http://repositori.uji.es/xmlui/bitstream/handle/10234/15473/ATT00019.pdf?sequence=1.

[35] González de Molina, M. and Toledo, V. 2014. The Social Metabolism. A Socio-Ecological Theory of Historical Change. Sgringer, New York.

[36] Gustavsson, E., Lennartsson, T. and Emanuelsson, M., 2007. Land use more than 200 years ago explains current grassland plant diversity in a Swedish agricultural landscape. Biol. Conserv. 138, 47-59.doi:10.1016/j.biocon.2007.04.004

[37] Guzmán, G.I. and González de Molina, M., 2009. Preindustrial agriculture versus organic agriculture: The land cost of sustainability. Land Use Policy 26(2), 502–510. doi:10.1016/j.landusepol.2008.07.004

[38] Guzmán, G., Aguilera, E., Soto, D., Cid, A., Infante, J., García-Ruiz, R., Herrera, A., Villa, I. and González de Molina, M., 2014. Methodology and conversion factors to estimate the net primary productivity of historical and contemporary agroecosystems. Working Paper of the Sociedad Española de Historia Agraria, DT-SEHA n. 1407.

Retrieved from: http://repositori.uji.es/xmlui/bitstream/handle/10234/91670/DT-SEHA%201407.pdf?sequence=3 (accessed 28/12/2014).

[39] Guzmán, G.I. and González de Molina, M., 2015. Energy efficiency in agrarian systems from an agro-ecological perspective. Agroecology and Sustainable Food Systems 39, 924-952.

doi: 10.1080/21683565.2015.1053587

[40] Haberl, H., 2001. The Energetic Metabolism of Societies. Part I: Accounting Concepts. J. Ind. Ecol. 5, 107–136. doi:10.1162/108819801753358481

[41] Hall, C. A. S., 2011. Synthesis to Special Issue on New Studies in EROI (Energy Return on 1 Investment). Sustainability 3, 2496-2499.doi:10.3390/su3122496

[42] Harper, K. A., MacDonald, S. E., Burton, P. J., Chen, J., Brosofske, K. D., Rosofske, S. C., Saunders, E. S., Euskirchen, D. R., Jaiteh, M. S. and Esseen, P.-A., 2005. Edge Influence on Forest Structure and Composition in Fragmented Landscapes. Conserv Biol 19, 768-82. doi:10.1111/j.1523-1739.2005.00045.x

[43] Henle, K., Alard, D., Clitherow, J., Cobb, P., Firbank, L., Kull, T., McCracken, D., Moritz, R.F.A., Niemelä, J., Rebane, M., Wascher, D., Watt, A. and Young, J., 2008. Identifying and managing the conflicts between agriculture and biodiversity conservation in Europe–A review. Agr. Ecosyst. Environ. 124, 60-71. doi:10.1016/j.agee.2007.09.005

[44] Ho, M.-W., 1998. The rainbow and the worm, the physics of organisms. Springer-Verlag, Berlin.

[45] Ho, M.-W., 2013. Circular Thermodynamics of Organisms and Sustainable Systems. Systems 1(3), 30–49. doi:10.3390/systems1030030

[46] Ho, M.-W., and Ulanowicz, R., 2005. Sustainable systems as organisms? BioSystems 82(1), 39–51. doi:10.1016/j.biosystems.2005.05.009

[47] Jackson, L. E., Pascual, U. and Hodgkin, T., 2007. Utilizing and conserving agrobiodiversity in agricultural landscapes. Agr. Ecosyst. Environ. 121(3), 196–210. doi:10.1016/j.agee.2006.12.017

[48] Jackson, L. E., Pulleman, M. M., Brussaard, L., Bawa, K. S., Brown, G. G., Cardoso, I. M., de Ruiter, P. C., García-Barrios, L., Hollander, A. D., Lavelle, P., Ouédraogo, E., Pascual, U., Setty, S., Smukler, S. M., Tscharntke, T., Van Noordwijk, M., 2011. Social-ecological and regional adaptation of agrobiodiversity management across a global set of research regions. Global Environ Chang 22(3), 623–639.doi:10.1016/j.gloenvcha.2012.05.002

[49] Johns, T. and Sthapit, B.R., 2004. Biocultural diversity in the sustainability of developing-country food systems. Food & Nutrition Bulletin 25(2), 143-155.

Retrieved from: http://www.ingentaconnect.com/content/nsinf/fnb/2004/00000025/00000002 /art00007?crawler=true&mimetype=application/pdf (accessed 28/12/2014)

[50] Krausmann, F., 2004. Milk, Manure, and Muscle Power. Livestock and the Transformation of Preindustrial Agriculture in Central Europe. Hum. Ecol. 32(6), 735–772. doi:10.1007/s10745-004-6834-y

[51] Krausmann, F., Haberl, H., Schulz, N. B., Erb, K., Darge, E., and Gaube, V., 2003. Land-use change and socioeconomic metabolism in Austria-PartI: driving forces of land-use change: 1950-1995. Land Use Policy 20, 1-20. doi:10.1016/S0264-8377(02)00048-0

[52] Krausmann, F., Erb, K.-H., Gingrich, S., Haberl, H., Bondeau, A., Gaube, V., Lauk, C., Plutzar, C. and Searchinger, T., 2013. Global human appropriation of net primary production doubled in the 20th century. Proc. Natl. Acad. Sci. 110, 10324-10329. doi:10.1073/pnas.1211349110

[53] Lambin, E. F. and Meyfroidt, P., 2011. Global land use change, economic globalization, and the looming land scarcity. Proc. Natl. Acad. Sci. 108(9), 3465–3472. doi:10.1073/pnas.1100480108

[54] Liu, L., Dietz, T., Carpenter, S. R., Alberti, M., Folke, C., Moran, E., Pell, A. N., Deadman, P., Kratz, T., Lubchenco, J., Ostrom, E., Ouyang, Z., Provencher, W., Redman, C. L., Schneider, S. H. and Taylor, W. W., 2007. Complexity of Coupled Human and Natural Systems. Science 317(5844), 1513-1516. doi:10.1126/science.1144004

[55] Loreau, M., Mouquet, N. and Gonzalez, A., 2010. Biodiversity as spatial insurance in heterogeneous landscapes. P. Natl. Acad. Sci. 100(22), 12765-12770. doi:10.1073/pnas.2235465100

[56] Margalef, R., 1991. Teoría de los sistemas ecológicos. Publicacions de la Universitat de Barcelona, Barcelona.

[57] Marull, J., Pino, J., Tello, E., and Cordobilla, M. J., 2010. Social metabolism, landscape change and land-use planning in the Barcelona Metropolitan Region. Land Use Policy 27(2), 497–510. doi:10.1016/j.landusepol.2009.07.004

[58] Marull, J., Tello, E., Wilcox, P., Coll, F., Pons, M., Warde, P., Valldeperas, N., Ollés, A., 2014. Recovering the landscape history behind a Mediterranean edge environment (The Congost Valley, Catalonia, 1854-2005): The importance of agroforestry systems in biological conservation. Appl Geogr 54:1-17. doi:10.1016/j.apgeog.2014.06.030

[59] Marull, J., Font, C., Tello, E., Fullana, N., Domene, E., Pons, M., Galán, E., 2015a. Towards an Energy-Landscape Integrated Analysis? Exploring the links between socio-metabolic disturbance and landscape ecology performance (Mallorca, Spain, 1956-2011). Landscape Ecol. doi: 10.1007/s10980-015-0245-x

[60] Marull ,J., Otero, I., Stefanescu, C., Tello, E., Coll, F., Pons, M., Diana, G.L., 2015b. Exploring the links between forest transition and landscape changes in the Mediterranean. Can forest recovery lead to lower landscape quality?. Agroforest Syst 89 (4):705–719. doi: 10.1007/s10457-015-9808-8

[61] Marull, J., Tello, E., Fullana, N., Murray, I., Jover, G., Font, C., Coll, F., Domene, E., Leoni, V., Decolli, T., 2015c. Long-term bio-cultural heritage: exploring the intermediate disturbance hypothesis in agro-ecological landscapes (Mallorca, c. 1850–2012). Biodiversity and Conservation 24 (13): 3217-3251. doi: 10.1007/s10531-015-0955-z

[62] Matson, P. A, Parton, W. J., Power, A. G. and Swift, M. J., 1997. Agricultural Intensification and Ecosystem Properties. Science 277, 504-509. doi:10.1126/science.277.5325.504

[63] McMichael, Ph., 2011. Food system sustainability: Questions of environmental governance in the new world (dis)order. Global Environ. Chang. 21(3), 804–812. doi:10.1016/j.gloenvcha.2011.03.016

[64] Muradian, R., Walter, M. and Martinez-Alier, J., 2012. Hegemonic transitions and global shifts in social metabolism: Implications for resource-rich countries. Introduction to the special section. Global Environ. Chang. 22 (3), 559–567. doi:10.1016/j.gloenvcha.2012.03.004

[65] Myers, N., Mittermeier, R. A., Mittermeier, C. G., da Fonseca, G. A. B. and Kent, J., 2000. Biodiversity hotspots for conservation priorities. Nature 403, 853-858. doi:10.1038/35002501

[66] Morowitz, H. J., 2002. The Emergence of Everything: how the world became complex. Oxford University Press, Oxford.

[67] Odum, E. P., 1993. Ecology and our Endangered Life-Support Systems. Sinauer Associates, Massachusetts.

[68] Odum, H. T., 1984. Energy Analysis of the Environmental Role in Agriculture. In: Stanhill, E. (Ed.), Energy and Agriculture, Springer Verlag, Dordrecht, 24-51.

[69] Odum, H. T., 2007. Environment, power, and society for the twenty-first century.The Hierarchy of Energy. Columbia University Press, New York.

[70] Olarieta, J. R., Rodríguez-Valle, F. L. and Tello, E., 2008. Preserving and destroying soils, transforming landscapes: Soils and land-use changes in the Vallès County (Catalunya, Spain) 1853–2004. Land Use Policy 25(4), 474–484. doi:10.1016/j.landusepol.2007.10.005

[71] Olarieta, J. R., Padrò, R., Masip, G., Rodríguez-Ochoa, R. and Tello, E. 2011. ‘Formiguers’, a historical system of soil fertilization (and biochar production?). Agr. Ecosyst. Environ. 140(1–2), 27–33. doi:10.1016/j.agee.2010.11.008

[72] Parcerisas, L., Marull, J., Pino, J. Tello, E., Coll, F. and Basnou, C., 2012. Land use changes, landscape ecology and their socioeconomic driving forces in the Spanish Mediterranean coast (El Maresme County, 1850-2005). Environ Sci Policy 23, 123-132. doi:10.1016/j.envsci.2012.08.002

[73] Passet, R., 1996. Principios de bioeconomía. Fundacion Argentaria-Visor, Madrid.

[74] Perfecto I. and Vandermeer, J., 2010. The agroecological matrix as alternative to the land-sparing/agriculture intensification model. P. Natl. Acad. Sci. 107(13), 5786-5791. doi:10.1073/pnas.0905455107

[75] Peterseil, J., Wrbka, T., Plutzar, C., Schmitzberger, I., Kiss, A., Szerencsits, E., Reiter, K., Schneider, W., Suppan, F. and Beissmann, H., 2004. Evaluating the ecological sustainability of Austrian agricultural landscapes—the SINUS approach. Land Use Policy 21(3), 307–320. doi:10.1016/j.landusepol.2003.10.011

[76] Phalan, B., Onial, M., Balmford, A. and Green, R. E., 2011. Reconciling Food Production and Biodiversity Conservation: Land Sharing and Land Sparing Compared. Science 333, 1289-1291. doi:10.1126/science.1208742

[77] Pierce, S.; 2014. Implications for biodiversity conservation of the lack of consensus regarding the humped-back model of species richness and biomass production. Funct Ecol 28, 253–257. doi: 10.1111/1365-2435.12147

[78] Prigogine, I. 1996. The end of certainity. Time, chaos and the new laws of nature. The Free Press, New York.

[79] Robson, J. P and Fikret Berkes, F., 2011. Exploring some of the myths of land use change: Can rural to urban migration drive declines in biodiversity? Global Environ Chang 21(3), , 844–854. doi:10.1016/j.gloenvcha.2011.04.009

[80] Roxburgh, S. H., Shea, K. and Wilson, J. B., 2004. The intermediate disturbance hypothesis, patch dynamics and mechanisms of species coexistence. Ecology 85, 359-371. doi:http://dx.doi.org/10.1890/03-0266

[81] Schaffartzik A., Mayer A., Gingrich S., Eisenmenger N., Loy C. and Krausmann F. (2014) The global metabolic transition: Regional patterns and trends of global material flows, 1950–2010. Global Environ Chang 26, 87-97.

[82] Schandl, H., Haberl, H. and Weisz, H., 2002. Handbook of physical accounting. Measuring bio-physical dimensions of socio-economic activities. MFA - EFA - HANPP. Social Ecology Working Paper 73. Institute of Social Ecology, Vienna. Retrieved from http://uni-klu.ac.at/socec/downloads/wp73.pdf (accessed 28/12/2014).

[83] Schrödinger, E., 1944. What is life? Cambridge University Press, Cambridge.

[84] Shannon, C. E. and Weaver, W., 1949. The Mathematical Theory of Communication. University of Illinois Press, Illinois.

[85] Smil, V., 2013. Harvesting the Biosphere: How Much We Have Taken from Nature. The MIT Press, Cambridge MA.

[86] Swift, M. J., Izac, A. M. N. and van Noordwijk, M., 2004. Biodiversity and ecosystem services in agricultural landscapes—are we asking the right questions? Agriculture, Ecosystems & Environment 104(1), 113-134. doi:10.1016/j.agee.2004.01.013

[87] Tainter, J., 1990. The Collapse of Complex Societies. Cambridge University Press, Cambridge.

[88] Tello, E., Garrabou, T.; Cussó, X., Olarieta, J. R. and Galán, E., 2012. Fertilizing Methods and Nutrient Balance at the End of Traditional Organic Agriculture in the Mediterranean Bioregion: Catalonia (Spain) in the 1860s. Hum. Ecol. 40(3), 369-383. doi:10.1007/s10745-012-9485-4

[89] Tello, E., Valldeperas, E., Ollés, N., Marull, J., Coll, F., Warde, P. and Wilcox, P., 2014. Looking backwards into a Mediterranean edge environment: Landscape changes in El Congost Valley (Catalonia), 1850-2005. Environ. Hist. 20, 347-384. http://dx.doi.org/10.3197/096734014X14031694156402

[90] Tello, E., Galán, E., Cunfer, G., Guzmán, G. I., González de Molina, M., Krausmann, F., Gingrich, S., Sacristán, V., Marco, I., Padró, R. and Moreno-Delgado, D., 2015. A proposal for a workable analysis of Energy Return On Investment (EROI) in agroecosystems. Part I: Analytical approach. Social Ecology Working Paper. Institute of Social Ecology, Vienna.

[91] Tello, E., Galán, E., Sacristán, V., Cunfer, G., Guzmán, G. I., González de Molina, M., Krausmann, F., Gingrich, S., Padró, R., Marco. I. and Moreno-Delgado, D., 2016. Opening the black box of energy throughputs in agroecosystems: a decomposition analysis of final EROI into its internal and external returns (the Vallès County, Catalonia, c.1860 and 1999). Ecol. Econ. 121, 160-174. doi:10.1016/j.ecolecon.2015.11.012

[92] Tilman, D., 1994. Competition and Biodiversity in Spatially Structured Habitats. Ecology 75(1), 2-16. doi:http://dx.doi.org/10.2307/1939377

[93] Tilman, D., 1999. Global environmental impacts of agricultural expansion: The need for sustainable and efficient practices. P. Natl. Acad. Sci. 96, 5995-6000. doi: 10.1073/pnas.96.11.5995

[94] Tilman, D., Cassman, K., G., Matson, P. A., Naylor, R. and Polasky, S., 2002. Agricultural sustainability and intensive production practices. Nature 418, 671-677. doi:10.1038/nature01014

[95] Tress, B., Tress, G., Décamps, H. and d'Hauteserre, A. M., 2001. Bridging human and natural sciences in landscape research. Landscape Urban Plan 57, 137-141. doi:10.1016/S0169-2046(01)00199-2

[96] Tscharntke, T., Klein, A. M., Kruess, A., Steffan-Dewenter, I. and Carsten Thies, C., 2005. Landscape perspectives on agricultural intensification and biodiversity-ecosystem service management. Ecol Lett 8, 857-874. doi: 10.1111/j.1461-0248.2005.00782.x

[97] Tscharntke, T., Clough, Y., Wanger, T. C., Jackson, L., Motzke, I., Perfecto, I., Vandermeer, J. and Whitbread, A., 2012. Global food security, biodiversity conservation and the future of agricultural intensification. Biol Conserv 151, 53-59. doi:10.1016/j.biocon.2012.01.068

[98] Ulanowicz, R. E., 1997. Ecology, the Ascendent Perspective. Columbia University Press, New York.

[99] Ulanowicz, R. E., 1986. Growth and Development. Ecosystems Phenomenology. Springer, Dordrecht.

[100] Ulanowicz, R. E., 2001. Information theory in ecology. Comput. Chem. 25, 393–399. doi:10.1016/S0097-8485(01)00073-0

[101] Ulanowicz, R. E., 2003. Some steps toward a central theory of ecosystem dynamics. Comput. Biol. Chem. 27(6), 523–530. doi:10.1016/S1476-9271(03)00050-1

[102] Urban, D. L., Minor, E. S., Treml, E. and Schick, R. S., 2009. Graph models of habitat mosaics. Ecol. Lett. 12(3), 260–73. doi:10.1111/j.1461-0248.2008.01271.x

[103] Vitousek, P. M., Ehrlich, P. R., Ehrlich, A. H. and Matson, P. A., 1986. Human Appropriation of the Products of Photosynthesis. BioScience 36(6), 363–373.

[104] Vranken, I., Baudry, J., Aubinet, M., Visser, M. and Bogaert, J., 2014. A review on the use of entropy in landscape ecology: heterogeneity, unpredictability, scale dependence and their links with thermodynamics. Landscape Ecol. doi:10.1007/s10980-014-0105-0

[105] Wrbka, T., Erb, K.-H., Schulz, N. B., Peterseil, J., Hahn, C. and Haberl, H., 2004. Linking pattern and process in cultural landscapes. An empirical study based on spatially explicit indicators. Land Use Policy, 21(3), 289–306. doi:10.1016/j.landusepol.2003.10.012

Chapter 5

General conclusions

In the work presented here, it has been seen that mathematical models give a new dimension to current issues of interest in agro-ecology, biodiversity conservation and landscape planning. Moreover, it is planned to publish part of the developed code to perform the required calculations as an R package in the near future.

To better understand the behaviour of the indices under analysis, we first have studied the indicators using training data, ie, values based on a (discrete) uniform distribution. Then we used the sample data from the cases of study of Mallorca and the Vallès County. Thus we have been able to obtain a theoretical frame in which the sample data lie.

In the chapter 2, a study of the Shannon entropy and human appropriation of net primary production ($HANPP$) is presented, showing the joint distribution of these two indicators. It is also introduced a resilience measure in agroecosystems. In Mallorca, the results clearly show that when intermediate levels of $HANPP$ are performed within high levels of complexity (H) in landscape patterns, like agro-forest mosaics, great bird species richness and high socio-ecological resilience can be maintained. Yet, these complex-heterogeneous landscapes are currently vanishing due to industrial farm intensification, rural abandonment and urban sprawl. The results make apparent the usefulness of transferring the concept of intermediate disturbance-complexity interplay to cultural landscapes. The spatial-explicit IDC model can be used as a tool for strategic environmental assessment of land-use policy.

Regarding to the chapter 3, the main contribution here is the possibility of summarizing a whole point cloud into a single curve. In this sense, the relationship between landscape patterns H and human appropriation A is reduced to $f(A) = E[H|A]$. This model is used to study temporal changes in Mallorca at regional scale. The results show how urban expansion affects landscape functionality, as well it is possible to see how combinations of land covers change for different time points.

The simulation method to obtain large new samples from real dataset can be done in for other cases of study. However, the whole process to obtain the bandwidth parameter is time requiring. Once one have the smoothing parameter for each subsimplex, next computations are straightforward.

The graph of the agroecosystems energy flows explained in the chapter 4 allows a new view of agroecosystems. Through the graph, it is possible to observe the energy interchange of the agroecosystems' internal loops. Moreover, new indicators to measure the properties of the internal energy flows have been proposed, they are E, energy storage, I, information (an improvement of this indicator is presented in the annex), and L, landscape functionality. These new indicators enable the study of the energy treatment into agroecosystems.

The results show that the landscape patterns of Mediterranean land use mosaics, created by traditional organic mixed-farming, have tended to vanish as a result of a simultaneous reduction in the complexity of the interlinking pattern of energy flows and the quantity of information carried by them. The model could help us to reveal how and why different agroecosystem managements lead to key turning points in the relationship of the energy profile with landscape ecological functioning. No doubt, these results will be very useful for designing more sustainable farm systems worldwide in the future.

Annex I

Information in agroecosystems

I.1 Introduction

Here we present a proposal to change the information indicator I. Our aim is to reflect the cultural knowledge of the farmers (agents) that drive the agroecosystem's processes according to their wisdom. For this purpose, a linear transformation is introduced, this will enable us to choose the combination of betas (proportions of energy flows in agroecosystems, see section 4.3.2 in previous chapter) at which I reaches its maximum. This implies that it is possible to stablish an ideal frame work and compare any case study to it. It should be said that this ideal combination of betas will be subject to a particular case study and time period.

I.2 Shifting maximum information

Due to its formulation, I (see equation [4.1]) achieves its maximum value for all $\beta_i = 0.5$, but there can be processes with different values of entropy. To tackle this issue, we propose to include a linear change in the I formula such that the placement at which the maximum value of this indicator is reached can be changed as needed. This linear change is applied to the betas before calculating the Shannon index in the information formula. It is defined as follows,

$$T(x,a) = \begin{cases} \frac{0.5}{a}x & x < a \\ 0.5 + \frac{0.5}{1-a}(x-a) & x \geq a\ . \end{cases}$$

This piecewise function translates the interval $(0, a)$ to the interval $(0, 0.5)$, and the interval $[a, 1)$ to $[0.5, 1)$, as can be seen in figure I.1a. This implies that the maximum value of the Shannon index applied to $(x, 1-x)$, after the transformation, is reached at the given value a instead of in 0.5. In figure I.1b this effect can be checked. So, we can take a vector of $\beta^* = (\beta^*_1, \ldots, \beta^*_s)$ to change where the maximum of any beta is given.

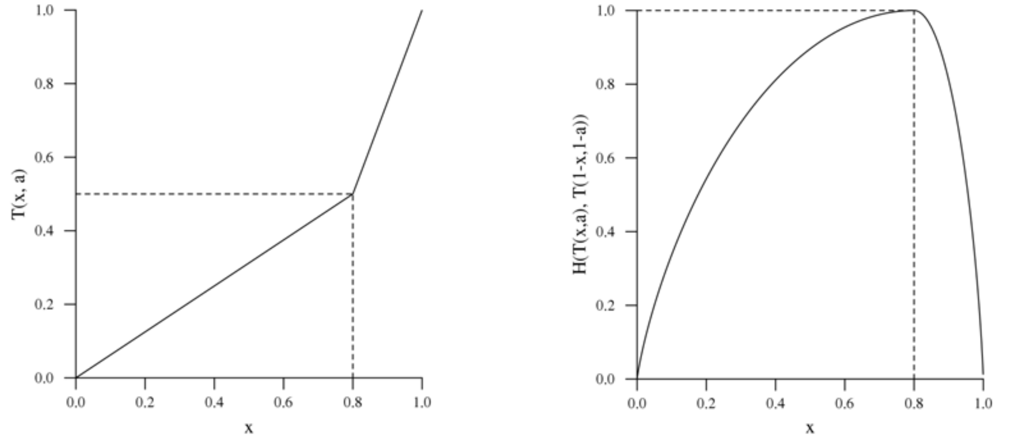

(a) Linear transformation T applied to x with $a = 0.8$. (b) Shannon index H applied to $(x, 1-x)$ with $a = 0.8$.

Figure I.1

We call I^* the information applied to $T(\beta, \beta^*)$. Now, the information indicator is written as

$$I^* = \left(-\frac{2}{s} \sum_{i=1}^{s} T(\beta_i, \beta^*_i) \log_2 T(\beta_i, \beta^*_i) \right),$$

where s is the number of betas we work with. Once the indicator is defined, we can add the penalization of waste (defined in section 4.3.6), $\gamma_W = (\gamma_{FW} + \gamma_{LW})/2$,

$$I^* = \left(-\frac{2}{s} \sum_{i=1}^{s} T(\beta_i, \beta^*_i) \log_2 T(\beta_i, \beta^*_i) \right) \gamma_W.$$

Note that taking $\beta^*_i = 0.5$ we recover the initial indicator I.